UiT Norges arktiske universitet

IFA – Department of Pharmacy

Molecular modelling of interactions between antipsychotic drugs and receptors mediating antipsychotic effects and important side effects

Halimatu Sadia T Issifou

Master thesis in Pharmacy FAR3911 May 2021

Table of contents

Abbreviations

AAP	Atypical antipsychotics
ADP	Adenosine diphosphate
ASP	Aspartic acid
ATP	Adenosine triphosphate
BBB	Blood brain barrier
cAMP	Cyclic adenosine monophosphate
CNS	Central Nervous System
COMT	Catechol-O-methyltransferase
CPU	Central processing unit
C-terminal	Carboxyl-terminal
DAG	Diacylglycerol
D_2S/D_2L	Dopamine D_2 receptor short/long
EC	Effective Concentration
ECL	Extracellular loop
EPS	Extrapyramidal side effects
FASTA	Text-based format of amino acid sequences
FDA	Food and drug administration
GABA	γ-aminobutyric acid

GDP	Guanosine diphosphate
$G_i/G_s/G_o$	G inhibitory/stimulatory/other
G-protein	Guanine nucleotide-binding protein
GPCRs	Guanine nucleotide-binding protein coupled receptors
GPU	Graphics processing unit
GTP	Guanosine triphosphate
ICL	Intracellular loop
IC_{50}	Half maximum inhibitory concentration
IFD	Induced Fit Docking
IP_3	Inositol triphosphate
K	Kelvin
K_i	Inhibitory constant
LBDD	Ligand-based drug design
LSD	Lysergic acid diethylamide
MAO-B	Monoamine oxidase B
MD	Molecular dynamics
NaCl	Sodium chloride
nM	Nanomolar
ns	Nanosecond
NPT	Isothermal-isobaric ensemble
N-terminal	Amino-terminal

OPLS	Optimized Potentials for Liquid Simulations
OPM	Orientations of proteins in membranes
PDB	Protein Data Bank
PDSP	Psychoactive Drug Screening Programme
PI-PLC	Phosphatidylinositol phospholipase C
PNS	Peripheral Nervous System
POPC	Palmitoyl-oleoyl-phosphatidylcholine
ps	Picosecond
RMSD	Root mean square deviation
RMSF	Root mean square fluctuation
SBDD	Structure-based drug design
SMILES	Simplified molecular input line entry system
SPC	Simple point-charge
TAP	Typical antipsychotic
TM	Transmembrane
UniprotKB	Universal protein resource knowledgebase
vdW	Van der Waals interaction
Å	Angstrom
5-HT	5-hydroxytryptamine
7TM	Seven transmembrane (synonym for GPCR)

Acknowledgements

In the name of Allah, the most Gracious, the most Merciful

This master thesis serves as a documentation of my final work in the Master of Pharmacy programme at The University of Tromsø – The Arctic University of Norway. It was written between August 2020 – May 2021 and achieved along with the Medical Pharmacology and Toxicology Research group at the faculty of Health Science.

First and foremost, I would like to commence by thanking the Almighty Allah for giving me strength and knowledge to complete this thesis. We as Muslims believe that in order to show gratitude to Allah, we must be thankful and recognize the people that helped us. On that note, I would like to sincerely express my gratitude, and acknowledge my supervisors Associate Professor Kurt Kristiansen and Professor Ingebrigt Sylte.

The support, guidance, encouragement and feedback I received from my supervisors through the whole process provided me with clarity, confidence in completing the project but also a great learning experience. Without them, I would probably find myself lost long time ago. I thank you for always being available and making me feel comfortable enough to ask you whatever came across my mind no matter how silly it was.

I also want to give thanks to my “room-mate” Sammy Chan for making this period enjoyable and less lonely by engaging in hour long conversations about random matters despite being in stressful times.

Lastly, I am forever grateful for my parents and siblings who continuously encouraged and believed in me even when I was doubtful myself. Once again, to everyone I thank you for the tremendous support.

Abstract

Dopamine and serotonin are two neurotransmitters that have strong functional interactions where one of the functions of serotonin is to inhibit the activity of dopamine. These neurotransmitters exert their actions through mediation of dopaminergic and serotonergic receptors, and the receptors in focus in the current study, are the dopamine D_2 and serotonin 5-HT_{2A} receptors. Common for both receptors is that they are class A G-protein-coupled receptors consisting of seven transmembrane helices embedded in the lipid membrane of neurons.

Imbalance and disruption of especially the dopamine system in the CNS may result in hallucinations, delusions, and lowered levels of motivation, which are important signs of schizophrenia and psychosis disorders. These disorders are treated with antipsychotic drugs that predominantly antagonize dopamine D_2 and serotonin 5-HT_{2A} receptors. Unfortunately, many patients on treatment with antipsychotics experience side effects like sedation, weight gain and extrapyramidal disturbances. Therefore, there is a need of more effective antipsychotic drugs with less adverse effects. The main aim of this thesis is to get a deeper understanding of the mechanisms of action and side effects of antipsychotics.

37 antipsychotic drugs were docked with induced fit docking (IFD) into four aminergic receptors, dopamine D_2, serotonin 5-HT_{2A}, 5-HT_{2C} and histamine H_1 receptor, scored according to energies associated with specific poses and finally ranked. Molecular dynamic (MD) simulations were further applied to thoroughly investigate the differences and similarities in binding modes between bromocriptine (agonist), aripiprazole (partial agonist) and risperidone (antagonist) in complex with the dopamine D_2 receptor, in addition to pimavanserin in complex with the serotonin 5-HT_{2A} receptor.

Our results suggest that there is a link between the binding affinities of the antipsychotic drugs to different aminergic receptors, and the most common side effect observed. Additionally, MD simulations revealed that antipsychotic drugs with different intrinsic activity, bind to the dopamine D_2 receptor in distinct ways. An agonist like bromocriptine on the dopamine D_2 receptor, established stable hydrogen bonds to serines in TM5 (Ser5.43, Ser5.42 and Ser5.46) that was not maintained in the partial agonist nor antagonist systems.

1 Introduction

1.1 The Nervous System

The human body consists of many complex organ systems from the integumentary, skeletal, muscular, endocrine, cardiovascular, lymphatic, respiratory, urinary systems to the nervous system. The nervous system is also the most complicated and comprehensive one as it is involved in all mentioned systems as the controlling, regulatory and communicating entity (1). Moreover, the nervous system is principally divided into two major regions, the central- and the peripheral nervous systems. The spinal cord and the brain are connected together and constitute what we call the central nervous system (CNS). This region is the executive control system in the body. The rest of the nervous structures in the body goes under the peripheral system, PNS, which mainly connects the central nervous system to muscles, organs, limbs and skin (2).

Shortly explained, the PNS can be divided into two subsystems named the autonomic and somatic nervous system. The somatic nervous system has voluntary control over the skeletal muscles, bones and skin while the autonomic nervous system has involuntary control over cardiac muscles, glands and smooth muscles found in many organs and blood vessels. This means that the functions of the autonomic nervous system are regulated and performed without our minds being involved and independently of our wishes. In this thesis we are focusing on the CNS.

1.2 The Central Nervous system

The central nervous system coordinates our actions, reflexes and sensations and consists of the brain and the spinal cord. While the brain is the "headquarters", the spinal cord acts as the "highway" for communication that combines the brain and the body (3). A vast network of cranial nerves from the PNS contains sensory receptors that are linked to the brain which again aids in processing changes in both external and internal environments. Nervous tissue consists of nerve cells, also referred to as neurons and is the largest and most important group of tissues in the nervous system. A neuron is built up of the cell body called soma. Dendrites and axons are extensions from the cell body that either pass or receive information from nearby neurons. In addition to nerve cells, neuroglial/glial cells are just as important but outnumbers neurons by a 3 to 1 ratio (3).

The major distinction between neuroglial and nerve cells is that glial cells do not participate directly in synaptic transmission nor electrical signalling, however they provide a framework of tissue that supports the neurons and their activities. Further, glial cells are also important in responding to tissue damage and maintaining the concentration of important chemical substances. They also play an essential role in what is known as the blood-brain barrier, BBB which is fundamental in drug delivery to the brain. The brain is an immune privileged organ that must be protected at all costs. The BBB is thereby present in the vasculature of the brain and one of the two systems involved in maintaining brain homeostasis. This is a physiological barrier that acts as a security system and protects neural tissues from exogenous substances like pathogens and toxins (4). It further separates circulating blood from cerebrospinal fluid of the brain (5). Structurally, the BBB consists of different classes of cells including mural cells, endothelial cells, glial cells and contractile proteins that can contract or stretch to regulate the diameter of the blood vessel. A simplified illustration of the barrier is provided in figure 1. Vital small molecules however, such as oxygen, hormones and carbon dioxide have free passage through the BBB. The other system involved in maintaining brain homeostasis is called the complement system and is a part of the immune system.

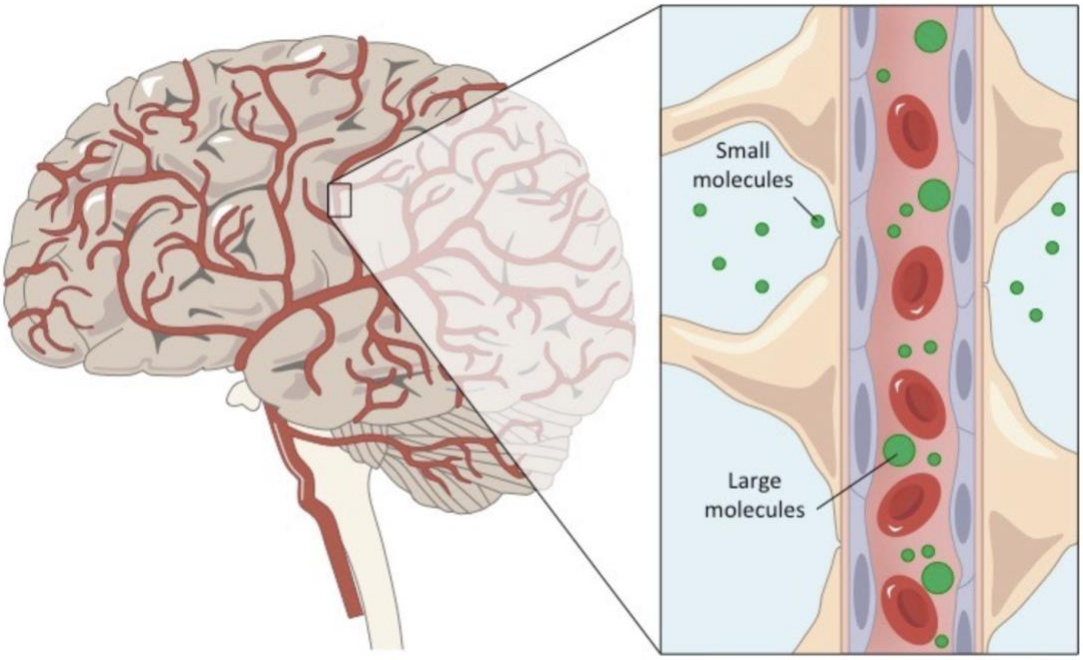

Figure 1: *simplified illustration of the blood-brain barrier in the brain. The BBB is composed of an inner lining of endothelial cells shown in purple, blood cells and mural cells that wrap around the endothelial cells. The mural cells (in beige) in addition to the endothelial cells are important in regulating the vascular permeability controlling the molecules that enter the blood stream in the CNS (5).*

One of the challenges seen in pharmaceutical drug design that target CNS disorders, is connected to the difficulties substances experience when penetrating the blood-brain barrier. This has to some extent been solved by for example creating smaller lipid-soluble substances that can penetrate the blood-brain barrier easier by transmembrane diffusion as drugs with low molecular weight and sufficient lipid solubility are more effective in transmembrane diffusion than polar substances (6).

1.3 Signal transmission

Endogenous neurotransmitters are chemical substances released by synaptic terminals which transmit signals between nerve cells upon binding to their respective receptors. These substances are fundamental for chemical cell to cell interactions and for control and regulation of behavioural and physiological functions (7). Most of the neurotransmitters are monoamines (e.g. dopamine, serotonin, histamine and noradrenaline), but there are also neurotransmitters that are simple amino acids like γ-aminobutyric acid (GABA), glutamate, and glycine. Biogenic transmitters modulate activities requiring fast responses like for instance, the fight or flight response where noradrenalin in particular is prominent (8). As a result, they are also inactivated quickly by degrading enzymes or specific uptake transporters to prevent continuous activation. Usually, neurotransmitters are synthetized and stored in vesicles in the presynaptic neuron. The release of the transmitters comes as a response to an action potential that has travelled along the axon and led to the opening of voltage gated calcium channels in the nerve terminal. The calcium ions (Ca^{2+}) then cause these vesicles to fuse with the membrane and release its content in the synaptic cleft by exocytosis. Following release they bind to their appropriate receptors on the postsynaptic neuron where they can exhibit their functions by initiating cascades of secondary effects leading to their biological responses (9).

The driving force for this process is the action potential. An action potential is caused by temporary changes in membrane permeability for diffusible ions. Neurons are filled with ions and at the resting state there is an equilibrium between cations and anions on the inside and outside. Potassium ions (K^+) and sodium ions (Na^+) are unequally distributed on the inside and outside of the neuronal membrane. The outer side of the neuron has a higher concentration of Na^+ ions compared to the inside, while the inside of the neuron contains a higher concentration of K^+ ions than the outside. In total, the extracellular space is more positively charged than intracellular. However, the concentrations are dynamic which means that ions constantly are flowing in and out of the neuron in an attempt of equalizing the concentration gradient. Despite of the attempt, at the resting membrane potential, the distribution of ions yields a net negative charge around approximately -70mV on the inside relative to the exterior.

In the initial step of neuron activation, hypopolarization, a few ion channels are open which allows Na^+ ions to enter the nerve cell which then renders the intracellular space more positive and less negative. This leads to an increase in the membrane potential to around -55 mV which influences the opening of voltage-gated sodium channels that causes an influx of Na^+ ions. The influx of Na^+ ions further make the neuron electropositive to + 30 mv. After this point, repolarization occurs which then brings the cell closer to the previous resting potential. The voltage-gated sodium channels get inactivated while specific potassium channels are activated simultaneously. Opening of the potassium channels leads to efflux of K^+ ions from the neuron and the neuron once again loses positively charged ions and returns back to its resting state. Finally, hyperpolarization happens due to the delayed inactivation of potassium channels that still allows K^+ ions to exit from the neuron. This causes the membrane potential to go even lower than the initial potential. As the potassium channels begin to close, the resting state is also re-established, and the process is repeated (10).

Following synthesis of the respective biogenic amine transmitters in presynaptic neurons, the transmitters are loaded and stored in vesicles. An action potential arrives at the nerve terminal which promotes opening of calcium channels and finally release of neurotransmitters into the synaptic cleft by exocytosis. Henceforth, the neurotransmitters diffuse across the cleft and binds to the respective receptors postsynaptically, i.e., dopamine binds to dopamine receptors while serotonin binds to serotonergic receptors. When the neurotransmitter is bound to its receptor, it activates the receptor resulting in the biological effect. The actions of dopamine and serotonin in particular, are mostly terminated by reuptake back into surrounding cells by selective presynaptic transporters. The actions of acetylcholine on the other hand, are terminated by enzymatic degrading (11, 12). A summary of dopaminergic synaptic transmission in the nervous system is displayed in figure 2.

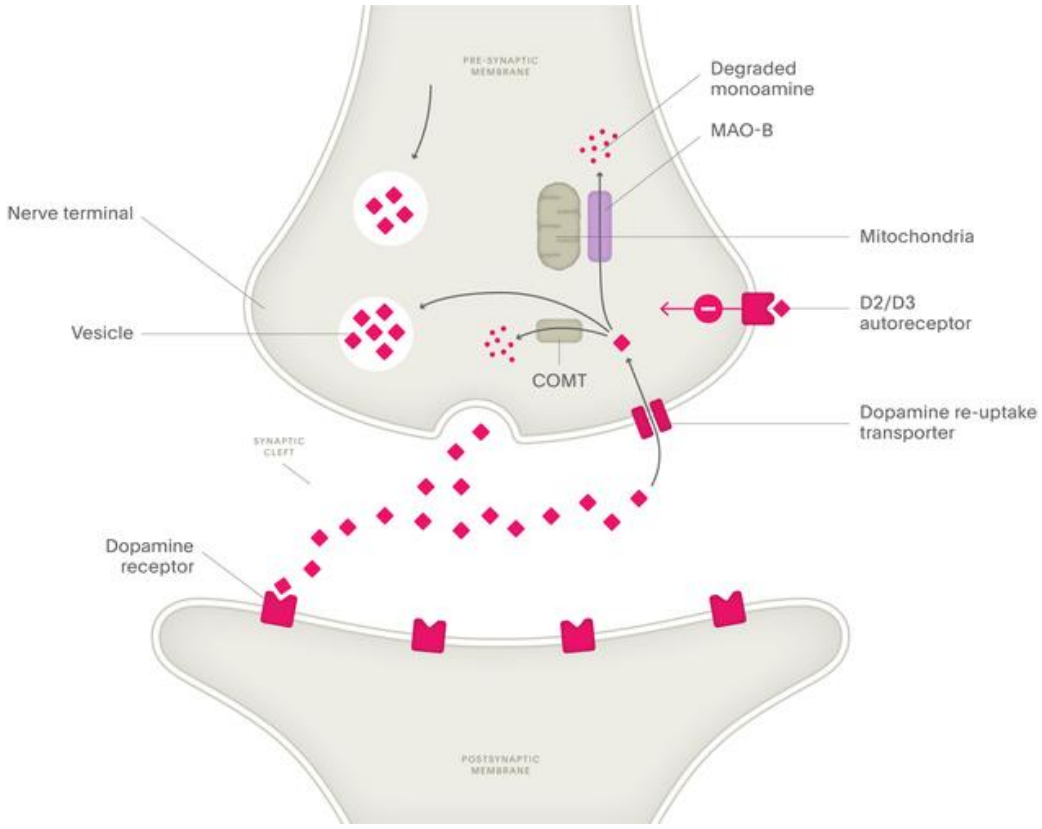

***Figure 2**: simplified illustration of the synaptic transmission in dopaminergic neurons. Dopamine (pink square) is released from the presynaptic terminal, diffuses over the synaptic cleft before it binds to and activates dopaminergic receptor (D_1-D_5). Dopamine is then taken up by transporters located presynaptically and finally broken down by enzymes such as catechol-O-methyltransferase (COMT) and monoamine oxidase B (MAO-B) (13).*

In this thesis the neurotransmitters dopamine and serotonin, also known as 5-hydroxytrypamine are of particular interest because they tightly interact. Moreover, imbalance and disruptions of mainly the dopamine systems are responsible for many disorders including psychosis, schizophrenia and Parkinson´s disease.

Supplementary, histamine for instance is also important due to the fact that some of the observed adverse effects of antipsychotic drugs are caused by unfavourable binding to histaminergic receptors and a subtype of serotonin receptors named the 5-HT_{2C} receptor. An earlier study (14) mentioned that obesity, diabetes and metabolic syndrome were prevalent comorbidities in schizophrenia patients especially those on treatment with antipsychotics. It also stated that antipsychotic drugs could impair metabolic regulation as these drugs are strongly associated with the core components of metabolic syndrome i.e., dyslipidaemia, hypercholesterolemia, weight gain and a lesser degree of hypertension.

1.4 Dopamine and serotonin

Dopamine is an essential neurotransmitter that is commonly studied for its role in physiological and cognitive functions including reward-based learning and movement but also disorders such as psychosis, Parkinson's disease and addiction (15). This neurotransmitter is a full agonist that naturally binds to and activate dopamine receptors (16).

In diseases like Parkinson's disease, it is especially the presynaptic substantia nigra neurons that are degenerated leading to impaired signalling between dopamine and dopamine receptors, resulting in dopamine deficiency in striatum. Consequences of dopamine deficiency can be psychiatric and movement pathologies. The main pathways of dopamine, and the locations of the dopamine receptors are defined as the mesolimbic, mesocortical, tubero-infundibular and nigrostriatal pathways and are all located within the central nervous system (17).

The mentioned pathways are responsible for different regulations where impaired signal transduction of any of these, results in positive or negative psychosis symptoms. The mesocortical and mesolimbic pathways are in control of phenomena like desire, pleasure, motivation and reward. For instance, when the mesolimbic system is hyperactive, it can result in positive psychosis symptoms like hallucinations and delusions. The nigrostriatal pathway is the pathway that rather controls and regulates motor function. Coordination of body movement through the skeletal system is mainly regulated via inputs from the substantia nigra to the major dopamine-containing area, corpus striatum. A clinically relevant example is in the pathology of Parkinson's disease where the dopaminergic neurons of substantia nigra degenerate leading to motor dysfunction symptoms like rigidity, tremor and bradykinesia. Secretion of the hormone prolactin is regulated from the anterior pituitary gland through the tubero-infundibular pathway. Situations where dopamine is not released properly or use of drugs such as antipsychotics that antagonize the dopamine D_2 receptor, can lead to hyperprolactinemia causing disruption of the menstrual cycle in women and abnormal lactation or breast formation in both genders.

The actions of dopamine are mediated by a family of G-protein-coupled receptors called dopamine receptors. This class of receptors constitutes 5 receptors and is further divided into D_1-like (D_1 and D_5) and D_2 like (D_2, D_3 and D_4) receptors. The dopamine D_2 receptor is of

particular interest in this thesis because it is the primary target for antipsychotic drugs. More on this is provided in later chapters.

Serotonin, 5-hydroxytryptamine (5-HT) is primarily found within the raphe region of the pons and in the upper brainstem. Neurons from these areas have widespread projections to the forebrain as well. Serotonin is commonly studied for its role in the headaches, sexual behaviours, circadian rhythms, emotions, mental arousal and emotions. Similarly to dopamine, impairments or disruptions of the serotonergic neurons have been implicated in various psychiatric disorders such as anxiety disorders, depression and in some cases schizophrenia (18). The actions of serotonin are mediated through serotonin 5-HT receptors which are expressed throughout both the central and peripheral nervous system. In total, there are 7 groups divided into 5-HT_1, 5-HT_2, 5-HT_3, 5-HT_4, 5-HT_5, 5-HT_6 and 5-HT_7 receptors. Only 5-HT_3 receptors are ligand gated ion channels while the rest are G-protein-coupled receptors. Further, the 5-HT_2 group of receptors consists of 5-HT_{2A}, 5-HT_{2B} and 5-HT_{2C} receptors that have similar ligand binding and signalling properties.

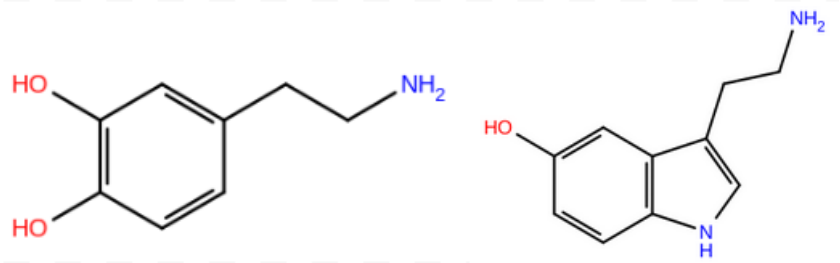

***Figure 3**: two-dimensional (2D) structures of the dopamine (left) and serotonin (right).*

1.4.1 Interplay between dopamine and serotonin

In previous papers (19-21) it has been described that the there is an interplay between serotonin and dopamine in the central nervous system. One of the mechanisms of the interplay, involves serotonin ability to inhibit dopamine production as we know that indeed, neurotransmitters do not act independently. Numerous studies have indicated that dopamine and serotonin system interact closely at synaptic levels (22-24), explaining that serotonin hypofunction or impairment may represent a biochemical trait that predisposes individuals to neurological diseases due to dopamine hyperfunction. Further, in the same review (20), it was

suggested that dysfunctional interactions between dopamine and serotonin systems perhaps is an important mechanism underlying the link between comorbid disorders and impulsive aggression. Consequently, impulsive behaviours among other CNS disorders, are undoubtably promoted by hyperactivity of the dopamine system as a result of a deficient serotonergic function. A modified stress model of impulsive aggression was proposed to further understand the interaction between the respective transmitters. Additionally, substance abuse associated with impulsive aggression is surely a result of dopamine dysregulation resulting from serotonergic deficiency.

Behaviours related to addictions and withdrawals are thought to be determined by the balance between the serotonin and dopamine, where dopamine is further thought to stimulate appetitive behaviours while serotonin promotes the opposite. This also explains some of the metabolic side effects patients treated with drugs interfering with the respective neurotransmitters experience. Some of these side effects include weight gain and increased cholesterol. The dopaminergic neurons receive serotonergic projections which also promote functional modulation of the terminals and cell bodies of dopamine neurons. More specifically, prior research (20) demonstrated that dopamine activity is inhibited by serotonin 5-HT_{2A} receptors.

1.5 Pathophysiology of psychiatric disorders

Neurological disorders are according to the world health organization (25) and other sources (26, 27) defined as diseases that affect both the central and peripheral nervous systems. Disorders that fall into this category can range from everything between migraines to Parkinson's disease, psychiatric disorders and multiple sclerosis. The world health organization further estimated in 2016 that neurological disorders and their consequences affected hundreds of millions of people worldwide and identified social discrimination and health inequalities such as wealth and power as major factors contributing to the associated disability and suffering (25).

Generally speaking, without differentiating between the various disorders, abnormalities in biochemical, structural and electrical system within the nervous system can result in a broad spectre of symptoms. Examples of symptoms include delirium, hallucinations, headache, pain

and altered levels of consciousness. Whilst the central nervous system is surrounded and protected by membranes, bones and isolated by the blood-brain barrier, it is still prone to damage or disruption if compromised.

Genetic disorders, infections, trauma, degeneration, environmental factors, lifestyle, health problems like malnutrition and even gluten sensitivity are among some of the proposed causes to neurological disorders (28). CNS issues may also be a result of injuries or problems in other parts of the human body as the whole body interacts with the nervous system. For example, problems with the cardiovascular system (blood vessels) that also supply the brain with blood, can lead to brain injuries due to insufficient blood supply.

Neurological disorders can be looked at as a tree. One of the branches from this tree, can be named psychiatric illnesses or mental disorders. Disorders in this category appear primarily as abnormalities of feelings, behaviour or thoughts like delusions, delirium, cognitive failure and hallucinations (27). In many cases, over time and depending on severity, these symptoms can produce distress or impairment of function. Examples of psychiatric disorders include psychosis, depressions, schizophrenia and anxiety disorders.

1.5.1 Schizophrenia

Psychoses such as schizophrenia are amongst the most severe mental illnesses and it often affects young people, is often chronic and is usually highly disabling (18). Schizophrenia is an example of a complex disorder that involves dysregulation and disruption of multiple pathways, especially dopaminergic systems. Deficits in acetylcholine muscarinic neurons and inflammation have been identified to play major roles in the development and exacerbation of schizophrenia. In addition, genetics are equally as important as there is a strong hereditary factor in the aetiology of schizophrenia (18).

The evidence suggestive features of schizophrenia mainly include what can be divided into cognitive, positive and negative symptoms (11). Positive symptoms are defined as symptoms that for instance are added to ones personality. Delusions, hallucinations, thought disorders, troubles with mobility and abnormal behaviours are amongst the most prominent positive symptoms. On the contrary, negative symptoms often reduces ones previous demeanour and

can include withdrawal from social contacts, reluctance to perform activities that once where fun, inability to experience pleasure and a reduction in emotional responses. The cognition aspect of schizophrenia often involves issues with memory and attention. Supplementary to the mentioned symptoms, anxiety, depression, and guilt are often present and in severe cases, some patients become suicidal (18).

A combination of genetic and environmental factors is believed to be the causes of schizophrenia. This is in view of the fact that a person may have a genetic trait that predisposes them for schizophrenia but exposure to certain environmental factors like viral infections, toxins or highly stressful situations are required for the disorder to develop (29). In addition to the genetics and environmental factors, there is a robust association with the neurochemical basis of schizophrenia because some of the affected genes control neuronal development, synaptic connectivity and neurotransmission. Different symptoms appear to be a result from malfunctions of different neuronal circuits. Decreased dopamine activity in the mesocortical pathway for example, is associated with negative symptoms while overactivation of dopamine receptors in the mesolimbic pathway is associated with positive symptoms (18).

In the medical field, preventative measures and rehabilitation in the form of therapy, pain management and in some situations, switching to a ketogenic diet are recommended and preferred. However, practicing this is extremely challenging so the introduction of medications to assist, is a quite common intervention. The class of medication used to treat many psychosis disorders including schizophrenia are called antipsychotics.

1.6 Antipsychotic drugs

Antipsychotic drugs, also named neuroleptics, are drugs used to treat and alleviate symptoms of psychotic disorders such as schizophrenia. Further, antipsychotic drugs are divided into typical or atypical, also known as first- and second-generation antipsychotics respectively. Typical antipsychotics (TAPs) work by antagonizing the dopamine D_2 receptor in all four dopamine pathways. In hyperactive mesolimbic pathways, the use of typical antipsychotics results in reduction in positive psychosis symptoms like hallucinations and delusion. Examples of substances in this class include haloperidol and chlorpromazine. In contrast to typical agents, atypical antipsychotics (AAPs) are weak D_2 receptor antagonists in addition to 5-HT_{2A} receptor antagonists. Risperidone, olanzapine, quetiapine and aripiprazole are among the most frequently used atypical antipsychotic drugs (30).

A ligand that works as a full agonist binds to its respective receptor and alters the receptor state which then results in a biological response. These ligands stabilize an active conformation of the receptor and increase receptor activity. A full agonist has in other words the capability of inducing a maximal response on its receptor. Contrarily, drugs that promote the antipsychotic effect mainly antagonize dopamine D_2 receptor activation and prevent dopamine from binding, also known as competitive dopamine D_2 receptor antagonism. Inverse agonists like risperidone stabilize an inactive state conformation of the receptor.

Further there are for instance D_2 receptor partial agonists that can modulate dopaminergic neurotransmission by producing the biological effect but at a much lower efficacy compared to a full agonist (31). A proposed mechanism explains that a partial agonist bind to the active site in a way that does not induce an ideal conformational change and receptor activation is therefore decreased (32). Alternatively, such pharmacologically active drugs don’t have the ability to elicit as large an effect, even at high concentrations so that all receptors would be occupied, as can a full agonist (33), figure 4.

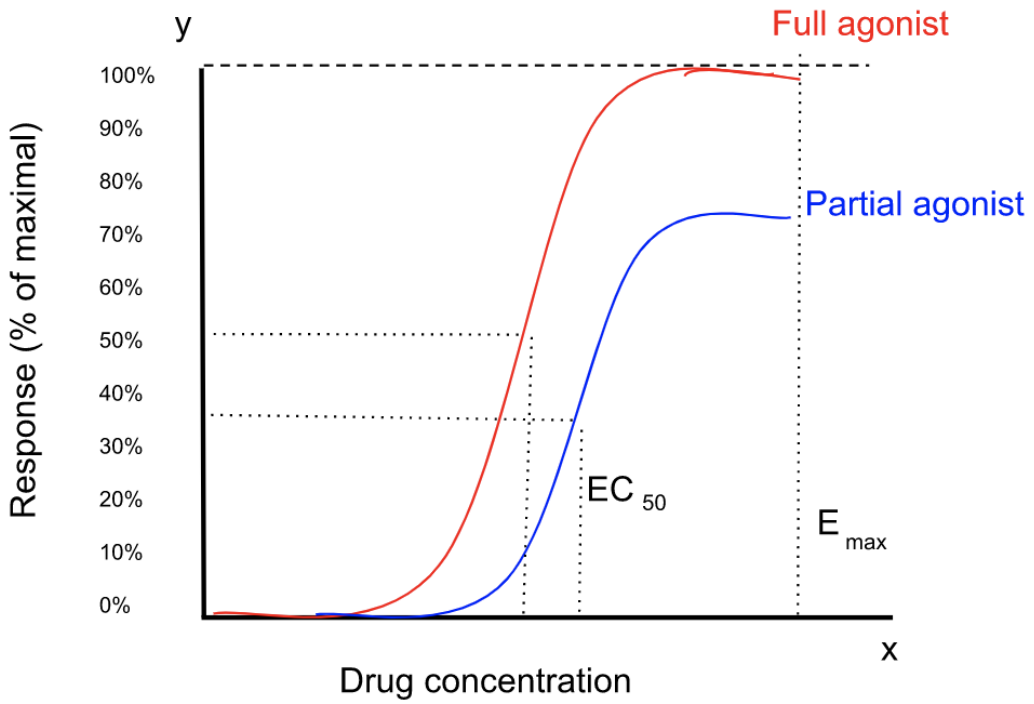

***Figure 4**: comparison between full agonist in red and partial agonist in blue. The half maximum effective concentrations EC_{50} and the maximum effective concentration E_{max} are marked with dotted lines.(34).*

Aripiprazole has a mechanism of action that is quite different from other antipsychotic drugs. It exerts its actions through partial agonism on both serotonin 5-HT_{1A} and dopamine D_2 receptors and also act as an antagonist on the serotonin 5-HT_{2A} receptor. Though aripiprazole was introduced in therapy over 15 years ago, the complexity of its action on signal transduction remains unresolved (35). Still new proposals in attempts to explain the mechanism of action of aripiprazole are presented, one of them which suggests that the term partial agonist is not sufficient. Rather, the conceptualization of this agent has shifted to "functional selectivity" referring to aripiprazole ability to display antagonistic and agonistic effects on dopamine D_2 receptor signalling pathways (35). It is suggested that aripiprazole may act as a agonist when dopamine concentrations are low and act as a antagonist when dopamine concentrations are elevated (36).

In clinical practice, the choice between using atypical or typical antipsychotics in treatment of patients is very complex and mostly dependent on the experience of the physician, the patients symptoms and conditions. Yet, there have been several studies (37-39) where the antipsychotics systematically have been compared in regards of clinical effect, tolerability, risk of side effects and quality of life. The conclusion from these studies was that atypical

antipsychotics such as olanzapine, risperidone and clozapine demonstrated a better outcome in aspects like improved pharmacological profile in reducing both negative and positive symptoms compared to typical antipsychotics (39). A portion of these results however, possibly owes to the absence/reduce in extrapyramidal symptoms which minimize the risk of developing secondary (negative) symptoms (40).

1.6.1 Unwanted effect of antipsychotic drugs

Unfortunately, many antipsychotic drugs produce serious and unacceptable side effects due to promiscuous activities against related receptors. Motor disturbances, collectively termed extrapyramidal side effects, include acute dystonia (involuntary movements like restlessness and muscle spasm), tremor and tardive dyskinesias and are among the main side effects antipsychotic drugs produce. Many of these extrapyramidal side effects are caused by dopamine D_2 receptor antagonism in the nigrostriatal pathway and is a common disadvantage of typical antipsychotics (11). In addition to antagonizing dopamine D_2 receptors, newer atypical agents concomitantly antagonize serotonin 5-HT_{2A} receptors which to some extent mitigates motor disturbances. It has been suggested that this is due to their differential binding kinetics and higher affinity for the 5-HT_{2A} receptor (41).

Apart from motor disturbances, endocrine, metabolic and sedating effects are commonly reported in patients treated with antipsychotic drugs. Abnormal breast growth in both genders, is a result of antagonism of dopamine D_2 receptors in the pituitary gland which again increase prolactin plasma concentration because dopamine inhibits prolactin secretion. Additionally, hyperprolactinemia is sometimes accompanied with estradiol reduction in women which could lead to increased appetite (18). Both TAPs and AAPs can disrupt metabolic regulation both in the central- and peripheral organs by activating the hunger centers and inhibiting satiety sensation. For instance, lipid and glucose metabolism in the liver can become impaired with weight gain leading to obesity. Results of this include increased risk of diabetes and cardiovascular diseases (30, 42).

On a molecular level, the mentioned adverse effects of antipsychotics stem from interactions with various receptors such as dopamine D_2, histaminergic H_1, α_1 adrenergic, serotonin 5-$HT_{2A/2C}$ and acetylcholine M_1/M_3 muscarinic receptors (32). Altered dopaminergic signalling

is a ubiquitous contributor to metabolic effects partially because dopamine regulates feeding behaviour. Overconsumption of palatable food seem to decrease dopamine D_2 signalling because the reward system adapts. This means that dopamine depletion could induce overeating. Serotonin modulates peripheral metabolism and circadian rhythms among others (43, 44). Additional antagonism of serotonin 5-HT_{2A} and 5-HT_{2C} receptors could induce hunger and increase food intake promoting weight gain. By altering serotonergic efflux in different brain regions, antipsychotic drugs can disturb serotonergic regulation of metabolic homeostasis and contribute to metabolic effects like increased glucose-dependent insulin secretion (45).

Drowsiness, sedation, dizziness, dry mouth and headaches are more examples of common adverse effects that many patients experience, again due to the fact that more antipsychotic drug are not fully selective and limited to specific receptors, hence they interfere with several molecular systems (11).

Finally, agranulocytosis and neutropenia are rare, yet severe adverse effects that are seen more frequently with clozapine (AAP) compared to other antipsychotic drugs in the same class and compared to conventional antipsychotics (11, 18). These adverse effects are reversible upon promptly withdrawal and are estimated to occur in 1-2 percent of patients treated with clozapine (32). Both agranulocytosis and neutropenia can be fatal and therefore require regularly hematologic monitoring. In refractory schizophrenia and treatment-resistant psychoses, clozapine is considered the gold standard, so the associated adverse effects are important reasons to find new effective agents devoid of severe side effects (46, 47).

1.7 G-protein-coupled receptors

GPCRs, which stands for G-protein-coupled receptors, form a large group of membrane-bound receptors that mediate cellular responses in response to activation by ligands such as neurotransmitters, proteins, neuropeptides, ions, lipids, nucleotides and hormones. More than 800 human GPCR sequences have been identified and they are categorized into six classes A to F, based on function and amino acid sequence (48). Class A GPCRs, also known as rhodopsin-like receptors, accounts for the largest and most diverse class of GPCRs found in humans (49). The architecture of class A is quite simple and both the ligand binding site and binding site of G-protein is located in the 7TM domain (seven transmembrane). The endogenous ligands on class A GPCRs include most biogenic amine neurotransmitters (such as histamine, dopamine, noradrenaline, histamine and serotonin), purines, cannabinoids and hormones among others (18). Class B GPCRs, also called the secretin and adhesion family, are mainly activated by peptides and hormones like glucagon, secretin and incretins. These receptors are characterized by their long amino-terminals and are important drug targets in diseases such as diabetes, psychiatric disorders and osteoporosis (50). Ligands are mainly recognized by a binding site in the extracellular domain and an additional binding site is found within the 7TM domain (51).

Metabotropic glutamate and $GABA_B$ receptors are examples of Class C GPCRs which are the receptors for the inhibitory and excitatory neurotransmitters GABA and glutamate respectively. In contrast to class A receptors, the orthosteric binding site in class C GPCRs is situated in an amino-terminal Venus flytrap domain which consist of two distinct lobes that close around the ligand (48). The allosteric site is located deep into the 7TM domain (52). Further, class D GPCRs – fungal mating pheromone receptors and class E being cAMP receptors, don't exist in humans and are believed to have many structural differences compared to class A GPCRs. One of these differences is that the highly conserved disulphide bond established between Cys(ECL2) and Cys(3.25) is not found in class D GPCRs (53). Finally, lipoglycoprotein Wnt is the endogenous ligand of class F frizzled/smoothened receptors. Class F receptors possess a long amino-terminal domain that is rich in cysteine residues and also holds the ligand binding site (48).

Common for all classes of GPCRs, is that they consist of seven hydrophobic transmembrane (TM) helices linked by three intracellular and three extracellular loops. The 7TM helices are

embedded within the membrane and forms a cavity that resembles a barrel. On the intracellular side is a carboxyl terminal (C-terminal) and an amino terminal (N-terminal) is located on the extracellular side. Both the C- and the N- terminal of the receptors are believed to be the most variable (54). Relevant for this project are dopamine D_2 and serotonin 5-$HT_{2A/2C}$ receptors which are classified as class A GPCRs.

1.7.1 Structure of class A GPCRs

Class A GPCRs share a common structural signature which consist of a heptahelical transmembrane domain. This domain is connected by three intracellular (ICL) and three extracellular loops (ECL) that are important for receptor function because they provide structure to the extracellular region, mediate movement of the helices and contribute to protein folding. The second extracellular loop, ECL2 in particular, has been known to be of significance for ligand binding as well as receptor activation (55-57).

Some parts of the GPCRs are more conserved among the diverse family of GPCRs and the residues that are important for transduction of the signal from the agonist binding site to the G-protein are conserved (49). The most variable segments, however, are the terminuses, both the amino and carboxyl terminus. In addition, great diversity is also observed for the intracellular loop (ICL3) between TM5 and TM6 (54). Monoaminergic class A GPCRs such as dopamine, serotonin and histamine receptors, have a disulphide bridge that constrains the ECL2 on top of the orthosteric binding site. Position identifiers based on the Ballesteros-Weinstein numbering scheme are used throughout this thesis to easily identify corresponding residues across class A GPCRs (58). In the dopamine D_2 receptor, two conserved residues Asn186(5.35) and Ile184(ECL2) are engaged in interactions with ligands and other residues in the binding site (59).

Aspartic acid residue 3.32 in TM3 is conserved among biogenic amine receptors and provides a strong salt bridge interaction with protonated amine in ligands. Other important residues that are as conserved are mentioned in later chapters. The binding site for the G-protein is located on the intracellular side and involves the carboxyl terminus. The most conserved regions of class A GPCRs can be summarized in the microswitch motifs CWxP, PIF, Na^+ pocket, NPxxY and DRY where the letters of the motifs stand for the residues and “x”

denotes any residue. For instance, CWxP (Cys, Trp, Pro) is situated in TM6, the PIF motif (Pro, Ile, Phe) combines TM5, TM6 and TM3, DRY (Asp, Arg, Tyr) and NPxxY (Asn, Pro, Tyr) motifs are located in TM3 and TM7 respectively (49). The NPxxY motif is known as the activation switch that moves inward during activation of the receptor. The ionic lock is a molecular switch formed between the highly conserved amino acids Arg(3.50) and Glu/Asp(6.50) from the D/ERY motif. In the inactive state of the receptor, the ionic lock is established (ionic interaction between mentioned amino acids) while the ionic lock is broken upon activation of the receptor as a result of outward movement of TM6 that allows for the binding of a G-protein (60).

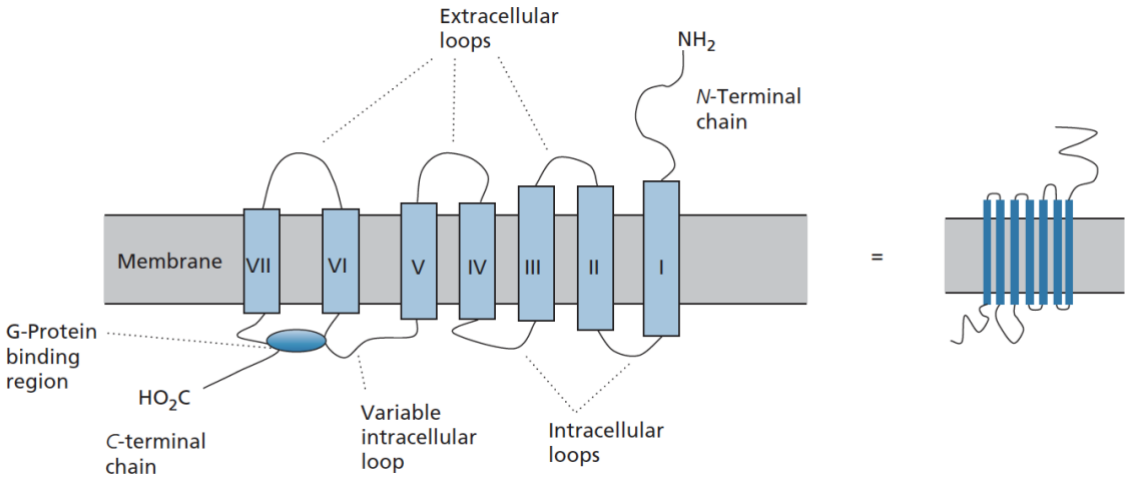

Figure 5: *simplified illustration of class A GPCR (31).*

1.7.2 Activation of class A GPCRs

For class A GPCRs, the binding site for endogenous ligands is formed between the seven transmembrane helices accessible from the extracellular surface. An additional binding site located on the inner surface of the receptor, opens up for the binding of a G-protein upon binding of endogenous ligands in the primary binding site. Binding of a ligand to the receptor induces conformational changes in the GPCRs which results in the binding of either GTP-binding proteins or the adaptor proteins called arrestins.

G-proteins consisting of three heteromeric subunits (α, β and γ) are anchored to the membrane through attached lipid residues. Coupling of α-subunit to the receptor causes the bound guanosine diphosphate (GDP) to be replaced by guanosine triphosphate (GTP). The α-GTP complex then dissociates from the β-γ complex and further interacts with effector proteins such as adenylyl cyclase or phospholipase C, resulting in either increased or decreased level of secondary messengers and ions which ultimately produce the cellular response (18).

Conformational change in the associated G-protein, triggers the release of GDP from the α-subunit, which is then replaced by GTP, as a result of receptor activation. This leads to that the α-GTP complex dissociates from the β-γ subunits and binds to a target enzyme or ion channel which then in return promotes inhibition or activation. The β-γ complex also mediates effects by stimulating or inhibiting effector proteins like ion channels and kinases. The G-protein is returned to inactive state within a short period of time as the α-subunit reassociate with the β-γ subunits. Adenylyl cyclase, an enzyme that catalyse the conversion of ATP to cAMP (cyclic AMP), is either activated by G_s protein or inhibited by the G_i protein. Upon activation, cAMP further activates protein kinase A by triggering the dissociation of regulatory subunits (α,β and γ) from the catalytic subunit. The catalytic subunits stimulate other target proteins through phosphorylation which then trigger the cellular response. A GPCR coupled to a G_i protein, which inhibits adenylyl cyclase, counteracts the actions of a GPCR coupled to G_s. Ultimately, the magnitude of the cellular response is proportional to the concentration of cAMP. Reduction in cAMP concentrations through active export or simultaneous enzymatic degradation result in the termination of the signal.

Another activation route for which GPCRs exert its action, involves the PI-PLC (Phosphatidylinositol phospholipase C) pathway. In this case the receptor is coupled to a G_q protein which activates the production of the secondary messengers DAG (diacylglycerol) and IP_3 (inositol triphosphate). DAG is lipid soluble and remains in the membrane. IP_3 on the other hand is water soluble and therefore diffuses into the cytoplasm where it triggers the release of calcium from intracellular storages. Released calcium can further bind to several intracellular proteins that through phosphorylation, stimulate a broad range of specific kinases among other (11). Figure 6 presents a summary of the activation mechanisms of GPCR.

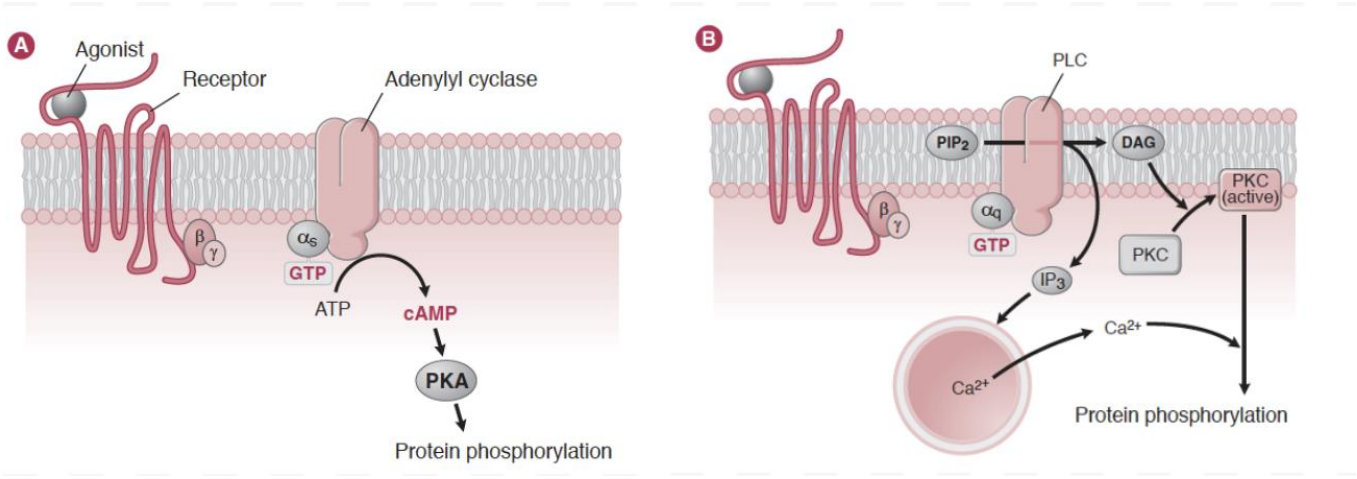

***Figure 6**: activation mechanism of GPCR (13).*

The other signalling pathway that can be activated and mediated through GPCRs, involves the binding of arrestins which functions to silence GPCR signalling and induce receptor internalization (61). In order for an arrestin to bind to the GPCRs, the receptors have to be phosphorylated by certain kinases before arrestins then can activate their own signalling independent of G-protein. This includes activation effector proteins that regulate cellular proliferation, apoptosis and differentiation. Receptor internalisation occurs through arrestin coupling and the receptor can then be dephosphorylated and reinserted into membrane. Alternatively, the receptors can be brought into lysosomes for degradation as an effect of arrestin binding (18). Regarding the structure of arrestins, a structural study revealed that arrestins are elongated molecules consisting of two domains with large N- and C-terminals (62). Interestingly, some ligands have been identified to favour one signalling pathway over the other in a concept known as biased signalling or functional selectivity. This means that certain ligand-receptor complexes (on the same receptor) preferentially signal through either

the arrestin or G-protein pathway with distinct efficacies and potencies which ultimately have distinct functional consequences (63).

1.7.3 Dopamine receptors

Human dopamine receptors, are mainly found within the central nervous system and especially expressed in the striatum, substantia nigra, hypothalamus, cortical areas, amygdalae and hippocampus (32). Dopaminergic neurotransmission have important roles in emotions, learning ability, addiction and the reward. The human dopamine receptors are class A GPCRs and also main targets for antipsychotic drugs. Imbalance of dopamine concentration in the CNS has been shown to be an important factor in disorders such as addiction, Parkinson's disease, bipolar disorder and schizophrenia (15).

The essential actions of dopamine are mediated by dopamine D_1-D_5 receptors which are closely related, have overlapping functions and pharmacology as well as conserved key residues (64). However, dopamine D_1 and D_5 receptor are located on both the pre-and post-synaptic neurons while dopamine D_2-D_4 receptors predominantly are located post-synaptically (65). An overview table of dopamine receptors is provided in supplementary material. Further, focusing on the dopamine D_2 receptor due to the fact that it is the most relevant in this thesis, it is interesting to notice that there are two isoforms of this receptor named D_2S (short) and D_2L (long). The short version is distributed in the mesencephalon and hypothalamus regions whereas the long type is mainly present in the striatum (66).

According to earlier publications (64, 67), the predicted binding site for agonists in the dopamine D_2 receptor is formed within the most hydrophobic segments of the seven membrane-spanning helices TM3, TM4, TM5 and TM6. The binding site crevice is extending from the extracellular surface of the receptor into the transmembrane domain in addition to this crevice being water accessible. Thus, the binding site is accessible to water soluble agonists like dopamine. Some of the conserved features in class A GPCRs, like the dopamine D_2 receptor that contribute to agonist binding, firstly include an electrostatic interaction between aspartic acid (Asp114(3.32)) in the third transmembrane (TM3) and protonated amine of the ligand. Secondly, serines in TM5 (Ser5.43, Ser5.42 and Ser5.46), form hydrogen bonds with polar atoms of the ligand while the hydrophobic aromatic cluster present in TM6

interact with aromatic features of the ligand (68). Another interesting feature especially observed in the dopamine D_2 receptor, is a hydrophobic pocket for antagonist located in TM7 and lastly the second extracellular loop which includes Ile184(ECL2) and Ile183(ECL2).

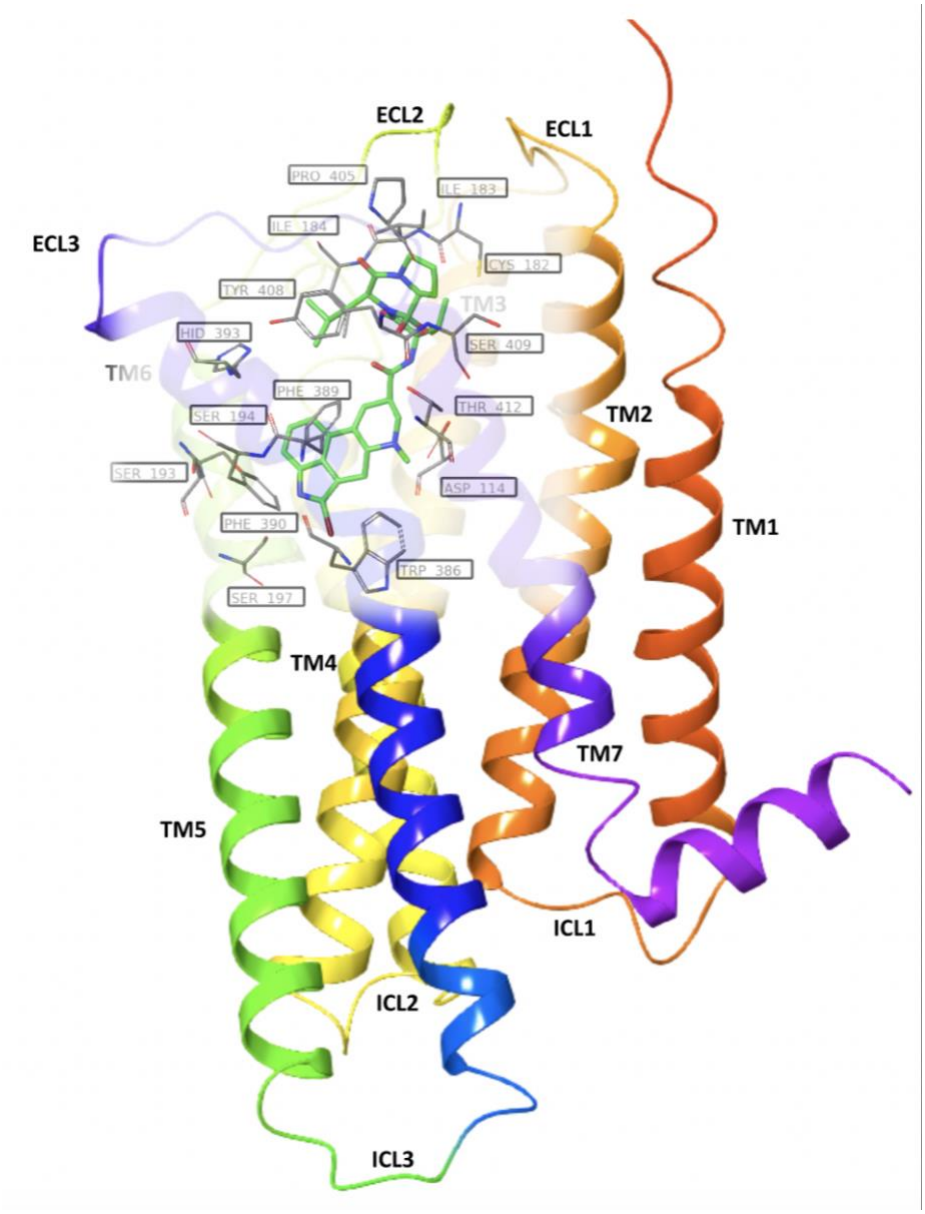

***Figure 7**: three-dimensional (3D) structure of the dopamine D_2 receptor. Agonist bromocriptine (green sticks) is bound in the ligand binding site and binding site residues are shown in gray with labels. Structure is based on information from the protein data bank (69).*

1.7.4 Serotonin receptors

Here we are focusing on the receptor subtypes of the serotonin 5-HT_2 class, serotonin 5-HT_{2A} receptor and 5-HT_{2C} receptor. Serotonin has been implicated in the pathogenesis of depression. It is a fact that suicidal and depressed patients have a depletion in the levels of serotonin and other monoamine neurotransmitters in the CNS compared to normal individuals which means serotonin concentrations in these patients are inadequate (70). The goal of antidepressant therefore is to increase the concentrations of monoamines, serotonin and/or noradrenaline in the synaptic cleft to further increase the biological functions e.g., through inhibiting reuptake of monoamines.

Uniformly to dopamine receptors, serotonin 5-HT_{2A} and 5-HT_{2C} are class A GPCRs and consist of seven transmembrane helices with one intracellular amphipathic helix 8 in the C-terminus. Both serotonin 5-HT_{2A} and 5-HT_{2C} receptors are densely distributed in cortex, however 5-HT_{2C} receptors are in addition found in limbic regions such as the hippocampus and striatum. The connection between serotonin and dopamine was explained in detail in previous chapters. Though other neurotransmitters like GABA and glutamate are involved, here we are narrowing it down to only concern dopamine and serotonin. In contrast to dopamine D_2 receptors, serotonin 5-HT_{2A}/5-HT_{2C} receptors are coupled to the G_q-protein and PI-PLC pathway. This pathway stimulates a cascade of events involving secondary messengers DAG and IP_3 which in turn activates protein kinase C and calcium release (11, 71). An overview table showing the classification and subtypes of the serotonin receptor is added in the supplementary material.

A relatively new atypical antipsychotic agent that was approved by FDA in 2016 called pimavanserin, acts as a selective antagonist/inverse agonist at the serotonin 5-HT_{2A} receptor which is distinct compared to conventional antipsychotic drugs. Currently it is only approved for treatment of Parkinson's disease psychosis and was proved to be well tolerated as monotherapy providing significant evidence for the relevance of 5-HT_{2A} and 5-HT_{2C} receptors in the treatment of psychotic symptoms.

It was pointed out in Kimura et al 2019 (44) that one of the most important features in the 5-HT_{2A} receptors include a side-extended cavity near the orthosteric site where antagonists selectively bind. This is located between TM4 and TM5 and adjacent to Asp155(3.32) which

is a strictly conserved residue essential for the interactions with ligands. In the 5-HT_{2C} receptor, this equals to Asp134(3.32). A hydrophobic cleft in the bottom of the ligand-binding pocket made up of highly conserved aromatic and hydrophobic amino acids like isoleucine(3.40), phenylalanine(5.47) and tryptophan(6.48), is another important feature that both the 5-HT_{2A} and 5-HT_{2C} exhibit. Correspondingly to the important features of the binding of drugs to the dopamine D_2 receptor, the protonated amine on pimavanserin establish a salt bridge with Asp155(3.32) in the serotonin 5-HT_{2A} receptor in addition to hydrophobic interactions with a hydrophobic cluster made up of Phe243(5.47), Phe332(6.44), Trp336(6.48) and Ile163(3.40) (44).

1.8 Computational methods

Computational methods and molecular modelling are terms used interchangeably and are a collection of various computer-based techniques applied for representation and manipulation of three-dimensional structures to relate them to their biological activity (31). Hence, these scientific methods are used to create logical assumptions that can be demonstrated in mathematical equations to facilitate reasonable predictions. Examples of some computational methods include virtual screening, induced fit docking (IFD) and molecular dynamic (MD) simulations. Applied in drug discovery, computational methods like IFD and especially MD simulations, have indeed proven to accelerate and reduce the immense cost, risk and time it takes to develop a new drug (72). In this thesis, these methods are utilized to examine interactions between antipsychotic drugs and the D_2 and 5-HT_{2A} receptors.

1.8.1 Induced fit docking and scoring

Induced fit docking (IFD) was one of the two computational methods that were most relevant in this project. In standard docking studies, ligands are placed or docked into binding sites of rigid receptors while the ligand itself moves freely. However, using static structures can lead to incomplete information especially since GPCRs are highly flexible and undergo dynamic changes upon ligand binding. Therefore, the main application of IFD was generating accurate complex structures for ligands that are antipsychotic drugs. Such methods allowed the receptor or target molecule to alter its conformation and shape of e.g., the binding site to better accommodate the ligand. Thus, producing all possible conformations (also referred to as poses) of the protein-ligand complexes that resemble biological systems. The scoring step in this process calculates the theoretical binding energy or affinities between the ligand and the target and further provides a docking score value for each of the poses which can be ranked from low to high (73). The binding energy, also known as Gibbs free energy (ΔG) is composed of enthalpic (ΔH) and entropic (ΔS) contributions summarized in following equation: $\Delta G = \Delta H - T\Delta S$ where T stands for temperature in kelvin.

1.8.2 Molecular dynamics simulations

The other computational method used was molecular dynamic (MD) simulations. MD simulations were applied to explore and account for macroscopic properties of several systems through calculation of energies, geometry, ligand binding, creating minimized structures and conformations. The main advantage with MD simulations is that it provides the means to very accurately solve equations of dynamic particles and capture the behaviours of biological systems over time in full atomistic detail with high resolution (72, 74). Further, it provides an insight into mechanisms and processes that would be time consuming, costly and complicated to investigate using traditional laboratory experimental studies. However, applying this method does not replace the need for traditional in vitro experiments in the laboratory, but it tremendously improves and simplifies the process.

1.8.3 Energy minimalization and force field

When utilizing computational methods, it is desired to find the arrangement of the ligand in the binding site with the lowest energy, hence the conformation with minimal energy strain. This process is called energy minimalization and helps to find the most stable conformation of the protein-ligand complex because it happens that during the construction process of the complex that i.e., steric hindrance, clashes, unfavourable bond angles and length arise (31). This will have a huge negative impact on the overall energy of the entire system. Following an energy minimalization, all unfavourable bonds are altered, and the system become more energetically stable (74).

For both the induced fit docking, scoring and the MD simulations, force fields were used to estimate the interacting energy between atoms and molecules in addition to calculating the potential energy of the systems. Force fields are used to describe the interactions within a molecule (intramolecular interactions) and the interactions that occur between molecules such as a ligand and its target (intermolecular interactions) (75). They consist of a set of potential energy formulas that include parameters that take both bonded, covalent atomic interactions, angle bending, bond stretching and nonbonded (non-covalent), van der Waals, electrostatic and hydrogen bonding interactions into account (76).

2 Aim

The Norwegian prescription database (77) revealed that a total of 131000 patients in all age groups and both genders had dispensed antipsychotic medications from Norwegian pharmacies in 2019. By roughly estimation in a population consisting of approximately 5,000,000 inhabitants, close to 3% of the Norwegian population had prescription on antipsychotic medications this year. The most commonly prescribed antipsychotics according to the prescription database, included levomepromazine, prochlorperazine, quetiapine, olanzapine, aripiprazole and risperidone. Further, pimavanserin (currently only available in USA) is the only non-dopaminergic antipsychotic as it performs its action through selective antagonism on the serotonin 5-HT_{2A} receptor. The previously mentioned antipsychotics on the other hand, exert their actions through antagonism mainly on the dopamine D_2 receptor, but also on the serotonin 5-HT_{2A} receptor.

The aim of this study is therefore to understand the structural mechanisms for which the most commonly prescribed antipsychotics act by and also get a deeper insight into putative structural mechanism that may explain how and why many patients experience certain serious adverse effects upon use. Interactions between ligands and respective targets are being investigated to comprehend how the desired effect is achieved but also to understand how the undesired adverse effects like sedation, weight gain, hormonal disturbance and motor dysfunction occurs. Additional aims included achieving more comprehensive understanding and training in the use of computational methods, especially IFD and MD simulations.

3 Methods

3.1 Software package

3.1.1 Schrödinger Maestro (release 2021-1)

Computational methods were utilized to investigate protein-ligand interactions and perform molecular dynamic calculations. The software package that was used was Schrödinger Maestro (Schrödinger release 2021-1) which is the graphical user interface and includes several programs that were used to create the antipsychotics drug, prepare the drugs (LigPrep), prepare the protein structures (Protein Preparation Wizard) and dock the drugs (Induced Fit Docking) into binding sites in structures of biogenic amine receptors. Additionally, Desmond (Schrödinger release 2021-1) from the same software was used to run high-performance molecular dynamic simulations.

3.2 Databases

3.2.1 The Protein Data bank

The protein structures of the receptors were retrieved from the Protein Data Bank (PDB) which is a resource that provides information about the three-dimensional shapes of proteins (78). The respective files from PDB were **6VMS** (69) – structure of dopamine D2 receptor G-protein complex in a lipid membrane with the agonist bromocriptine, **6CM4** (79) - structure of dopamine D_2 receptor bound to antagonist risperidone, **3RZE** (80)- human histamine H_1 receptor in complex with antagonist doxepin, **6A93** (81) - serotonin 5-HT_{2A} receptor in complex with antagonist risperidone and lastly **6BQH** (82) - serotonin 5-HT_{2C} receptor in complex with the antagonist ritanserin. There was no need of homology models due to the fact that all protein structures of interest, were already solved and accessible in the Protein Data Bank. The datafiles from PDB for 6CM4, 3RZE,6BQH and 6A93 have been solved using x-ray crystallography and had resolutions on 2.87 Å, 3.10 Å, 2.70 Å and 3.00 Å respectively. 6VMS on the other hand, was solved with cryo electron microscopy with 3.80 Å in resolution.

3.2.2 Orientations of Proteins in Membranes

OPM, Orientations of Proteins in Membranes, is a database that was used to optimize the spatial arrangement of the receptor transmembranes in lipid bilayers based on the PDB files (83). In the present study, the files that were downloaded from this database included 6VMS, 6CM4 and 6A93.

3.2.3 Psychoactive Drug Screening Programme

Another useful database was The PDSP (Psychoactive Drug Screening Programme) K_i database which provided information about antipsychotic drugs and their published binding affinities (K_i value) on different target molecules such as GPCRs (84). The K_i values for all 37 antipsychotic drugs that were docked, were obtained from The PDSP K_i database with some exceptions as explained in later chapters. Finally, computational methods in the form of IFD calculations and MD simulations were the main methods utilized in this thesis**.**

3.3 Induced Fit Docking

First step in the process was to set up the three-dimensional (3D) structures of the drugs. The structures of 37 established antipsychotic drugs (approved for treatment of psychosis and pimavanserin approved for treatment of psychosis in patients with Parkinson's disease in U.S) were created in Maestro based on their SMILES codes and further prepared using the ligand preparation module LigpPrep (Schrödinger release 2021-1). The following antipsychotic drugs were created: Fluphenazine, Risperidone, Paliperidone, Pimozide, Amisulpride, Brexpiprazole, Sulpiride, Ziprasidone, Sertindole, Haloperidole, Droperidole, Iloperidone, Pimavanserin, Perospirone, Zuclopenthioxol, Zotepine, Lurasidone, Mesoridazine, Cariprazine, Asenapine, Pipotiazine, Chlorprothiexene, Flupentixole, Thioridazine, Chlorpromazine, Thiothiexene, Aripiprazole, Prochlorperazine, Perphenazine, Clozapine, Quetiapine, Levomepromazine, Loxapine, Olanzapine, Trifluoperzine and Cyamemazine.

The two-dimensional (2D) structures of the drugs are presented in figure 8. After running this preparation in physiological pH 7.0 +/- 2.0, all drugs gained a positive charge that was crucial for interaction with an aspartic acid residue in transmembrane helix 3, Asp(3.32) that is conserved among biogenic amine receptors. This application generated low-energy 3D structures of the antipsychotics based on their 2D structure with correct chirality, conformations, stereochemistry and ionization state. The force field used to estimate the forces and prepare the ligands in IFD was OPLS3e which stands for optimized potentials for liquid simulations (85).

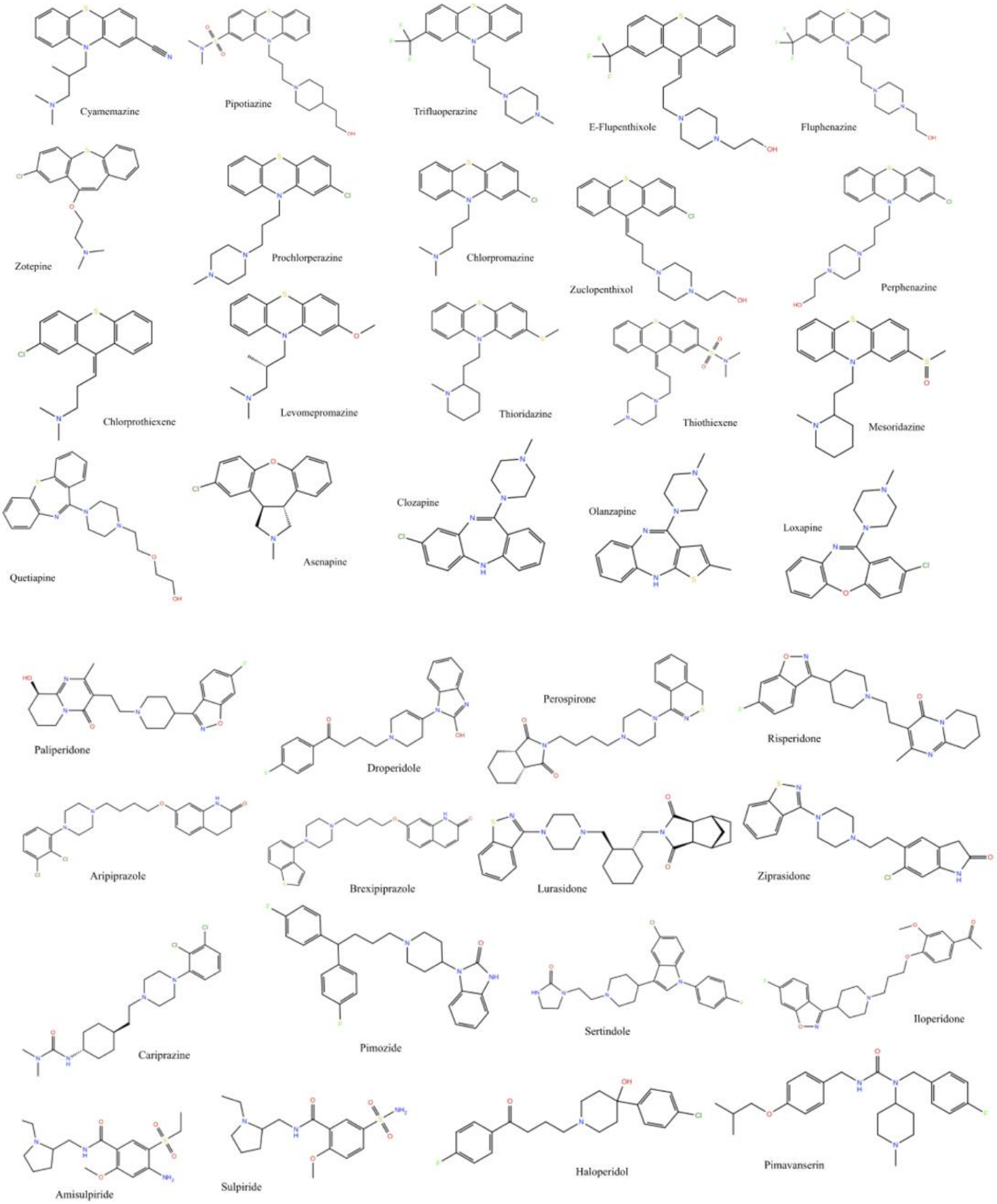

Figure 8: *two-dimensional (2D) chemical structures of the 37 antipsychotic drugs docked*

3.3.1 Protein preparation and induced fit docking calculations

All 37 established drugs were docked using induced fit docking (IFD) based on the IFD protocol (86). IFD was implemented to accurately fit and predict most favourable conformation of ligand-protein complex. The receptors were run through protein preparation wizard (Schrödinger release 2021-1) (87) with the purpose of locating and fixing structural defects in the imported protein structure and thereby preparing them for use. This included adding missing loops and hydrogen atoms, correcting charge states and conformations. The workspace was then analysed and unnecessary molecules such as cholesterol, palmitic acid, pentaethylene glycol, oleic acid and dihydroxyethylether were removed from the protein structures.

To make sure that all poses/conformations had the most desired interactions (i.e., those involving protonated amino group in drug and an Asp residue in transmembrane helix 3, (Asp3.32), constraints were used to run the IFD. The exact constraints that were used, are shown in figure 1 in the supplementary material. In addition to the constraints, a grid was generated to specify the binding site by choosing the aspartic acid (3.32) in transmembrane helix 3 of the receptor as the centre and the docking box. In order to be able to identify corresponding residues across class A GPCRs, position identifiers have been used according to the Ballesteros-Weinstein numbering scheme (58). According to this numbering scheme, residues within the TM helices are numbered relative to the most highly conserved residue within each residue that is given the number 50. The first number denotes the helix (1-7) while the second number indicates its position relative to the most conserved position in that helix. In Asp(3.32), this means that the residue is located in TM3, 18 positions N-terminal of the most conserved residue. In all GPCRs within class A, the position identification is the same while the receptor sequences vary. Asp(3.32) equals to Asp114 in the dopamine D_2 receptor and Asp155 in the serotonin 5-HT_{2A} receptor.

The maximum box size used for docking was 20 angstroms in each direction (20 $Å^3$). The advantage of using IFD compared to conventional glide docking is that IFD provides both ligand and protein flexibility and is thus more realistic. The best poses, those that were energetically favourable, were chosen based on mainly docking scores. Lastly, the induced fit docking processes were run on 12 central processing units (CPU´s).

3.4 Molecular Dynamics simulation

MD simulations were performed to analyse the physical motions of drugs and receptors at atomistic and molecular levels, but also gain detailed information about fluctuations. In short, MD simulations were used to investigate the structure and dynamical behaviours in biological environments. This computational method was used to properly understand how different types of antipsychotic drugs interact with several amine receptors by inducing conformational changes into the receptor structure during MD simulations. Bromocriptine - a D_2 agonist, risperidone - a D_2 antagonist, aripiprazole - a D_2 partial agonist and pimavanserin – a 5-HT_{2A} antagonist were used to compare how their mechanisms of actions affect the structure of the dopamine D_2 and serotonin 5-HT_{2A} receptors. Since there were no PDB files for pimavanserin in the serotonin 5-HT_{2A} receptor, pimavanserin was docked into this receptor structure using PDB file of the 5-HT_{2A} (PDB: 6A93), after removing risperidone. Besides the mentioned ligand-bound complexes, three ligand-free systems were constructed to further study and compare the influence of the ligands on the dynamic profiles (structural motions) of the receptors. This was done by removing the ligand from the D_2 agonist protein (PDB: 6VMS), D_2 antagonist protein (PDB: 6CM4) and 5-HT_{2A} antagonist protein (PDB: 6A93).

MD simulations of the systems were performed using the 2020-4 release of the Desmond module in the Schrödinger software. To successfully run the simulations, the Desmond protocol (75) was implemented and run on a single graphics processor (GPU).

3.4.1 Constructing the systems

The PDB file 6VMS (69) – structure of dopamine D_2 receptor G-protein complex in a lipid membrane with bromocriptine was used as a starting point because the ligand bromocriptine was already bound to the system in addition to a G-protein complex. The system consisted of chain A (guanine nucleotide-binding protein G_i subunit alpha-1), chain B (guanine nucleotide-binding protein $G_i/G_s/G_t$ subunit beta-1), chain C (guanine nucleotide-binding protein $G_i/G_s/G_o$ subunit gamma-2), chain E (svFv16 single chain antibody) and chain R (dopamine D_2 receptor). During protein preparation chain E was removed since the antibody

is only present to stabilize the receptor structure during crystallization without interfering with ligand binding.

Before running the MD simulations, all systems were prepared with the protein preparation wizard like described in earlier sections. After preprocessing, unnecessary molecules such as cholesterol, palmitic acid, pentaethylene glycol, oleic acid and dihydroxyethylether were removed from the protein structures and only ligand remained. However, when preparing the dopamine D_2 receptor for MD with risperidone without the G-protein (PDB: 6CM4), there were still missing loops in the structure after running the protein preparation, that manually had to be corrected. This was done by implementing the crosslinker protein panel (88). Utilizing this panel, it was assumed that the missing loops were not included in the sequence (because it failed to fill in the missing loops with protein preparation wizard several times) so that the "loose ends" could be cross-linked. This was quickly performed by defining the attachment points on both ends of the structure, defining the monomer set and multi-residue set of the linker. Following this process, the residues were refined and the whole system minimized before running MD simulation on the finished structure. In this part of the study, no constraints were used.

After running MD simulation with bromoergocriptine in the active site, bromocriptine was removed for aripiprazole to be docked with IFD in the same protein structure. The pose with the best docking score was chosen for MD simulations. MD simulations were run for risperidone with PDB file 6CM4 (structure of dopamine D_2 receptor bound to antagonist risperidone) without the G-protein complex on the receptor protein. There was no need to perform an IFD prior to the MD because risperidone was already bound to the dopamine D_2 receptor. However, protein preparation wizard was run as usual before starting MD simulations. Pimavanserin was docked into the serotonin 5-HT_{2A} receptor (PDB: 6VMS) and the pose with the best docking score was selected for MD. This pose had a docking score of –11.40 kcal/mol.

In each turn, all the ligand-bound systems were merged with a palmitoyl-oleoyl-phosphatidylcholine (POPC) membrane bilayer environment, based on Orientations of Proteins in Membranes server, OPM (83). The OPM provided structural and spatial arrangements of membrane proteins with respect to the lipid bilayer. The solvent model that was used in all systems was SPC which stands for simple point-charge. SPC solvent model is an empirical model where water molecules are modelled as rigid triangles with charges

distributed over all atoms and is thus among the simplest water models utilized in molecular dynamic simulations (89).

After downloading the PDB files with correct orientation via OPM, a FASTA file from UniprotKB database (90) was also incorporated to ensure the right structure for dopamine D_2 receptor. The FASTA file included the amino acid sequence of the human dopamine D_2 receptor and had the code P14416. In the case where the OPM was not specific enough to place the membrane, for instance when preparing the serotonin system, the membrane was manually added by selecting the residues within all seven TMs and finally placing it. Further, the embedded systems were neutralized with salt solutions of 0.15 M NaCl. The boundary conditions were set to an orthorhombic box shape with the edges of the box 10 Å away from the protein ligand-complex in all directions. The overall number of atoms in the bromocriptine and aripiprazole systems including the G-protein, water molecules, ions and POPC was approximately 138000 each. Figure 9 displays the whole bromocriptine – D_2 + G_i complex. For the risperidone system without a G-protein and serotonin 5-HT_{2A} receptor – pimavanserin complex, including water molecules, ions and POPC, the total numbers of atoms was 38000 and 46500 respectively.

Before running the MD simulations, all of the systems were gradually relaxed through equilibration and minimization using the default protocols of Desmond. Interactions between atoms were calculated with the OPLS_2005 force field. The isothermal-isobaric ensemble NPT maintained a constant temperature at 300 K and pressure at 1.01325 bar during the simulations. 1000 ns long atomistic MD simulations with a recording interval of 250 ps were run for seven systems (four ligand-bound and three ligand-free) and provided 4000 frames each. An additional MD simulation was run for bromocriptine in dopamine D_2 receptor without the G-protein over a period of 100 ns with a recording interval of 100 ps for later comparisons. Ultimately, the trajectory frames from the MD simulations were used to process and analyse the simulation results.

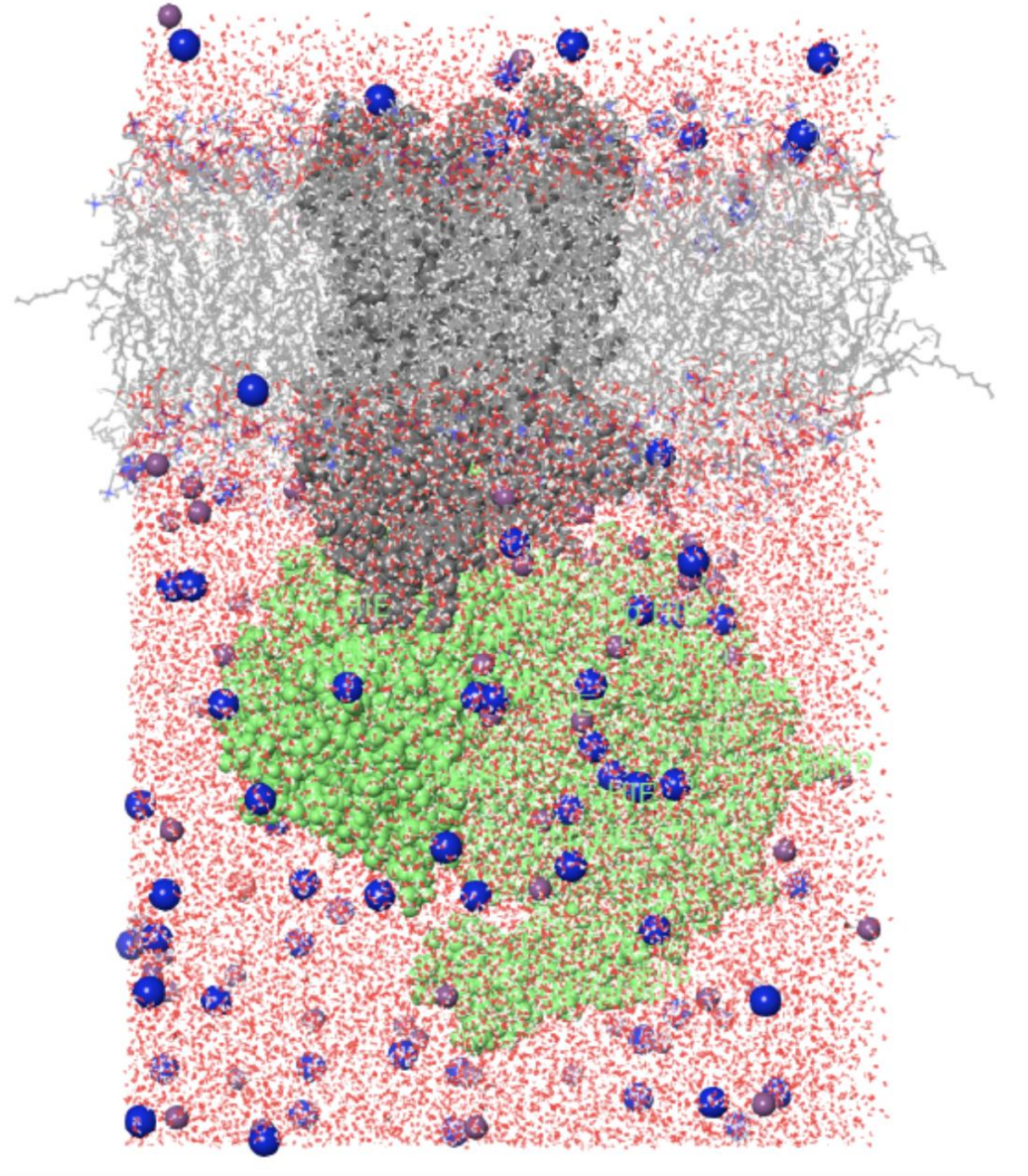

Figure 9: *bromocriptine – D_2 + G_i including the G-protein (large green unit below the membrane, CPK model), water molecules and ions (chloride (Cl^-) ions as purple spheres, Na^+ ions blue spheres, CPK model) and POPC (membrane displayed in grey). The D_2 receptor is embedded within the membrane and TM helices are shown as a grey CPK model.*

4 Results

4.1 Induced fit docking

All of the 37 ligands were docked into the orthosteric binding site domain of the four receptor structures dopamine D_2, serotonin 5-HT_{2A}, 5-HT_{2C} and histamine H_1 receptor using the Schrödinger IFD protocol (schrödinger release 2021-1). The results from the IFD scoring values, their intrinsic activity and inhibition constants for the four receptors, are presented in tables 1- 4. Only the lowest energy IFD scores were selected and matched up with affinity values, K_i, from the PDSP database (84). The affinities for levomepromazine, asenapine, pimavanserin and paliperidone on these receptors were not available in the database so they were retrieved from their supplementary protection certificates; asenapine (91) and pimavanserin (92) and previous articles, levomepromazine (93) and paliperidone from McLeod 2015 (94). No affinity data was found for some of the ligands and therefore left blank with a hyphen.

As a rule of thumb, the lower the K_i, the greater the binding affinity. A low K_i indicates greater ability for a ligand to bind to its target. High affinity ligands require lower concentrations to produce desired effect (95). To systematically classify the ligands based on affinity, the K_i values were rated on a four-point scale according to Yonemura et.al 1998 (93). Ligands with K_i values on the order of 1nM or less were defined as high affinity. K_i values on the 10 nM order, meaning under 100 nM was categorized as moderate affinity while ligands with K_i values on 100 nM order were relatively low affinity. Finally, low affinity ligands were those with values over 1000 nM. Regarding the docking scores, generally they are only describing favourable binding or orientation of a ligand in the target but alone does not serve as useful surrogates for binding affinity. Nevertheless, the general interpretation of docking scores is that the lower/more negative the number is, the better the binding (96).

*Table 1 – **Dopamine D_2 receptor** binding affinity (K_i) and IFD docking score corresponding to the best docking pose for antipsychotic drugs.*

Ligands	Intrinsic activity	K_i (nM)	IFD score (kcal/mol)
Amisulpride	Antagonist	3.0	-8.4
Aripiprazole	Partial agonist	0.3-0.9	-8.8
Asenapine	Antagonist	1.3	-8.4
Brexpiprazole	Partial agonist	0.2	-10.7
Cariprazine	Partial agonist	0.5-0.7	-8.1
Chlorpromazine	Antagonist	7.2	-8.3
Chlorprothixene	Antagonist	3.0-5.6	-8.6
Clozapine	Antagonist	44-330	-7.9
Cyamemazine	Antagonist	5.8	-7.4
Droperidol	Antagonist	-	-9.6
Z-Flupentixol	Antagonist	0.4	-9.9
E-Flupentixol	Antagonist	120	-8.6
Haloperidol	Antagonist	0.3-10	-9.6
Fluphenazine	Antagonist	0.2-1.4	-9.1
Iloperidone	Antagonist	0.4-21.4	-9.5
Levomepromazine	Antagonist	5.9	-6.9
Loxapine	Antagonist	5.2-71.4	-7.8
Lurasidone	Antagonist	1.7	-10.9
Mesoridazine	Antagonist	4.4-19	-8.5
Olanzapine	Antagonist	3.0-106	-7.3
Paliperidone	Antagonist	2.5	-10.2
Perospirone	Antagonist	0.6	-10.5
Perphenazine	Antagonist	0.2-1.4	-8.9
Pimavanserin	-	-	-9.5
Pimozide	Antagonist	0.06-29	-13.2
Pipotiazine	Antagonist	0.2	-9.2

Prochlorperazine	Antagonist	0.2-7.0	-8.9
Quetiapine	Antagonist	78-1000	-8.7
Risperidone	Antagonist	0.3-19	-9.8
Sertindole	Antagonist	0.6-9.1	-10.7
Sulpiride	Antagonist	4.2-206	-9.2
Thioridazine	Antagonist	0.4-26.7	-8.0
Tiothixene	Antagonist	0.03-1.4	-8.0
Trifluoperazine	Antagonist	-	-7.9
Ziprasidone	Antagonist	0.8-9.7	-9.8
Zotepine	Antagonist	5.4-11	-9.5
Zuclopenthixol	Antagonist	-	-10.1

Main source: PDSP K_i database
No data – marked with hyphen (-)
Some drugs have varying K_i values (based on different sources) and are therefore listed as intervals

*Table 2 – **Serotonin 5-HT$_{2A}$ receptor** binding affinity (K_i) and IFD docking score corresponding to the best docking pose for antipsychotic drugs.*

Ligands	**Intrinsic activity**	**K_i (nM)**	**IFD score (kcal/mol)**
Amisulpride	Antagonist	8.3	-9.2
Aripiprazole	Partial agonist	3.4-35	-9.7
Asenapine	Antagonist	0.06	-9.6
Brexpiprazole	Antagonist	0.5	-11.2
Cariprazine	Antagonist	18.8	-8.5
Chlorpromazine	Inverse agonist	2.8	-9.0
Chlorprothixene	Antagonist	0.3-0.4	-9.4
Clozapine	Inverse agonist	5.4	-9.8
Cyamemazine	Antagonist	1.5	-10.4
Droperidol	-	-	-9.5
Z-Flupentixol	Antagonist	87.5	-10.9

E-Flupentixol	Antagonist	-	-10.8
Haloperidol	Antagonist	25-120	-10.5
Fluphenazine	Antagonist	3.2	-9.6
Iloperidone	Antagonist	0.1-5.6	-9.8
Levomepromazine	Antagonist	0.07	-9.5
Loxapine	Inverse agonist	1.7-13.5	-8.7
Lurasidone	Antagonist	2.0	-11.3
Mesoridazine	Antagonist	4.8-11.7	-11.4
Olanzapine	Antagonist	1.5-24	-8.9
Paliperidone	Antagonist	1.2	-11.2
Perospirone	Antagonist	1.3	-10.0
Perphenazine	Antagonist	5.6	-10.2
Pimavanserin	Antagonist/inverse	0.09	-11.4
Pimozide	Antagonist	14.3-77.7	-12.0
Pipotiazine	Antagonist	-	-11.31
Prochlorperazine	-	7.2-15	-9.0
Quetiapine	Antagonist	31-2500	-8.6
Risperidone	Inverse agonist	0.1-7.0	-9.8
Sertindole	Antagonist	0.3-6.0	-11.2
Sulpiride	-	4.8	-8.9
Thioridazine	Antagonist	1.1-60.0	-10.5
Tiothixene	Antagonist	50.0	-9.7
Trifluoperazine	Antagonist	-	-9.5
Ziprasidone	Antagonist	0.08-1.7	-8.9
Zotepine	Antagonist	2.6	-10.4
Zuclopenthixol	Antagonist	-	-10.8

Main source: PDSP K_i database
No data – marked with hyphen (-)
Some drugs have varying K_i values (based on different sources) and are therefore listed as intervals

*Table 3 – **Serotonin 5-HT$_{2C}$ receptor** binding affinity (K_i) and IFD docking score corresponding to the best docking pose for antipsychotic drugs*

Ligands	Intrinsic activity	K_i (nM)	IFD score (kcal/mol)
Amisulpride	-	>10000	-7.7
Aripiprazole	Partial agonist	15-180	-9.1
Asenapine	Antagonist	0.03	-8.8
Brexpiprazole	Partial agonist	12-34	-9.2
Cariprazine	Inverse agonist	134	-8.3
Chlorpromazine	Antagonist	25	-9.0
Chlorprothixene	Antagonist	4.5	-9.3
Clozapine	Inverse agonist	9.4	-9.5
Cyamemazine	Antagonist	12	-8.4
Droperidol	-	-	-9.4
Z-Flupentixol	-	102.2*	-10.3
E-Flupentixol	-	-	-10.7
Haloperidol	Antagonist	>10000	-9.6
Fluphenazine	Antagonist	174-2570	-10.1
Iloperidone	Antagonist	14-251	-9.1
Levomepromazine	Antagonist	0.07	-8.9
Loxapine	Inverse agonist	9.5	-9.1
Lurasidone	-	415*	-11.3
Mesoridazine	Antagonist	157	-10.5
Olanzapine	Inverse agonist	4.1-71	-9.3
Paliperidone	Antagonist	48	-10.7
Perospirone	-	-	-10.2
Perphenazine	Antagonist	132	-9.5
Pimavanserin	Antagonist/inverse	0.44	-10.2
Pimozide	-	570-3359	-10.5

Pipotiazine	-	-	-10.9
Prochlorperazine	-	122	-9.1
Quetiapine	Antagonist	615-3500	-9.5
Risperidone	Inverse agonist	10.0-64.0	-9.1
Sertindole	Inverse agonist	0.3-6.0	-11.5
Sulpiride	-	-	-7.4
Thioridazine	Antagonist	53.0	-10.4
Tiothixene	-	1350	-8.7
Trifluoperazine	Antagonist	-	-9.7
Ziprasidone	Inverse agonist	0.7-13.0	-9.0
Zotepine	Inverse agonist	3.2	-10.4
Zuclopenthixol	Antagonist	-	-9.5

Main source: PDSP Ki database
No data – marked with hyphen (-)
Species measured on deviates from human – marked with asterix (*) Lurasidone = pig, Z-flupentixol = rat
Some drugs have varying K_i values (based on different sources) and are therefore listed as intervals

*Table 4 – **Histamine H_1 receptor** binding affinity (K_i) and IFD docking score corresponding to the best docking pose for antipsychotic drugs*

Ligands	Intrinsic activity	K_i (nM)	IFD score (kcal/mol)
Amisulpride	-	>10000	-9.6
Aripiprazole	Antagonist	25.1-61	-9.6
Asenapine	Antagonist	1.0	-8.9
Brexpiprazole	Antagonist	19.0	-11.0
Cariprazine	Antagonist	23.2	-8.5
Chlorpromazine	Antagonist	4.25	-9.7
Chlorprothixene	Antagonist	0.9-3.8	-8.7
Clozapine	Antagonist	1.1	-8.9
Cyamemazine	Antagonist	9.3*	-9.3
Droperidol	-	-	-10.7

Z-Flupentixol	-	0.9	-11.7
E-Flupentixole	-	5.7	-12.5
Haloperidol	Antagonist	1800	-9.7
Fluphenazine	Antagonist	7.3-70	-12.5
Iloperidone	-	12.3	-10.1
Levomepromazine	Antagonist	0.6	-8.4
Loxapine	Antagonist	2.2-3981	-7.6
Lurasidone	-	>1000*	-10.8
Mesoridazine	Antagonist	1.8	-12.0
Olanzapine	Antagonist	0.09-4.9	-9.8
Paliperidone	Antagonist	-	-11.5
Perospirone	-	-	-11.4
Perphenazine	Antagonist	2.6-8.3	-10.8
Pimavanserin	-	-	-8.9
Pimozide	Antagonist	25.0-692.0	-12.7
Pipotiazine	-	-	-11.5
Prochlorperazine	Antagonist	6.0-19.0	-11.3
Quetiapine	Antagonist	2.2-12.9	-10.8
Risperidone	Inverse agonist	3.5	-9.5
Sertindole	Antagonist	130.0	-12.7
Sulpiride	-	72443	-9.4
Thioridazine	Antagonist	2.5-17.0	-9.9
Tiothixene	Antagonist	4.0-12.0	-11.9
Trifluoperazine	Antagonist	-	-11.0
Ziprasidone	Antagonist	4.6-47.0	-9.9
Zotepine	Antagonist	0.6-5.8	-10.8
Zuclopenthixol	Antagonist	-	-10.9

Main source: PDSP Ki database
No data – marked with hyphen (-)
Species measured on deviates from human – marked with asterix (*) Lurasidone and Cyamemazine = guniea pig
Some drugs have varying K_i values (based on different sources) and are therefore listed as intervals

4.1.1 Binding affinity K_i and docking scores

Levomepromazine, prochlorperazine, quetiapine, olanzapine, risperidone and aripiprazole are the most prescribed antipsychotic drugs in Norway based on the Norwegian prescription database. On that account, they will be exclusively pointed out even though there are drugs in the tables with "better" affinity values and docking scores. These numbers alone do not predict how effective the agents are, nor if they actually are on the marked for use under the indication of being antipsychotic. The affinity of levomepromazine, prochlorperazine, olanzapine, aripiprazole and risperidone on the dopamine D_2 receptor was high as their K_i values were on the order of 1 nM and ranged from 0.2 nM to 5.9 nM. Quetiapine on the other hand, recorded moderate affinity because the lowest reported K_i value was 78 nM on the dopamine D_2 receptor. Of the 37 docked drugs, none could be classified as low affinity drugs on the dopamine D_2 receptor because their K_i values were all below 1000 nM.

In addition to looking at levomepromazine, prochlorperazine, quetiapine, olanzapine, risperidone and aripiprazole, investigating pimavanserin is of interest especially since it is the only antipsychotic drug known that does not interact with the dopamine D_2 receptor as an antagonist or partial agonist. On the serotonin 5-HT_{2A} receptor, levomepromazine, prochlorperazine, quetiapine, olanzapine, risperidone and aripiprazole had K_i values on 0.07 nM, 7.2 nM, 31 nM, 1.5 nM, 0.1 nM and 3.4 nM respectively which rate them high to moderate affinity. Pimavanserin had no reported value on the dopamine D_2 receptor but had very high affinity on the serotonin 5-HT_{2A} receptor with a K_i value of 0.09 nM. Other drugs that showed high affinities on this receptor, were chlorprothixene, sertindole and ziprasidone with affinity values ranging between 0.08 – 6.0 nM.

High affinity for the serotonin 5-HT_{2C} receptor was registered for levomepromazine, olanzapine and pimavanserin with affinity values of 0.07 nM, 4.1 nM and 0.44 nM respectively. The lowest reported K_i value for risperidone was 10 nM and 15 nM for aripiprazole which rendered them as moderate affinity drugs on the 5-HT_{2C} receptor. Relatively low affinity, with K_i values on the order of 100 nM, was shown by prochlorperazine and quetiapine. The K_i values of these drugs were 122 nM for prochlorperazine and 615 nM for quetiapine. Among the drugs that exhibited low affinity for 5-HT_{2C} receptor, were amisulpride and haloperidol, both with K_i values over 1000 nM.

The affinity of the selected drugs (levomepromazine, olanzapine, prochlorperazine, quetiapine, aripiprazole and risperidone) for the histamine H_1 receptor was high to moderate with K_i values ranging from 0.09 – 25.1 nM. Sertindole was the only drug that had relatively low affinity for the H1 receptor with a K_i value of 130 nM. Out of all 37 drugs, olanzapine had the highest affinity with 0.09 nM while lowest affinity was seen for sulpiride with a K_i value of 72443 nM.

Concerning the docking scores, pimavanserin had -9.5 kcal/mol on the dopamine D_2 receptor and -11.4 and -10.2 kcal/mol on the serotonin 5-HT_{2A} and 5-HT_{2C} receptors respectively. The docking scores for aripiprazole were -8.8, -9.7, -9.1 and -9.6 kcal/mol on the dopamine D_2, serotonin 5-HT_{2A}, 5-HT_{2C} and histamine H_1 receptors respectively. Conclusively, all of the selected drugs had good docking scores on all receptors as seen in the tables. Some of the drugs that stood out with extremely good scores below -10 kcal/mol on the histamine H_1 receptor were brexpiprazole, Z and E-flupentixol, fluphenazine, lurasidone and sertindole. Their docking scores were -11.0 kcal/mol for brexpiprazole, -11.7 kcal/mol for Z-flupentixol, -12.5 kcal/mol for E-flupentixol and fluphenazine, -12.5 kcal/mol for lurasidone and -12.7 kcal/mol for sertindole. The docking score of pimozide was the highest on the dopamine D_2 receptor with a value of -13.2 kcal/mol while the reported K_i values for pimozide ranged between 0.06-29 nM.

4.2 Molecular dynamics simulations

Three ligand-free complexes were constructed in addition to the four ligand-bound complexes to better understand the influence of ligand binding on the proteins. These were, dopamine D_2 receptor including G-protein without a ligand, dopamine D_2 receptor without G-protein or a ligand and lastly serotonin 5-HT_{2A} receptor without a ligand. The ligand-bound complexes were bromocriptine and aripiprazole bound to the dopamine D_2 receptor including G-protein, risperidone bound to dopamine D_2 receptor without G-protein and pimavanserin bound to serotonin 5-HT_{2A} receptor.

4.2.1 Structural stability analysis

The stability of the protein in complex with ligands relative to its conformation was determined by the deviations from the starting structures, produced during the 1000 ns long MD simulations. Principally, the smaller the deviations the more stable the protein structure. In the present thesis, the root mean square deviation (RMSD) and root mean square fluctuation (RMSF) for the backbone atoms were measured. RMSD measured the average difference between the backbone atoms of the respective proteins from its initial structural conformation to the final position by superimposing all frames on the reference frame over the course of the simulation. RMSF on the other hand, was measured to characterize the degree of fluctuation of the residues in the receptors in complex with the different ligands. Additionally, secondary structure elements like α-helices and β-strands are displayed in the figures. α-helical and β-strand regions are highlighted in red and blue backgrounds respectively.

4.2.1.1Root mean square deviation

RMSD value for the backbone was measured for all MD simulations that were run in order to study the stability of the simulations. The evolution plots from the MD simulations for bromocriptine, aripiprazole, risperidone and pimavanserin with average and maximum RMSD values are profiled in figure 10. The protein structure systems for 1000 ns simulations of bromocriptine and aripiprazole included the dopamine D_2 receptor plus G-protein, while the risperidone system only included the dopamine D_2 receptor. The 100 ns long MD simulation of bromocriptine was without the G-protein. RMSD for the pimavanserin system was calculated on the serotonin 5-HT_{2A} receptor (without G-protein as well). Three ligand-free simulations were also run, the first one being dopamine D_2 receptor including G-protein, the second being dopamine D_2 receptor without G-protein and lastly the serotonin 5-HT_{2A} receptor.

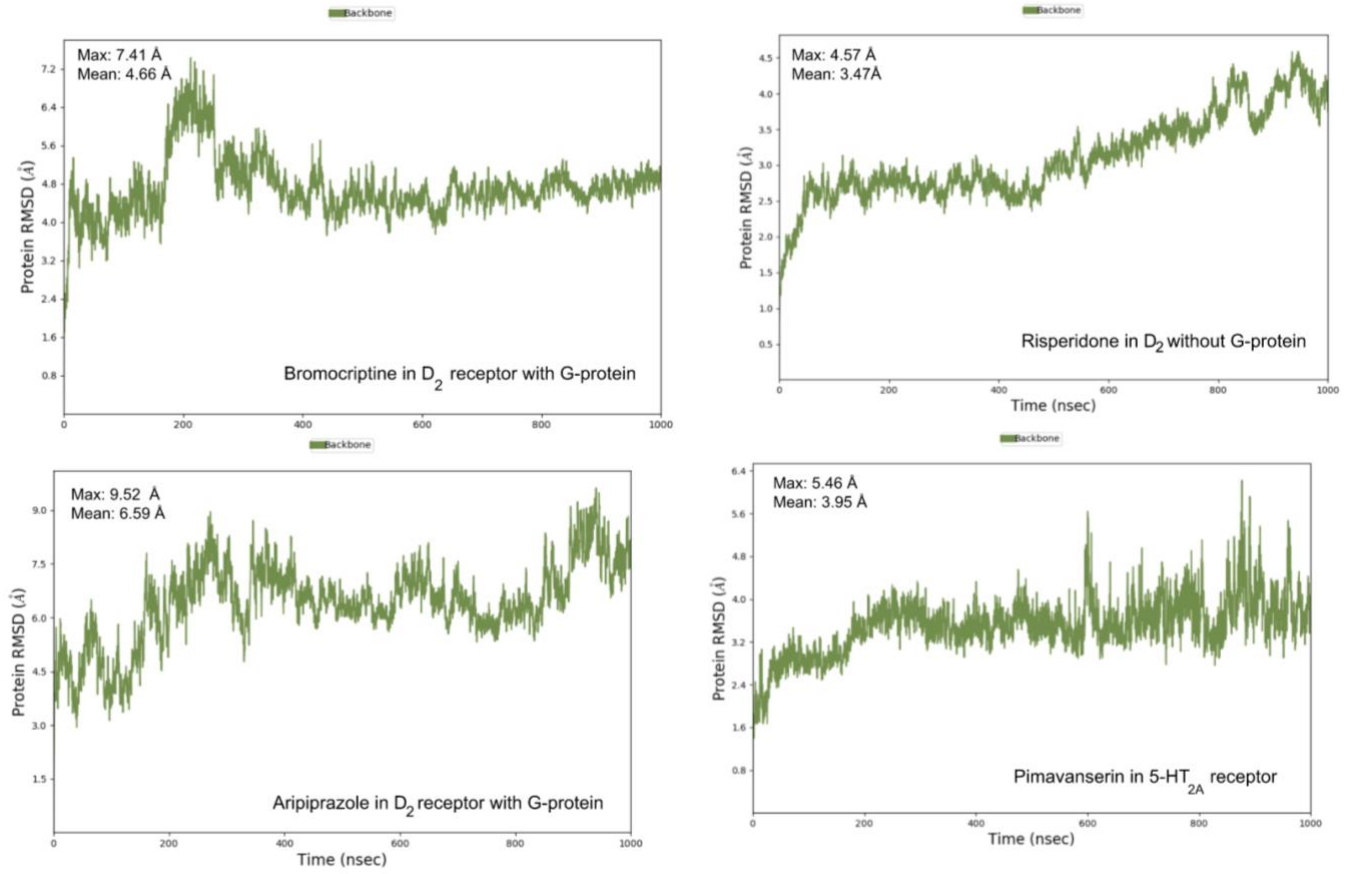

***Figure 10**: RMSD plots of backbone atoms for bromocriptine, aripiprazole, risperidone and pimavanserin. Maximum RMSD values were calculated after superimposing frame 849,3780, 3780 and 3524 (highest peaks) on the starting structure respectively.*

For the bromocriptine – receptor complex, the highest observed RMSD value was 7.41 Å approximately 200 ns into the simulation as the system had a slight increasing trend in the beginning. Approaching 250 – 300 ns into the simulation, the system equilibrated at around 4.66 Å for the remaining course of the simulation. Interestingly, the aripiprazole–receptor complex never seemed to fully equilibrate and the highest noticed RMSD was 9.52 Å towards the end of the simulation. Nonetheless, the mean RMSD was 6.59 Å. The curve for the ligand-free dopamine D_2 receptor including G-protein system (figure 11), appeared to slowly increase in a straight pathway during the simulation with the highest RMSD value calculated at 12.01 Å 9.15 Å at average.

Maximum and average RMSD values for the risperidone system was 4.57 Å and 3.47 Å respectively. The conformational deviation from the initial structure appears to harmonically change in an increasing manner. Judging from the previously mentioned RMSD analysis, pimavanserin in the 5-HT_{2A} receptor with mean and highest RMSD values 3.95 Å and 5.46 Å respectively, represents the most stable conformers among the simulations. It increases at the onset up to 200 ns before it maintains a more or less straight path with a few peaks out the simulation. The highest observed peak was measured at 5.18 Å. The measured RMSD values for ligand-free system number two, D_2 without G-protein, were 3.85 Å at mean and 5.27 Å at maximum. For ligand-free system number three, 5-HT_{2A}, RMSD values were 5.42 Å (maximum) and 3.81 Å (mean) respectively. The plots for the ligand free systems are shown in figure 11.

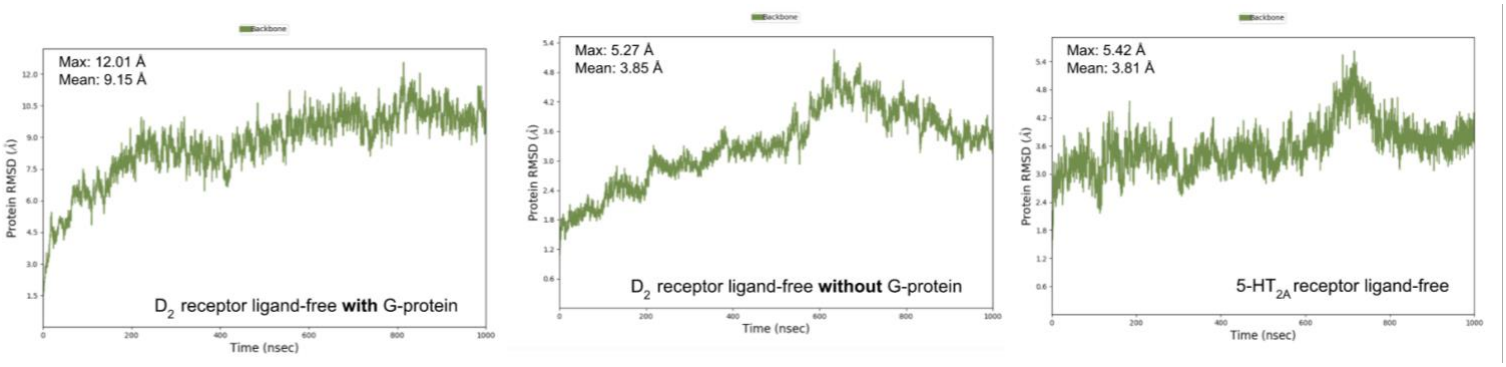

Figure 11*: RMSD plots of backbone atoms for ligand-free systems, D_2 receptor with and without G-protein and also 5-HT2A receptor. Maximum RMSD values were calculated after superimposing the frames with the highest peaks on the starting structure.*

4.2.1.2Root mean square fluctuation

RMSF analysis based on the backbone atoms were carried out along with RMSD to fully obtain a picture of the movement and conformational changes of the systems over the simulation period. The relevant plots are presented in figure 12. For both bromocriptine and aripiprazole in dopamine D_2 receptor with G-protein, the section in the middle is coloured blue which indicates β-strands. These β-strands are a part of the G-protein (chain B – guanine nucleotide binding protein G_i, subunit β) and thus, is not found in the risperidone and pimavanserin systems. This region shows a relatively low and stable RMSF value of approximately 2.0 Å which is in good agreement with the fact that β-strands usually are rigid and fluctuate less compared to loop regions for instance.

Following the β-strands section, comes an α-helical region, (after the 600-residue index mark), which is the α-helices of the dopamine D_2 receptor. A few peaks with RMSF values of 5.61 Å and 3.36 Å were observed in the bromocriptine system and these two peaks represented the amino terminals ACE (acetyl group, N-terminal) and NMA (N-methyl amide of C-terminal) respectively. In the aripiprazole system, more peaks were observed in the receptor region and highest peak to the far left had a RMSF value of 7.46 Å while RMSF value of the peak at the very end was 6.05 Å. Another peak was observed right after the 800-residue index mark and RMSF value this residue, Leu222, was 6.04 Å. Besides from the peaks, the average RMSF values for the receptor regions were around 3.0 Å for bromocriptine and aripiprazole. The RMSF plot for aripiprazole further shows more fluctuations than the bromocriptine curve.

Maximum RMSF values measured for risperidone and pimavanserin were 4.21 Å for Ile394 and 3.98 Å for Glu351 respectively. Similarly to bromocriptine and aripiprazole, the most fluctuating parts and highest peaks in the risperidone and pimavanserin plots are all situated in the loop regions (ICLs and ECLs) which are known to be more flexible than β-strands and α-helices. For the ligand-free dopamine D_2 receptor with G-protein, the highest measured RMSF values were 8.11 Å and 4.75 Å (ACE and NMA respectively) compared to the average value around 4 Å. In the plot for the D_2 receptor without a G-protein, Asn35 had a RMSF value of 5.13 Å while the value was 5.33 Å for Asp400. Values for ACE and NMA were not applicable. Finally, the maximum RMSF values observed in the ligand-free 5-HT_{2A} system were 8.01 Å for Thr69 and 3.88 Å for NMA (no available data for ACE).

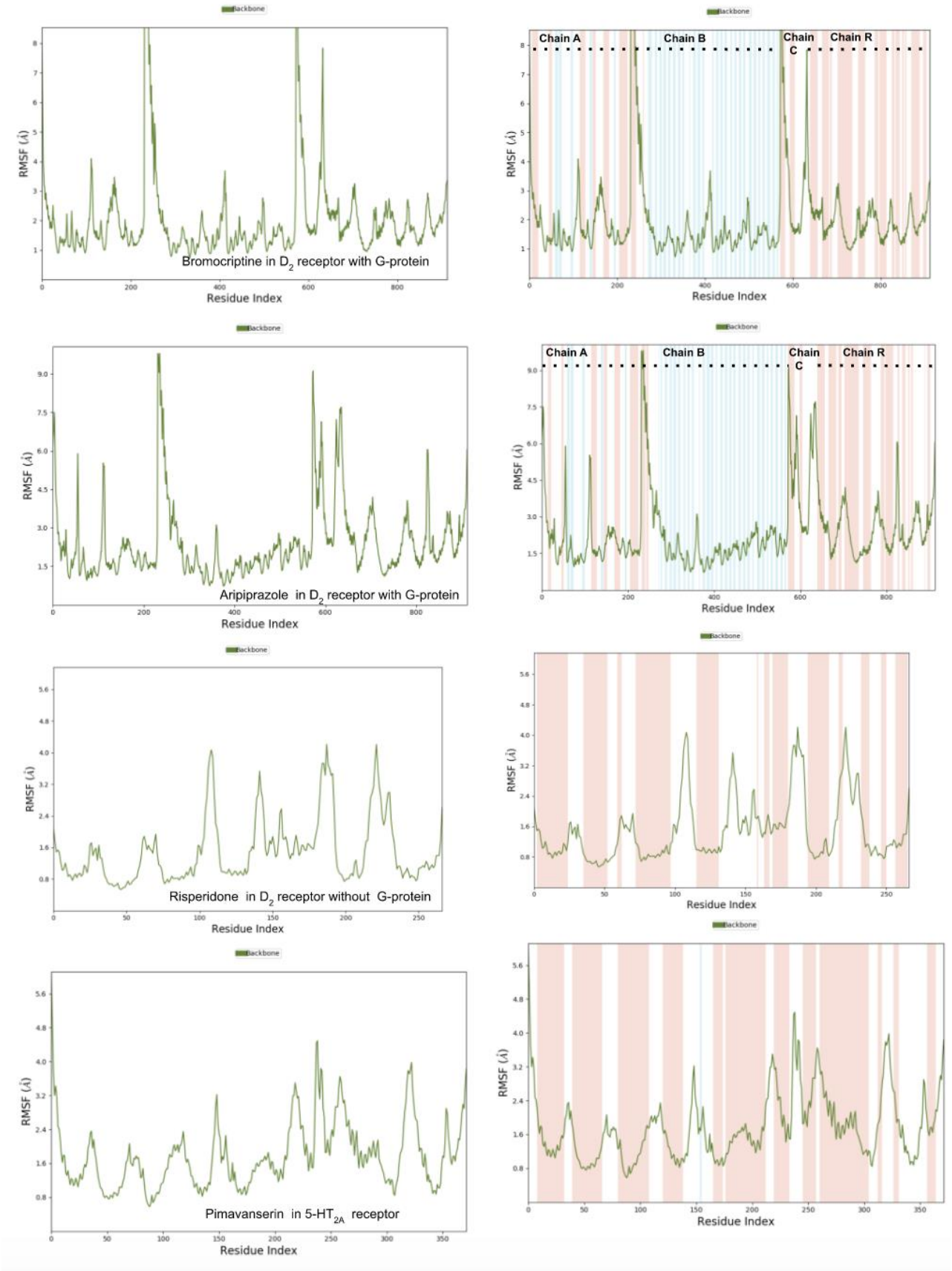

***Figure 12**: RMSF plots of backbone atoms for bromocriptine-, aripiprazole-, risperidone- and pimavanserin systems for each residue in the protein chains. RMSF value describes time-averaged fluctuation of the residues over the entire simulation time and is calculated after superposition on reference (starting) frame. Chain A is subunit α of the G-protein, Chain B is subunit β, Chain C is subunit γ and Chain R is the dopamine D_2 receptor. Red, blue and white fields display α-helical, β-strands and loop regions respectively.*

Both RMSD and RMSF analysis were carried out for the 100 ns MD simulation run on bromocriptine without the G-protein, figure 13. Highest RMSD value observed was 3.41 Å while the average value was 2.79 Å. The highest peak in the RMSF plot as seen in figure 13 was registered for ACE which had a value of 6.20 Å. The mean and NMA RMSF values were 1.71 Å and 4.39 Å respectively. In accordance with the previous RMSF plots all peaks were observed in loop regions.

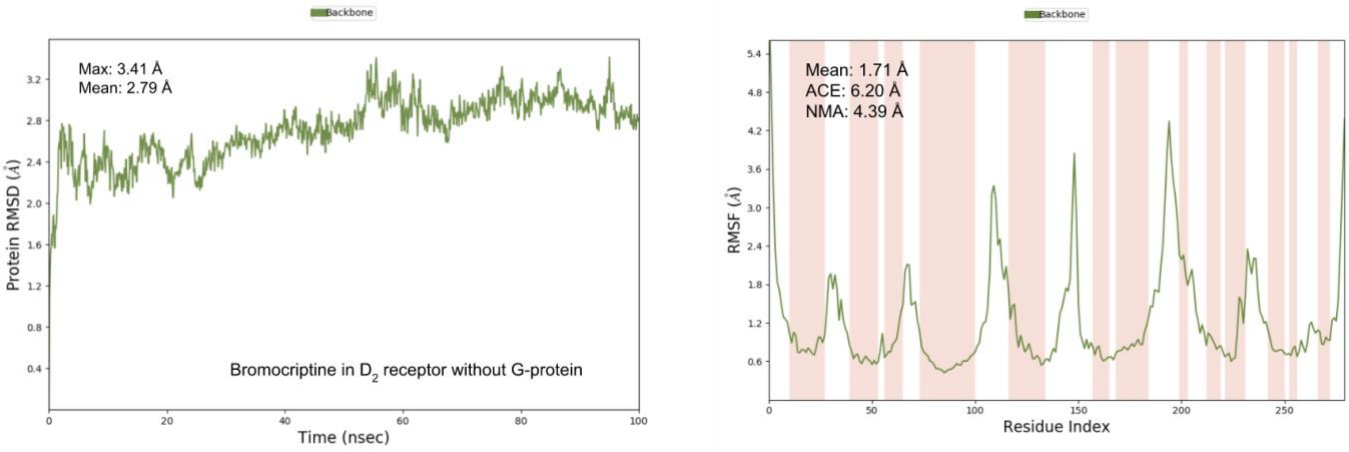

***Figure 13**: Left: RMSD plot of backbone atoms for bromocriptine 100 ns MD simulation. Maximum RMSD values was calculated after superimposing frame 556 (highest peak) on the starting structure. Right: RMSF plot also based on backbone atoms. Red and white fields display α-helical and loop regions respectively.*

4.2.2 Investigation of selected frames throughout the simulations

In order to visualize the motion and dynamics of the drugs upon binding to the receptor, a conformational transition analysis for all systems were performed. The analysis was based on the MD simulation trajectory for each of the four systems, bromocriptine and aripiprazole in the dopamine D_2 receptor including G-protein, risperidone in the dopamine D_2 receptor without G-protein and finally, pimavanserin in the serotonin 5-HT_{2A} receptor. Five snapshots were taken from the 1000 ns long simulation. The trajectory snapshots display multiple superimposed frames and evolution of ligand position with respect to the MD time where the first snapshot was captured at frame number 1. In figure 14 this is displayed in the colour blue. The following snapshots, frame 1001, 2001, 3001 and 4001 are coloured in lilac, white, beige and red respectively. A distinct deviation from the initial pose was seen for all systems from early in the simulation but the largest was seen for aripiprazole. The deviation was much

smaller for bromocriptine and risperidone when looking at the initial pose (frame 1, blue colour) and the final pose (frame 4001, red colour). These results were consistent with the findings obtained from the RMSD and RMSF analysis as the RMSD aripiprazole plot from figure 10 fluctuated more compared to the other plots.

Each of the frames were studied thoroughly to investigate eventual differences in ligand-protein contacts with respect to the dynamic receptor. However, since the frames were captured at five separate points during 1000 ns long simulations that generated 4000 frames, they are not representative for the whole simulation. Rather, they give a snapshot at the interactions formed at that exact time.

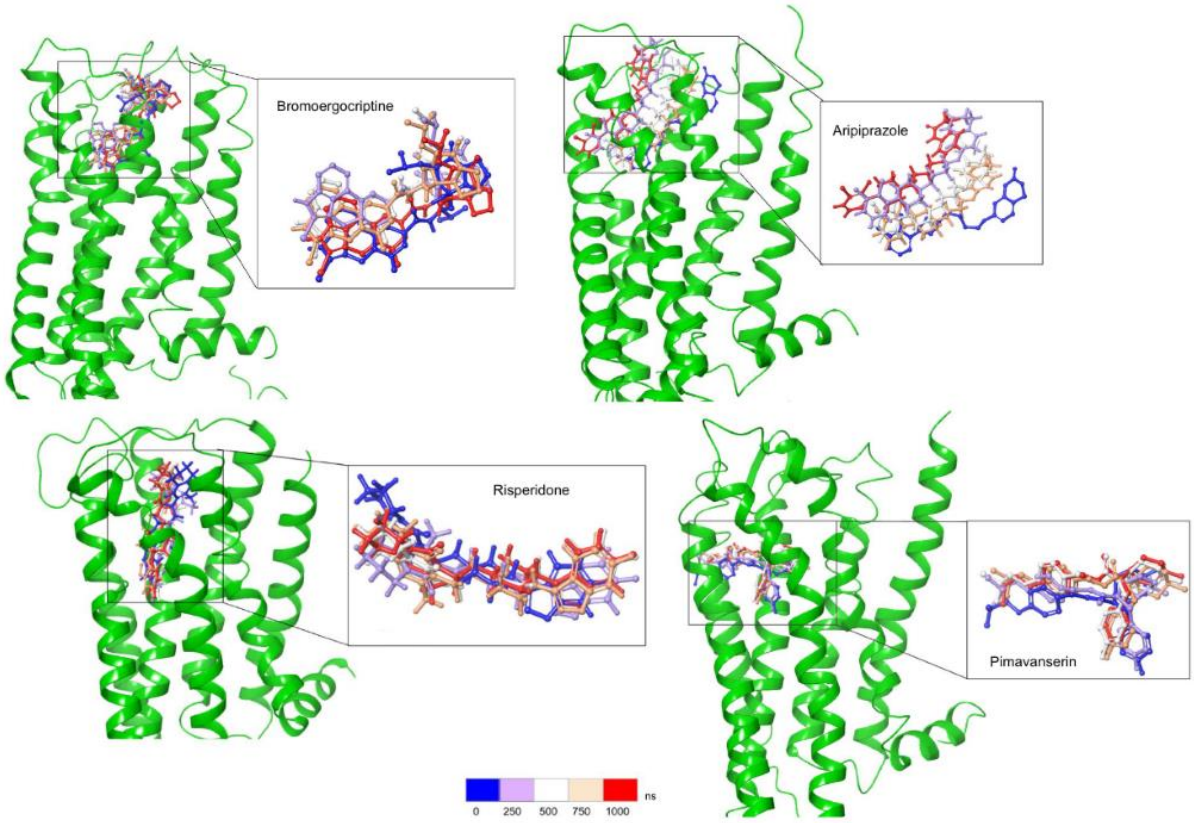

***Figure 14**: Conformational transition analysis of agonist, antagonist and partial agonist on the dopamine D_2 receptor and antagonist on the serotonin 5-HT_{2A} receptor (pimavanserin) during MD simulation. Colour scale is initiated from left to right and shows the evolution of ligand position with respect to simulation time.*

In frame 1, 1001, 2001 and 3001 bromocriptine created a salt bridge with Asp114(3.32) in the D_2 receptor that was not present in frame 4001. Asp114(3.32) additionally established a hydrogen bond with the drug in all frames between the protonated amine group in bromocriptine and the carboxylate of Asp114(3.32). $\pi - \pi$ stacking interactions with

Phe390(6.52) were present in all frames with varying numbers. Bromocriptine in frame 1, 2001, 3001 and 4001 made two interactions with this residue while bromocriptine in frame 1001 only made one $\pi - \pi$ stacking interaction to Phe390(6.52). In addition, Phe389(6.51) also created a $\pi - \pi$ stacking interaction with the ligand in frame 1 but not in the other frames. However, bromocriptine in frame 4001 established a $\pi - \pi$ stacking interaction with His393(6.55) that was not seen in the other frames. Hydrogen bonds between both Ser197(5.46) and Ile184(45.52) and the ligand were present in all frames.

Protonated amine on aripiprazole made salt bridge interactions with negatively charged oxygen on Asp114(3.32) in all frames. Similarly to bromocriptine, a hydrogen bond was formed in all frames with the carboxyl group of Asp114(3.32). Hydrogen bonds with Cys182(45.50) and Trp413(7.40) were present in all frames and so were $\pi - \pi$ stacking interaction with Phe390(6.52). Interestingly, a $\pi - \pi$ stacking interaction with Phe389(6.51) and halogen interaction between chlorine from the ligand and Ser193(5.42) were only observed in frame 2001.

The ligand in all of the frames in the risperidone system made as expected, salt bridge interactions to Asp114(3.32). A hydrogen bond was also present in all frames between the protonated amine group in bromocriptine and the carboxylate of Asp114(3.32). While risperidone in frames 1, 3001 and 4001 engaged in two $\pi - \pi$ stacking interaction with Trp386(6.48), the positively charged nitrogen in the ligand in frames 1001 and 2001, formed $\pi - cation$ interaction with the same residue. A $\pi - \pi$ stacking interaction with Phe189(5.38) was seen in frame 3001.

Finally, for pimavanserin in the 5-HT_{2A} receptor, apart from a salt bridge interaction and hydrogen bond between the ligand and carboxylate of Asp155(3.32) in all frames, two $\pi - \pi$ stacking interactions were observed with Trp336(6.48) in frame 1. No hydrophobic interactions seen in frame 1001. In frame 2001 one $\pi - cation$ interaction was established with Trp336(6.48) and a $\pi - \pi$ stacking interaction with Phe234(5.38). Two $\pi - cation$ interactions were formed with Trp336(6.48) and Phe339(6.51) in both frame 3001 and 4001.

Conclusively, hydrogen bonds mediated through water molecules, so called water bridges, were present in all frames for all of the ligands but in varying amounts. It seems like bromocriptine and risperidone for instance, mainly had these interactions in the top of the binding cavity while aripiprazole and pimavanserin additionally had interactions deep in the

pocket. Most of the water bridges were not in direct contact with the ligand, but other residues that affected the overall binding profile. Figures of all frames in all systems are added in supplementary material figures 2-5.

4.2.3 Protein-ligand interaction analysis

Protein-ligand and Ligand-protein contact interaction analysis were conducted based on the simulation interaction diagram module (Schrödinger release 2021-1) in Desmond. These modules created graphical and schematic displays of the ligand interactions with various protein residues over the simulation period. Only interactions between ligand and receptor were studied, therefore it is highly possible that interactions between residues were present. The representative structures (average RMSD structures) of the MD trajectory frames were prepared for all complexes and presented as both 2D and 3D structures. Bromocriptine was properly accommodated in the binding cavity of the dopamine D_2 receptor. The protonated nitrogen of the ligand formed a hydrogen bond, an ionic interaction and a water bridge with Asp114(3.32) in TM3 for 97%, 3.6% and 57% of the simulation time respectively. Ser197(5.46) contributed to a hydrogen bond as an acceptor with bromocriptine for 96% of the simulation. The aromatic residues Trp386(6.48), Phe389(6.51), Phe390(6.52) and His393(6.55), created a hydrophobic field in the binding site that had non-polar interactions such as vdW, $\pi - \pi$ stacking and cation- π interactions with bromocriptine for a total of 100%. In addition, His393(6.55) and Thr412(7.39) had polar interactions with bromocriptine mediated by water molecules. Ile184(45.52) in ECL2 had hydrogen bond contacts as a donor to the ligand, in addition to water bridge and hydrophobic interactions. Apart from the mentioned main interactions, Phe110(3.28), Val111(3.29), Val115(3.33), Ile183(45.52), Phe189(5.38), Pro405 (7.32) and Tyr408 (7.35) had weak hydrophobic contacts with bromocriptine. These findings are shown in figure 15 and 16.

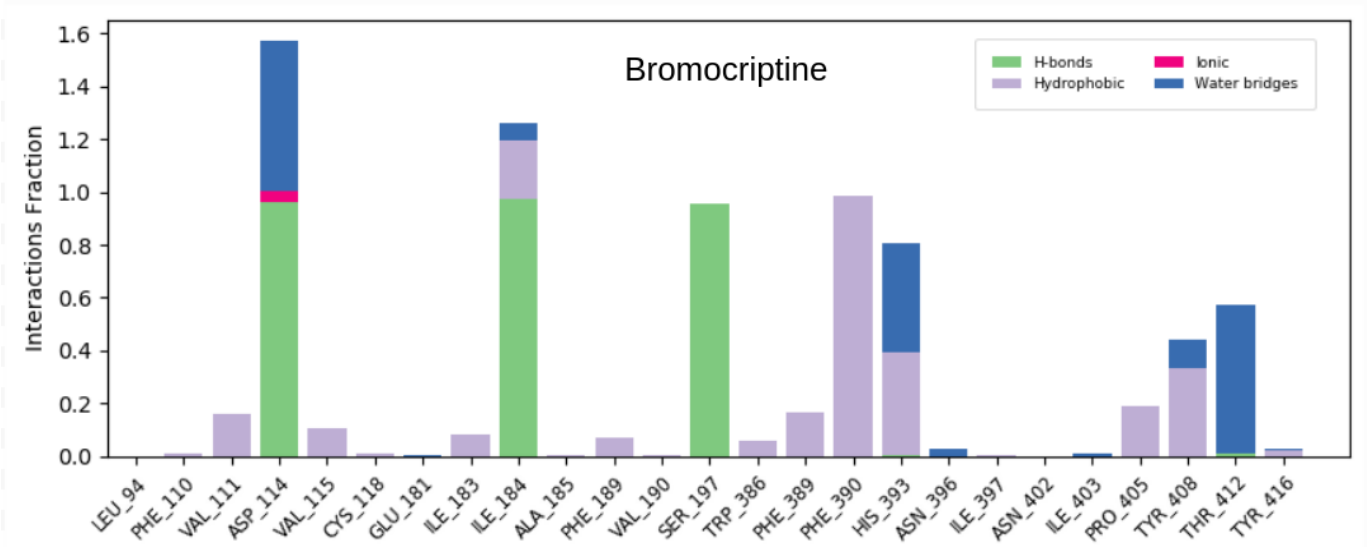

***Figure 15**: Fraction of Interactions between ligand and binding site residues presented as bar-diagram. Green is hydrogen bonds, pink is ionic interaction, blue represents water bridges and lilac are hydrophobic interactions.*

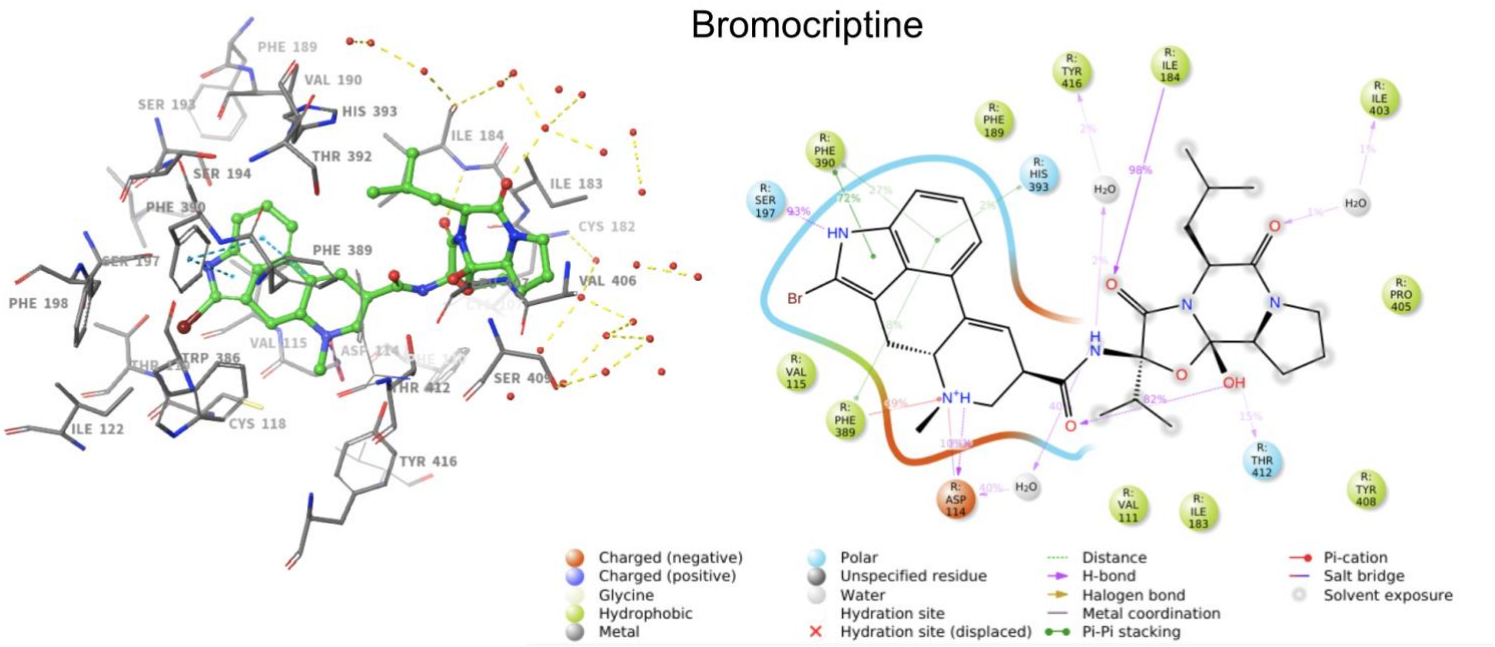

***Figure 16**: Protein-ligand contact analysis of bromocriptine in dopamine D_2 receptor. In left panel: 3D representation of binding site residues in gray and bromocriptine in green. Dotted line in blue shows $\pi - \pi$ stacking interactions, pink dotted line shows ionic interactions, yellow line shows hydrogen bonds and red spheres represent water molecules. In right panel: 2D representation of binding site residues in bubbles and ligand in black.*

The dopamine D_2 partial agonist, Aripiprazole, also had interactions with Asp114(3.32) in the binding cavity. Asp114(3.32) formed strong hydrogen bond and ionic interaction with the positively charged nitrogen of aripiprazole for 86% and 14% of the simulation time respectively. Cys182(45.50) participated in two hydrogen bonds with the NH group in aripiprazole as a donor for 95% and as an acceptor for 97% of the time. Other critical amino acids involved Phe389(6.51), Phe390(6.52) and Trp413(7.40) which established hydrophobic $\pi - \pi$ stacking interaction with aripiprazole. In addition to hydrophobic interactions, Trp413(7.40) also contributed to a hydrogen bond with the oxygen ether group in aripiprazole as a donor. The amino acids Val91(5.39), Leu94(2.64), Val115(3.33), Cys118(3.36), Ile183(45.51) and Ile184 (45.52) engaged in less significant hydrophobic contact with aripiprazole as presented in figure 17 and 18.

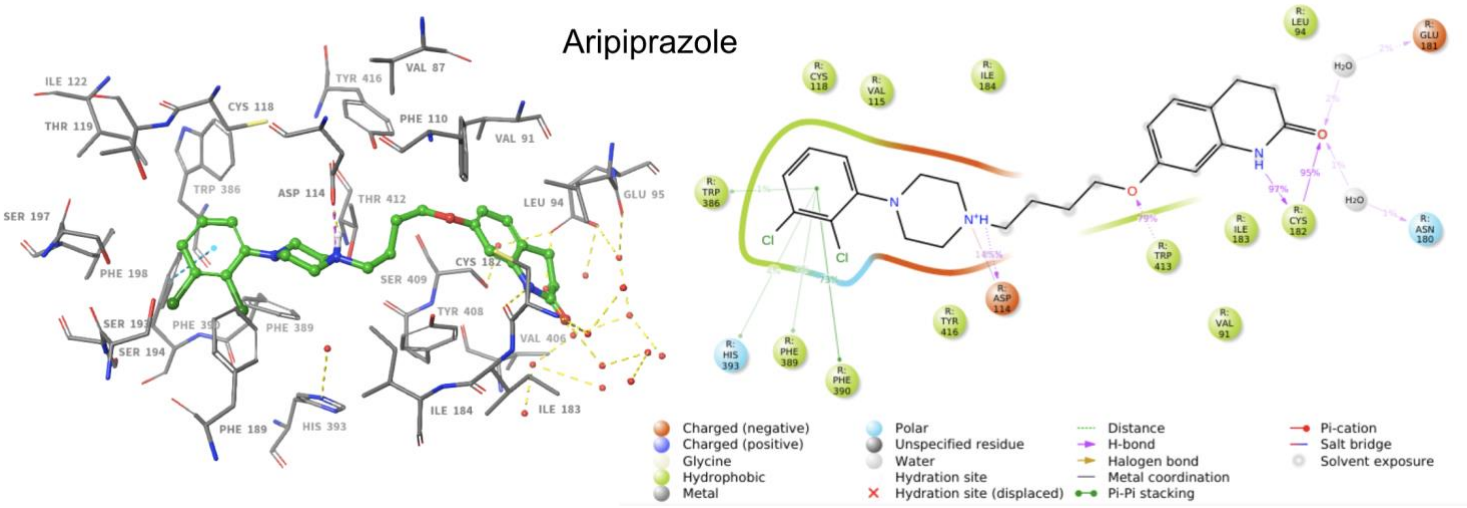

***Figure 17**: Protein-ligand contact analysis of aripiprazole in dopamine D_2 receptor. In left panel: 3D representation of binding site residues in gray and aripiprazole in green. Dotted line in blue shows $\pi - \pi$ stacking interactions, pink dotted line shows ionic interactions and yellow line shows hydrogen bonds. In right panel: 2D representation of binding site residues in bubbles and ligand in black.*

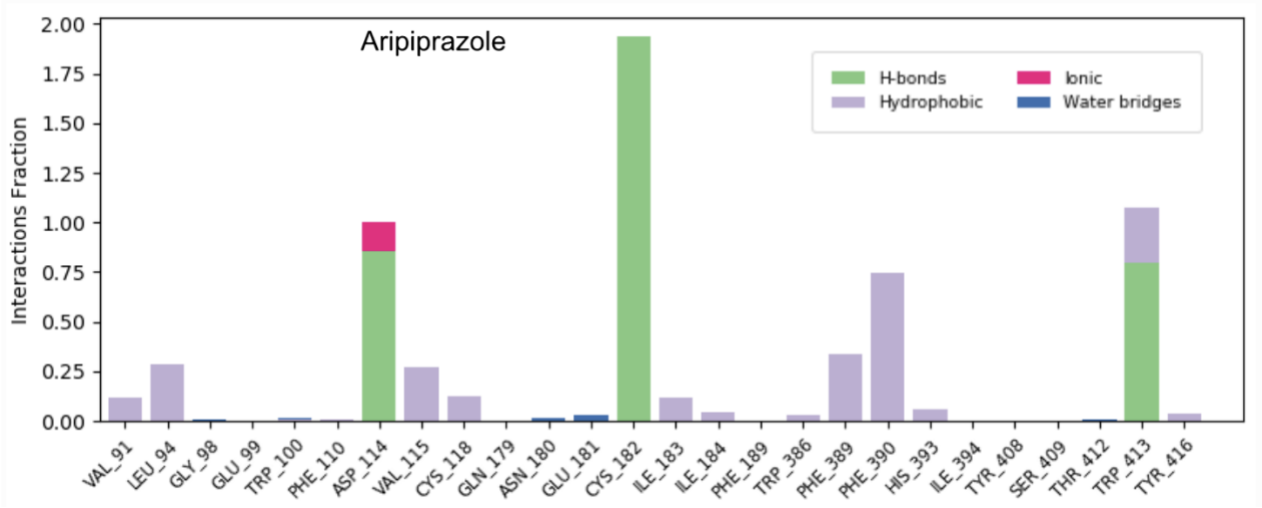

***Figure 18**: Fraction of Interactions between ligand and binding site residues presented as bar-diagram. Green is hydrogen bonds, pink is ionic interaction, blue represents water bridges and lilac are hydrophobic interactions.*

The key interactions that were identified between risperidone and residues within the binding pocket cavity of D_2 receptor involved a hydrogen bond, water bridge and ionic interaction with Asp114(3.32). The hydrogen bond was maintained for approximately 90% of the simulation time, while the salt bridge and water bridge were maintained for 12% and 3% respectively. The interaction analysis further suggested that Pro201(5.50), Phe202(5.51), Phe189(5.38), Phe382(6.44), Trp386(6.48), Phe389(6.51), Tyr408(7.35), Tyr416(7.43) and Trp413(7.40) established hydrophobic non-polar interactions with the ligand in the form of vdW, $\pi - \pi$ stacking and cation- π interactions for up to 57% of the simulation time. A hydrogen bond and water bridge were created between risperidone and Ser193(5.42) in addition to an insignificant hydrogen bond with Thr119(3.37) as seen in figure 19. A bar diagram of the interaction fractions is presented in figure 20.

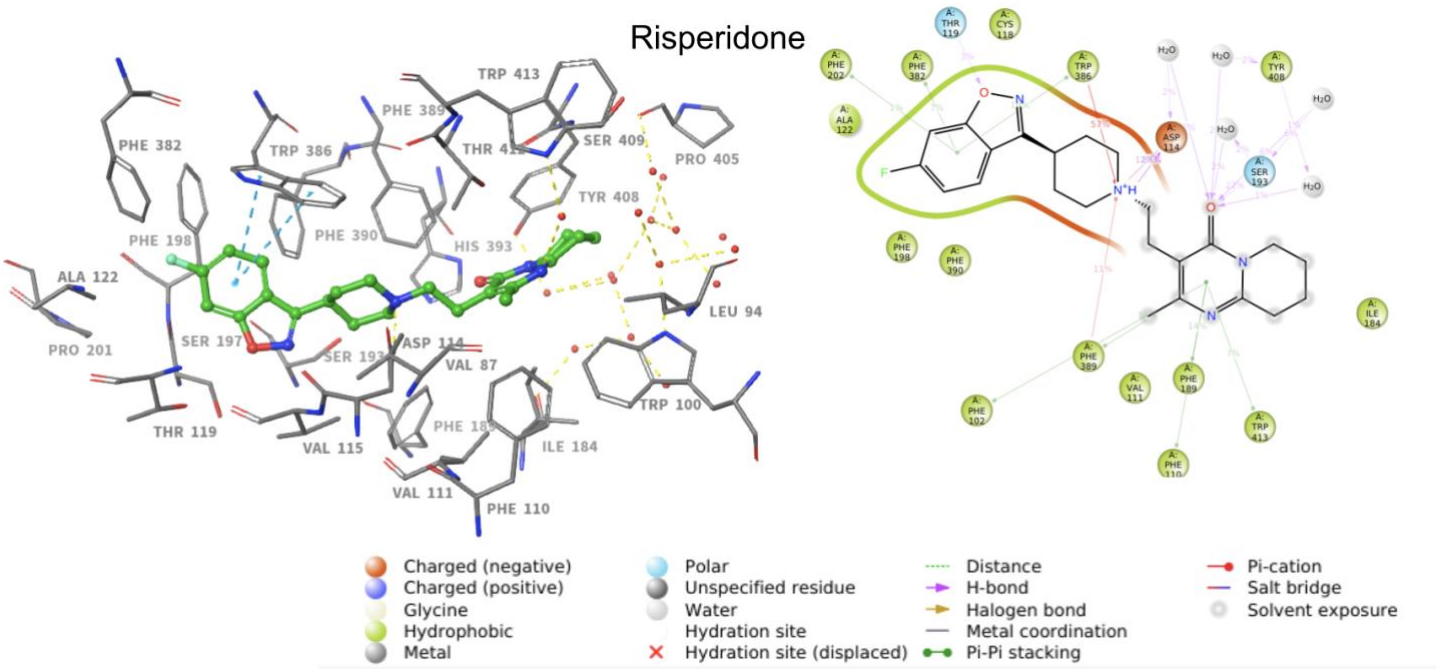

Figure 19: *Protein-ligand contact analysis of risperidone in dopamine D_2 receptor. In left panel: 3D representation of binding site residues in gray and risperidone in green. Dotted line in blue shows $\pi - \pi$ stacking interactions, pink dotted line shows ionic interactions, yellow line shows hydrogen bonds and red spheres represent water molecules. In right panel: 2D representation of binding site residues in bubbles and ligand in black.*

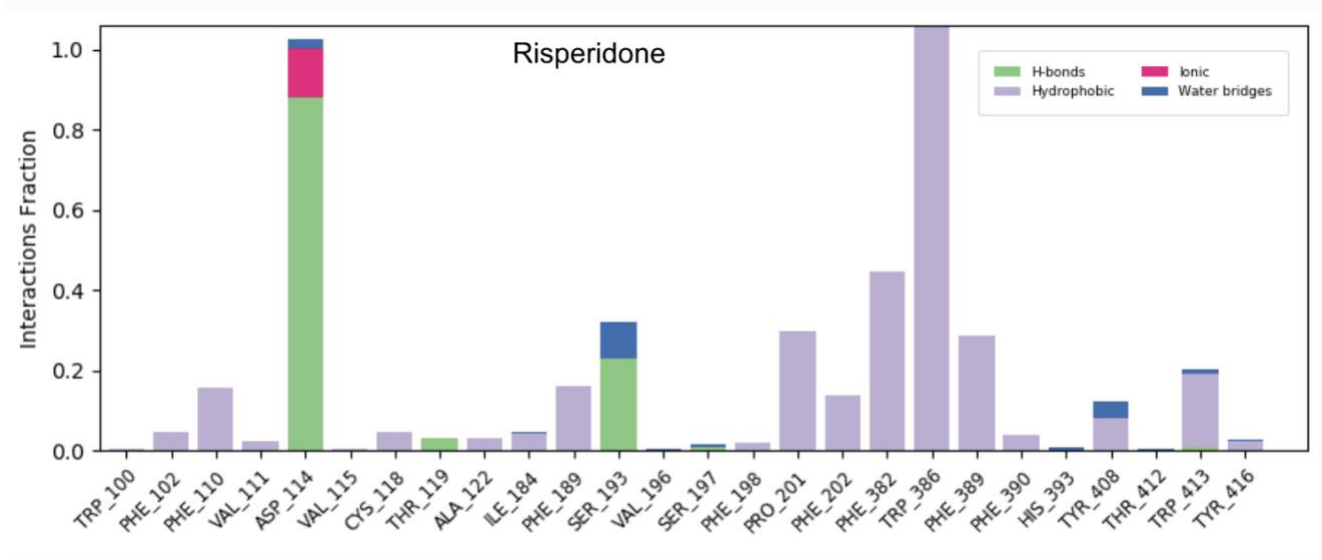

Figure 20: *Fraction of Interactions between ligand and binding site residues presented as bar-diagram. Green is hydrogen bonds, pink is ionic interaction, blue represents water bridges and lilac are hydrophobic interactions.*

Pimavanserin was docked into the serotonin 5-HT_{2A} receptor and among the main interactions were a hydrogen bond and a salt bridge between protonated nitrogen on ligand and Asp155(3.32) in binding cavity. The hydrogen bond was maintained for 94% of the simulation time while the ionic interaction was maintained for 6.4%. Comparably to previous structures, the 5-HT_{2A} receptor has an aromatic hydrophobic network in the binding site

consisting of the residues Trp336(6.48), Phe339(6.51), Phe340 (6.52), Phe243(5.47) and Phe234(5.38) which participate in vdW, $\pi - \pi$ stacking and cation- π interactions throughout the simulation period. Both Asn343(6.55) and Ser239(5.43) contributed to water bridge interactions with the ligand for 47% and 14% of the simulation time respectively while an additional hydrogen bond with Ser239(5.43) was created. Ultimately, for 67% and 45% of the MD simulation time, a water bridge and vdW interaction respectively, were established between Leu229(ECL2) and pimavanserin. Visual representations in figure 21 and 22. Common to all systems was that none of the ligands had significant interactions with amino acids in TM1, TM2 or TM4.

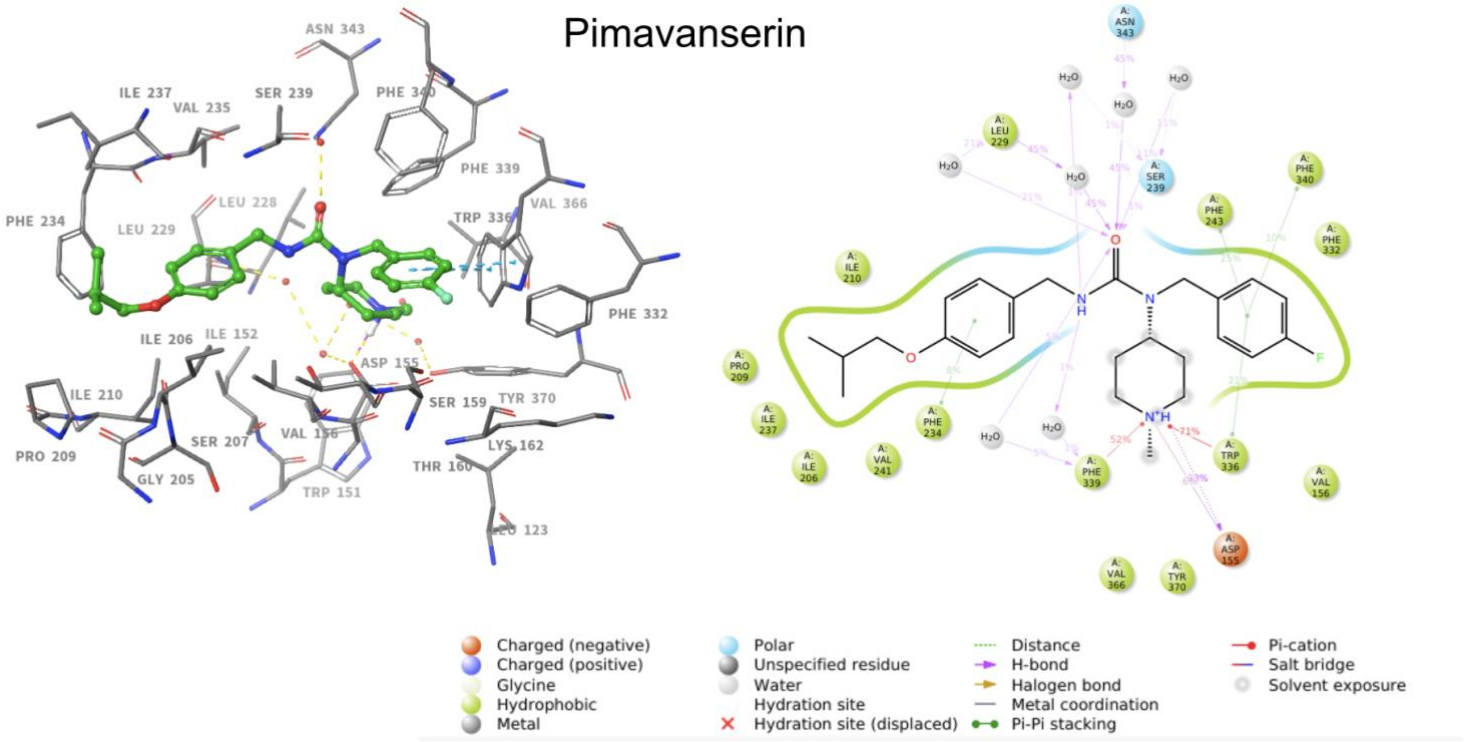

***Figure 21**: Protein-ligand contact analysis of pimavanserin in serotonin 5-HT$_{2A}$ receptor. In left panel: 3D representation of binding site residues in gray and pimavanserin in green. Dotted line in blue shows $\pi - \pi$ stacking interactions, pink dotted line shows ionic interactions, yellow line shows hydrogen bonds and red spheres represent water molecules. In right panel: 2D representation of binding site residues in bubbles and ligand in black.*

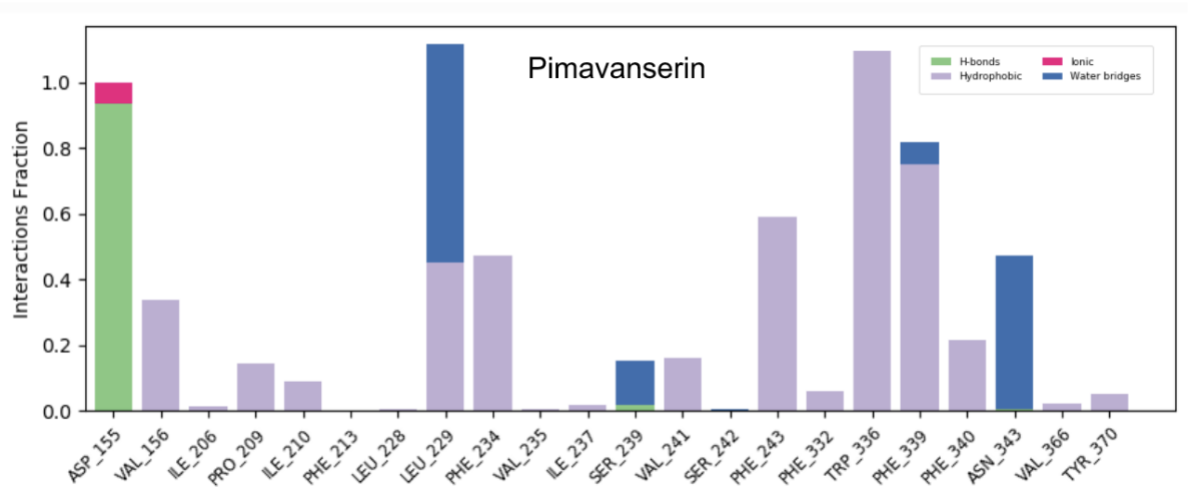

***Figure 22**: Fraction of Interactions between ligand and binding site residues presented as bar-diagram. Green is hydrogen bonds, pink is ionic interaction, blue represents water bridges and lilac are hydrophobic interactions.*

Bromocriptine in the shorter simulation, exhibits more or less the same interactions that were revealed in the bromocriptine 1000 ns with G-protein system. The main differences lie in the fraction of the interactions, for instance, the ionic interaction with Asp114(3.32) is established for approximately 11% of the simulation time, while hydrogen bond and water bridge with the same residue is maintained for 89% and 41% respectively. Ile184(45.52) participated in hydrogen bond as a donor with bromocriptine for 94% while also creating hydrophobic interactions. Ser197(5.46) also made a stable hydrogen bond to the ligand. Phe390(6.52), Phe389(6.51), His393(6.55) were making $\pi - \pi$ stacking interactions with bromocriptine throughout the whole simulation time (figure 23).

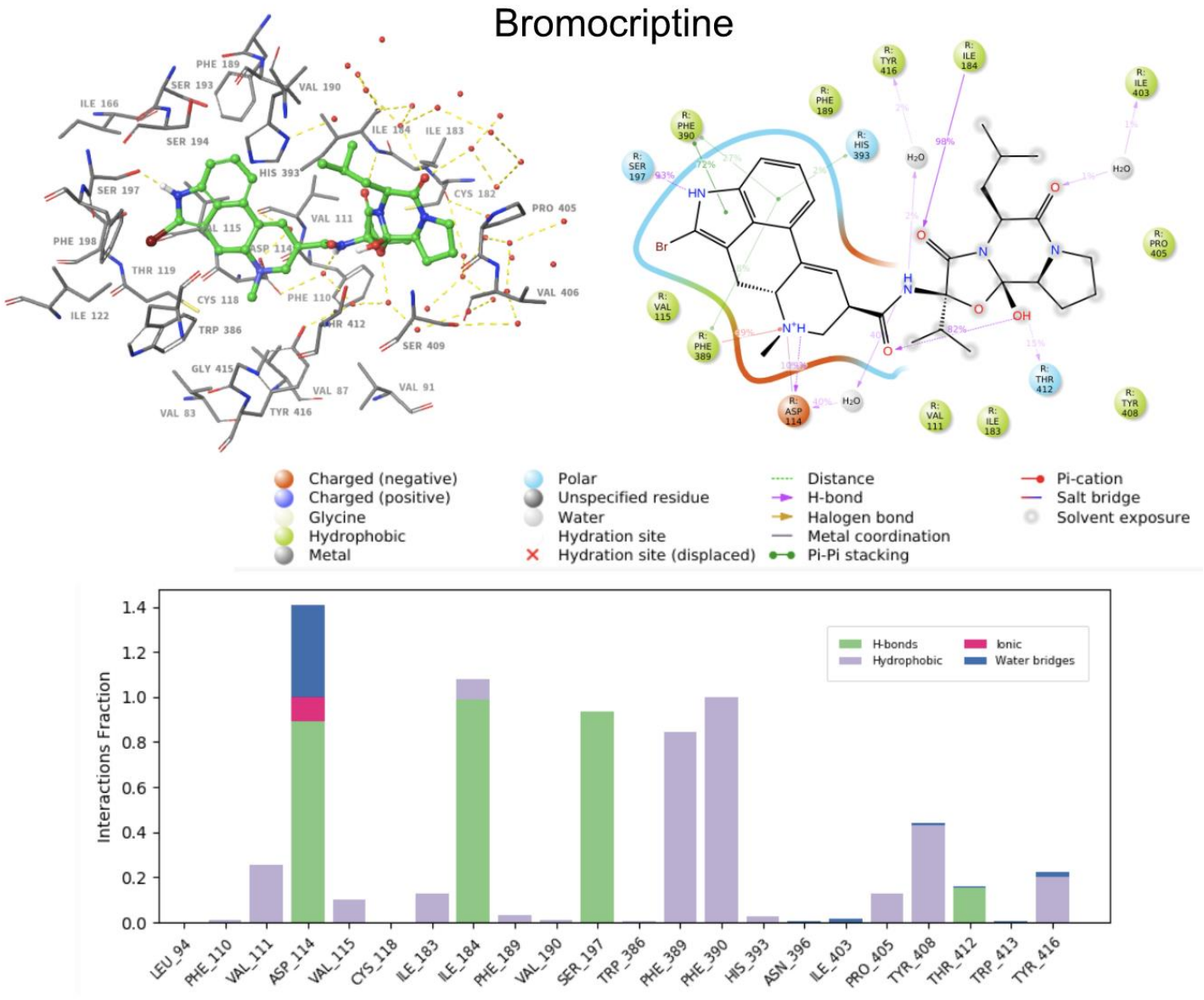

Figure 23: *Top: Protein-ligand contact analysis of bromocriptine in dopamine D_2 receptor* ***without*** *G-protein. In left panel: 3D representation of binding site residues in gray and bromocriptine in green. Dotted line in blue shows $\pi - \pi$ stacking interactions, pink dotted line shows ionic interactions, yellow line shows hydrogen bonds and red spheres represent water molecules. In right panel: 2D representation of binding site residues in bubbles and ligand in black. Bottom: Fraction of Interactions between ligand and binding site residues presented as bar-diagram. Green is hydrogen bonds, pink is ionic interaction, blue represents water bridges and lilac are hydrophobic interactions.*

4.2.4 Comparison of active and inactive dopamine D_2 receptor

The conformations of inactive (bound to antagonist risperidone PDB: 6CM4) and active dopamine D_2 receptors (bound to agonist bromocriptine PDB: 6VMS) were thoroughly looked at to identify the major structural differences. The most obvious differences in these structures that were observed, involved a rearrangement of the helices in the seven transmembrane domains, the most considerable being in TM3 and TM6. In figure 24, TM6 is coloured in dark green while TM3 is coloured in light green. In the inactive conformation, the cytoplasmic halves of TM3 and TM6 are oriented towards each other creating an ionic interaction between well conserved Arg132(3.50) and Glu368(6.30) also known as an ionic lock. The ionic lock is disrupted in the active conformation as the cytoplasmic halves of TM3 and TM6 are pointing in different directions. Further, in the active state, the residues Ile184(ECL2) and Phe189(5.38) seem to have a greater distance between them as the extracellular loop 2 changes conformation and thus creates more room. Collectively, the inactive conformation of the dopamine D_2 receptor seems to be more compact compared to the active form.

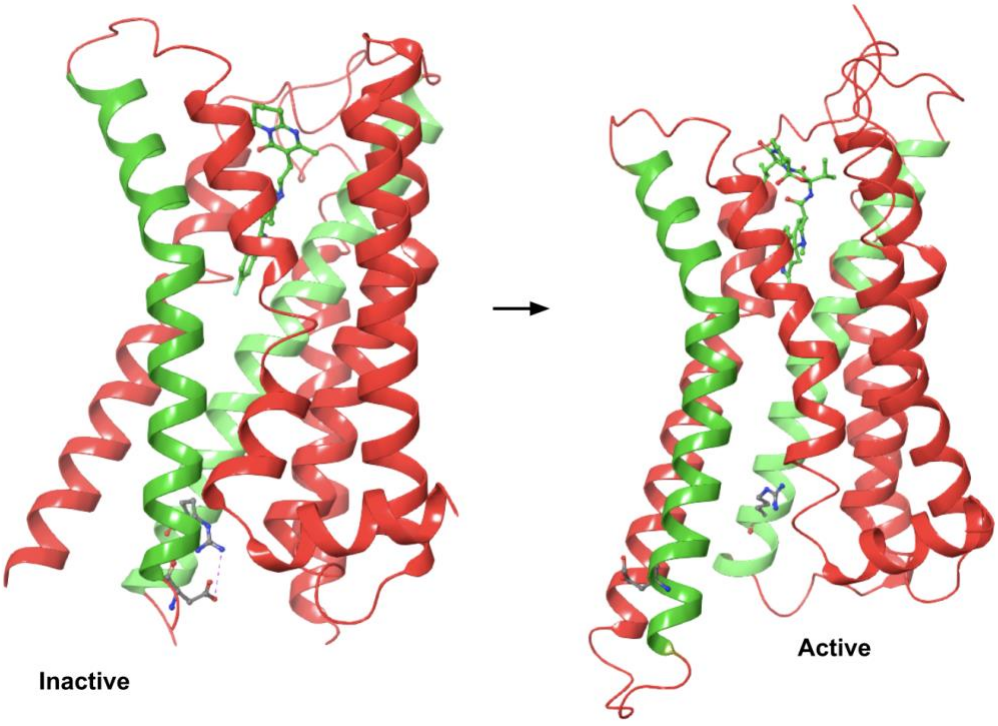

***Figure 24**: presentation of the dopamine D_2 receptor in inactive (left) and active (right) conformation. The inactive structure is bound to risperidone while the active is bound to bromocriptine. TM6 and TM3 are coloured dark and light green respectively. Pink dotted line in inactive receptor displays a salt bridge (ionic lock) between Glu368 and Arg132 which is disrupted in the active conformation. ICL2 and ICL3 loop in inactive structure are not shown, nor the G-protein in the active form.*

Further, the structures were superimposed as seen in figure 25 under. The calculated RMSD value was 10.10 Å and the biggest deviation between the superimposed structures seemed to be the orientation of especially TM6 as the bottom part of this helix did not align as well as the other TMs. The rest of the TMs seem to align decently even though none of them are 100% overlapped as understood from the RMSD value. A low RMSD value, usually around 3 Å according to the Desmond user manual software (75), indicates a perfect fit.

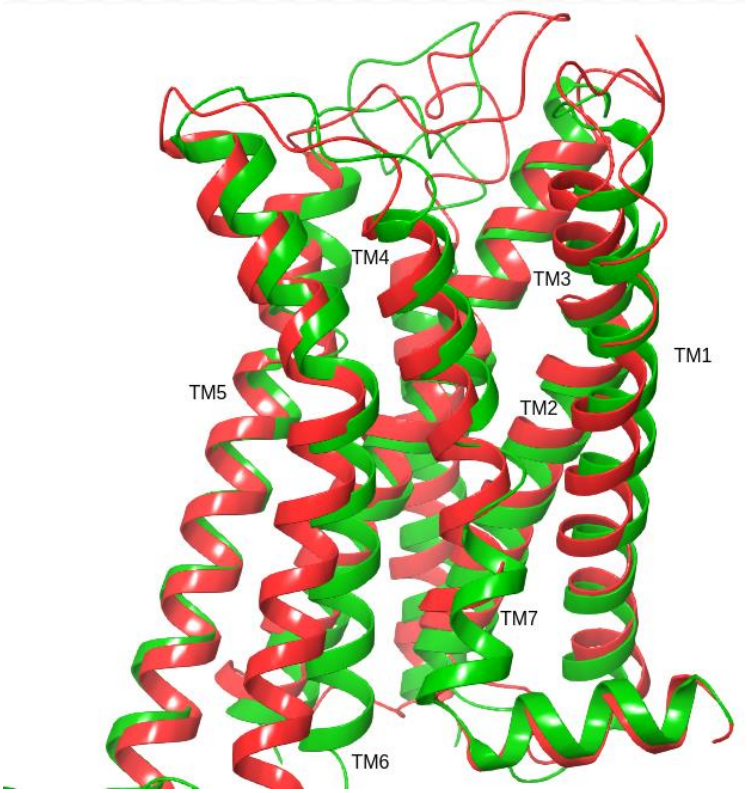

***Figure 25**: inactive (green) superimposed on active (red) dopamine D_2 receptor. Calculated RMSD value based on backbone atoms = 10.10 Å*

Additionally, the conformation of aripiprazole (partial agonist) in the dopamine D_2 receptor was also studied. When it comes to accommodation in the orthosteric binding site, the phenylpiperazine part of aripiprazole and the multiple ring system in bromocriptine, occupy the same regions, interacting with ECL2, TM3, TM5, TM6 and TM7. The benzioxazole moiety of risperidone on the other hand, extends into a deep binding pocket consisting of TM3, TM5 and TM6 as seen in figure 26. These residues were mentioned in earlier sections presenting protein-ligand interactions. Exclusively, bromocriptine established a stabile hydrogen bond to Ser197(5.46) in TM5 and also $\pi - \pi$ stacking and water bridge interactions to His393(6.55) that were not found in the partial agonist nor antagonist system.

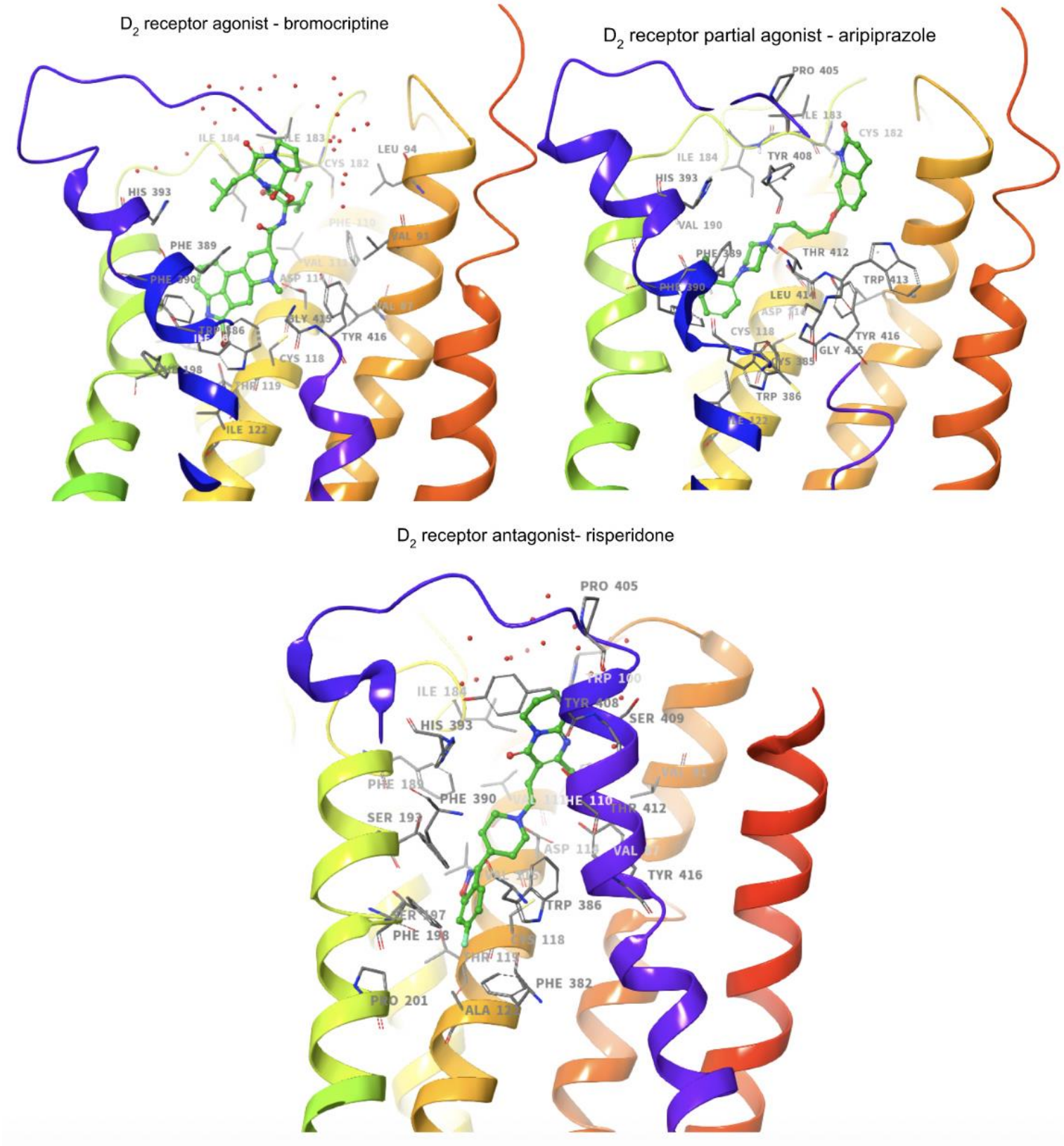

Figure 26: *comparisons of agonist (top left), partial agonist (top right) and antagonist (bottom) in the dopamine D_2 receptor. Ligands and residues are displayed in green and gray respectively. TM6 (blue) and TM7 (purple) were partially removed to visualize the accommodation better. All structures are based on the starting structure*

In the binding site of the serotonin 5-HT_{2A} receptor, the fluorobenzyl ring of pimavanserin occupied a region located deep within the receptor as seen in figure 27. Two of the interactions that were established in this region were hydrophobic involving Trp336(6.48). The chemical structure of pimavanserin deviates excessively from to structures of bromocriptine, aripiprazole and risperidone and is much smaller and compact. In addition to pimavanserin extending to a deeper region, it also seems to occupy a side extended cavity in TM5 with the isobutoxybenzyl group of the drug (to the far left). A side extended cavity like this, was not observed in the D_2 receptor. Some of the residues in this cavity in close vicinity to pimavanserin, included Gly238(5.42) and Leu229(ECL2) contributed with both polar (through water molecules) and non-polar interactions.

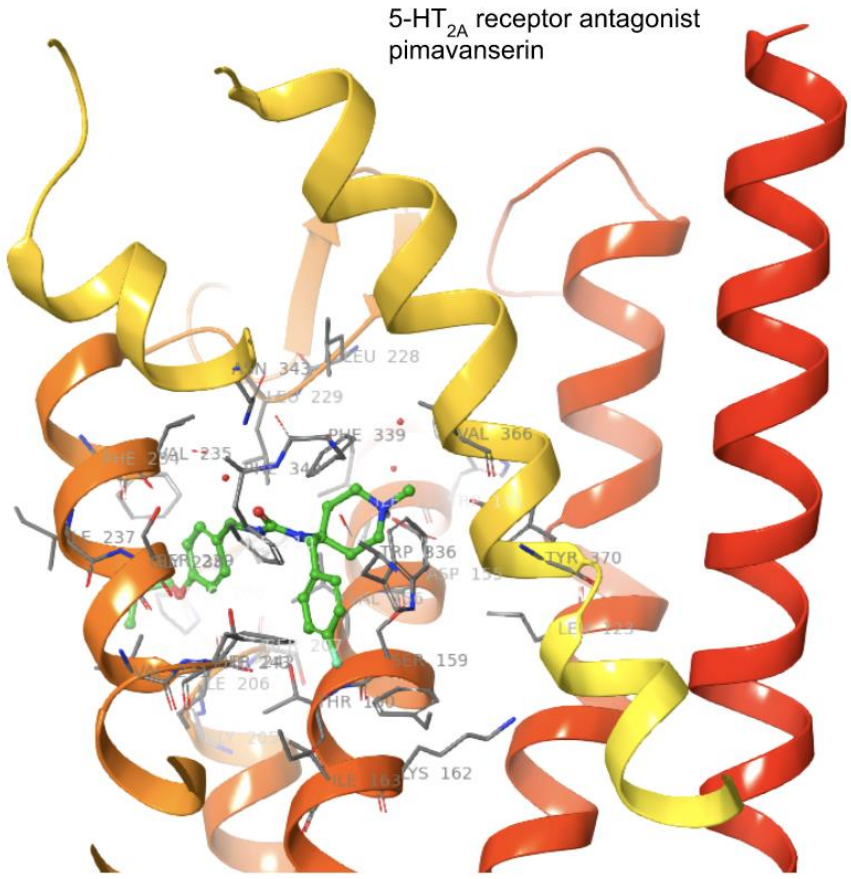

***Figure 27**: representation of pimavanserin in the binding site of the serotonin 5-HT_{2A} receptor. Pimavanserin is displayed in green, TM6 (yellow to the left) was partially removed to visualize the accommodation better.*

5 Discussion

The main aim of this present study was to obtain a deeper understanding of how antipsychotics interact with specific G-protein coupled receptors at a molecular level, that are important for their therapeutic effects (dopamine D_2 and serotonin 5-HT_{2A} receptors) and adverse side effects (dopamine D_2, 5-HT_{2C} and histamine H_1 receptors). Firstly, the binding affinity and docking scores of 37 antipsychotic drugs for the four G-protein-coupled receptors, dopamine D_2, serotonin 5-HT_{2A}, 5-HT_{2C} and histamine H_1 receptors were studied. Secondly, the binding poses of bromocriptine which is an agonist on the dopamine D_2 receptor were compared to the binding poses of aripiprazole and risperidone, a partial agonist and antagonist on the same receptor respectively. Pimavanserin, a selective 5-HT_{2A} antagonist that is currently only marketed in the U.S as an antipsychotic drug in the treatment of Parkinson's disease psychosis, was also investigated. Methods within computational chemistry e.g., IFD and MD simulations were used to accomplish this, and a huge advantage is that this approach accelerates and reduces the cost, risk and time it takes to obtain valuable information about interesting compounds.

5.1 Induced fit docking

The ability to model IFD provides more accurate conformations compared to standard glide docking where ligands are docked into rigid or semi rigid protein structures. Upon binding of a drug to its target in reality, the protein structure of the target undergo dynamic changes to perfectly accommodate the ligand and this is taken into consideration with IFD. Normally, standard glide docking takes much shorter time but the negative side of this is the introduction of sensitivity for the reason that only one or very few conformations are used to represent the receptor and thereby overlooking all conformational changes in the ligand binding pocket induced by a ligand (97). The docking of all 37 ligands in the four receptors (D_2, 5-HT_{2A}, 5-HT_{2C} and H_1) was specified with constraints to ensure that the protonated amine in the ligand formed a salt bridge interaction with the carboxylate group of Asp(3.32). This interaction is known to be important for both binding and activation of agonists and also important for binding of antagonists to biogenic amine class A G-protein-coupled receptors (16, 44, 59, 80).

Even though IFD is a more time-consuming process than standard glide docking, applying constraints definitely reduced the number of poses and helped to further save time during the analysis. For the purpose of only docking 37 drugs in four different receptors, this approach was sufficient and effective.

Upon docking of the drugs in their respective target receptors, the binding sites were defined in advance by using grids or enclosing boxes. A grid is a box-shaped lattice consisting of spaced points surrounding and centered on interesting regions of the target protein and was set to include 20 $Å^3$ (98). This was done to ensure that the drugs were incorporated or embedded into the regions within the receptor that defined the binding site interacting with important residues. This process however has some limitations, among them that by using grids, all conformational changes that might occur on both the drug and the target are not taken into consideration simply because we only obtain information that is generated after the drug is placed into the binding site.

The results from the IFD, were further based on a "scoring approach" where the binding affinity or energy of a protein-ligand complex was calculated and ranked. To process the number of molecules involved in a docking process, the scoring calculations have to be rapid. However, they also have to be accurate enough to give good measures of the binding affinities. This is a difficult compromise as increased computational speed can include applying simplifications or short cuts as well as assumptions. This in turn, reduce the accuracy, hence, the evaluation of a drugs affinity to its target is affected (31, 73). Force fields that estimate binding affinities by summarizing the contribution of different interactions (such as vdW and electrostatic interactions) and bond bending/angles/stretching etc, were applied which creates an uncertainty. This is further discussed in detail later.

Another drawback with scoring function is that water molecules were not taken into consideration although the biological systems are located in aqueous environment. Water molecules can form interactions with surrounding molecules including the drug, and thereby have an impact on the docking score (60, 83, 84). Finally, all of the drugs that were docked were alkaline with pKa values above 7 (common for alkaline compounds) while the aqueous environment utilized in the process pH of 7.0 ± 2.0. Due to differences in acidity in the environment and the actual compounds, the drugs exist in both protonated and unprotonated states. It is the protonated state of the drug that establishes a salt bridge interaction to Asp3.32 (in all of the aminergic receptors used in this thesis), hence that state is docked. The

unprotonated state is not payed regards to, and the fraction of unprotonated versus protonated state remains unknown. Determination of the concentration needed of the drug to occupy 50 percent of the receptors is therefore not 100 percent accurate.

5.1.1 The context between receptor binding profiles and side effects

Among the most recurrent side effects of antipsychotic drugs levomepromazine, prochlorperazine, quetiapine, olanzapine, risperidone and aripiprazole are sedation or drowsiness. Sedation and drowsiness are mainly associated with antagonism on the histamine H_1 receptor according to previous articles (32, 93). This can also be seen in light of the affinity values reported for these drugs on the histamine H_1 receptor. The reported K_i values of levomepromazine, prochlorperazine, quetiapine, olanzapine, risperidone and aripiprazole on the H_1 receptor presented in table 4, were 0.6 nM, 6.0 nM, 2.2 nM, 0.09 nM, 3.5 nM and 25.1 nM respectively. Thus, mostly classified as high affinity with the exception of aripiprazole that would be classified as a moderate affinity drug on the histamine H_1 receptor. The induced fit docking scores were -8.4 kcal/mol for levomepromazine, -11.3 kcal/mol for prochlorperazine, -10.9 kcal/mol for quetiapine, -9.8 kcal/mol for olanzapine, -9.5 kcal/mol for risperidone and -9.6 kcal/mol for aripiprazole. Twenty of the 30 drugs with reported binding affinity values from PDSP on the H_1 receptor could be classified as high affinity drugs. This more or less demonstrates why many patients experience sedation or drowsiness upon antipsychotic treatment. For patients that are agitated and suffer from acute psychosis though, these side effects can have a beneficial effect and are generally more tolerable (32). Further, such side effects tend to decrease with continued use and are «mild» compared to other side effects described later in this chapter.

The histamine H_1 receptor is a G-protein-coupled receptor with many structural similarities to both the dopamine and serotonin receptors such as the conserved CWxP, PIF, NPxxY and DRY motifs as well as a conserved disulphide bridge between ECL2 and the top of TM3 (56, 57). However, according to Shimamura et al. 2012 (80), the overall size of the ligand binding pocket of the histamine H_1 receptor seems to be more spacious because the ECL2 constitute more residues which increases the distance between TM3 and TM5 compared to dopamine and serotonin receptors. This ultimately results in better accommodation of histamine H_1

selective antagonists such as doxepin, a tricyclic antidepressant, as they tend to be quite bulky and large. The main residues that are involved in interactions with doxepin are Asp107(3.32) forming a salt bridge, and Ile115(4.40), Phe24(6.44), Trp428(6.48) and Phe432(6.52) participating in hydrophobic interactions such as $\pi - \pi$ stacking. For reference, the reported K_i value of doxepin on the H_1 receptor is 0.09 nM (99) and comparably to the antipsychotics discussed in the present study, the most pronounced side effect of doxepin too, is sedation.

Extrapyramidal side effects (EPS) being acute dystonia, tardive dyskinesia, akathisia, rigidity, tremor and bradykinesia are usually explained by antagonism at D_2 receptors especially in the nigrostriatal pathway and are thus more prevalent with TAPs (11, 18, 100). It is believed that the severity of EPS produced by the drugs, increases with its affinity for the D_2 receptor (11). Levomepromazine and prochlorperazine are two of the most prescribed TAPs in Norway and their K_i values on the dopamine D_2 receptor are 5.9 nM and 0.2 nM respectively. This renders them both high affinity and using these drugs over long time increases the risk of developing EPS. AAPs on the other hand, act by simultaneous antagonism on the 5-HT_{2A} receptor, decreasing the inhibitory effect serotonin has on the dopaminergic system in the nigrostriatal pathway and thereby reducing the severity of dopamine D_2 antagonist-induced EPS (44). Therefore, the frequency of EPS in AAPs in general is lower. In the present study, some examples of AAPs are risperidone, olanzapine, quetiapine, aripiprazole and clozapine. The K_i values for risperidone for instance on the D_2 and 5-HT_{2A} receptor were 0.3 nM and 0.1 nM respectively, which means its binding affinities to both these receptors are high. This is in good agreement with the findings in Kimura et al 2019 (44). The same trend was seen in Yonemura et al 1998 (93) and Kondej et al 2018 (47).

Besides side effects such as such as sedation and motor disturbances i.e., EPS, some antipsychotic drugs are further known to affect metabolic regulation. Endocrine disturbances can occur by antagonism on D_2 receptors in the anterior pituitary gland, leading to hyperprolactinemia and abnormal breast enlargement in both genders. This side effect is much more prevalent in TAPs compared to AAPs (101). Another effect, antipsychotic-induced weight gain, can quickly result in obesity which in the worst case can develop into diabetes (102, 103) . It is believed that this most likely involves antagonism at both the histamine H_1 receptor and the 5-HT_{2C} receptor and is a result of altered glucose tolerance as well as increased food intake (11, 18, 103-105).

Clozapine has moderate affinity for the dopamine D_2 receptor (K_i value of 44 nM) but high binding affinity to 5-HT_{2A}, 5-HT_{2C} and histamine H_1 receptors with reported values of 5.4 nM, 9.4 nM and 1.1 nM respectively. It is associated with absence of EPS but a significant risk of weight gain. The affinity of olanzapine on the 5-HT_{2C} and histamine H_1 receptors was 4.1 nM and 0.09 nM respectively. These findings confirm what was found in previous articles (11, 42, 103-105) where it was concluded that clozapine and olanzapine are amongst the antipsychotics with most pronounced risk of weight gain. In two articles (105, 106) where antipsychotic drug-induced weight gain was investigated, it was concluded that individuals on treatment with clozapine and olanzapine, gained a mean of approximately 12 kg and 7-12 kg respectively over a period of 12 months. Nasrallah et al (106) further stated that compared to clozapine and olanzapine, use of risperidone was associated with a mean weight gain of 2-3 kg over the same period. Additionally, in 2004 Bitter et al found no statistically significant difference in weight gain between clozapine and olanzapine (107). The similar behaviour observed with clozapine and olanzapine is probably due to the similarities in their chemical structures, figure 8.

Interestingly, haloperidol which is a TAP, has much lower affinities for histamine H_1 and 5-HT_{2C} receptors with K_i values of 1800 nM and >10000 nM respectively and is known to have an insignificant effect on weight gain (38, 105). Patients on AAP treatment gained more weight than patients on TAPs according to a Cochrane meta-analysis from 2010 (108). However, the same pattern was not observed for other TAPs like levomepromazine and prochlorperazine as their affinities were moderate to high on H_1 and 5-HT_{2C} receptors. Finally, it is worth noting that despite not being mentioned in this study, TAPs are commonly divided into low- and high potency drugs which are equally efficacious. The groups nonetheless differ in tolerability and side effects and can explain why different trends are seen in different TAPs even though they belong to the same category (38).

Pimavanserin is very selective to the serotonin 5-HT_{2A} receptor with a K_i value of 0.087 nM and 0.44 nM for the serotonin 5-HT_{2C} receptor (92). No appreciable affinity values (K_i value over 300 nM) were reported for pimavanserin on any other aminergic receptor, and one can speculate that that is the reason why most of the common side effects of pimavanserin differ from those of conventional antipsychotics. Some of these side effects include nausea and constipation. However, more severe psychiatric disturbances upon pimavanserin treatment such as hallucination, delirium and gait disturbance, have been reported (92).

For many years, clozapine has been the gold standard in treatment-resistant schizophrenia and related disorders when treatment with other antipsychotic drugs remains inadequate (18, 102, 103). In addition to previously mentioned side effects, agranulocytosis and neutropenia (lowered white blood cell count) are rare, yet life-threatening side effects that are estimated to occur in 1-2 percent of clozapine treated patients (46). These drug-induced haematological reactions are most likely results of hypersensitivity reactions and not directly linked to binding affinity on any of the respective receptors. The exact mechanism remains unclear, but one theory proposes that antibodies against neutrophils may be produced upon treatment with clozapine which ultimately leads to a deficit in white blood cells (109). It is impossible to predict the risk of these side effects so diligent monitoring is required. The risk of agranulocytosis is however believed to be higher among women and increases with age (46).

Just like with all drugs, it is more than the actual drug that determines whether a patient develops side effects or not. Background variables like gender, genetics and age are important factors that help explain the reasons why some patients are more prone compared to others. The severity of the side effects is extremely difficult to prognosticate, and in some cases, the side effects occur in the beginning of the treatment but lessen with time. Other times the side effects are so severe that discontinuation is the only option. Receptor binding profiles are partially useful in predicting side effects but are not alone advance enough to properly understand the physiologic and pharmacologic mechanisms involved.

5.2 Molecular dynamics simulations

In part two of this study, MD simulations were run, and detailed descriptions are provided in earlier chapters. In comparison to IFD, the MD simulations incorporated information about structural conformational states important for understanding the pharmacology and physiology of GPCRs, that could not be obtained solely based on IFD. Further, the MD simulations yielded valuable information about the strength of ligand-protein interactions in terms of contact frequencies. This was very helpful in the identification of key interactions established between the ligands and the receptors, especially when comparing the intrinsic activity of different ligands on the same receptor. Ultimately, utilizing MD simulations gave insights into the differences between activated and inactivated D_2 receptor, highlighting some of the interactions that were formed. An advantage with the MD simulations was its ability to successfully carry out the simulations despite the fact that the systems were quite large, consisting of over 100,000 atoms each.

Conclusively, MD simulations have improved performance compared to IFD and also allows simulation of larger systems over longer periods of time. However, the running time can be up to several weeks, which sometimes is regarded as a limitation (72). This method is more resource-consuming than docking studies but in return, it provides a much higher accuracy and reliability.

One drawback that limits the usability of MD simulations in this thesis, is the use of force fields because they are generally based on approximations and experimental measurement and are thus not 100 percent accurate. The OPLS_2005 force field was utilized, however, there are newer and more updated force fields such as OPLS3e that achieve a higher level of accuracy in e.g., predicting protein-ligand binding. The improvements that have been introduced, include extensive parameterization of valence and torsional terms, virtual sites that better compute partial charges and represent lone pairs and charge distributions as well (110). These are indeed enhancements that lead to improved performance, nevertheless, there is always room for improvement. As more knowledge of even more complex chemical systems is obtained, new challenges with the fidelity of force fields are exposed. Further, as more reference data become available, additional refinements like improved torsion types to better determine e.g., conformation energies, will be necessary to ensure more robust and meaningful results (110).

Another important challenge is the simulation timescale step which is the time length between evaluations of the potential. In many cases the timestep is not small enough to capture the fastest relevant molecular events and movements, and one fears that valuable information is lost or left out. The consequence of this would be poor characterization of the proteins dynamic behaviour. There are techniques such as simplifying the models, metadynamics and simulated annealing that can be applied to overcome this limitation and fortunately, advances in algorithms, hardwares and softwares have increased the effectiveness of timesteps (72).

The application of MD simulations definitely provides valuable information that is useful in particularly drug design and is less resource consuming compared to experimental methods. This approach is faster, cheaper and more accessible and can for instance improve lead optimization e.g., by refining them to improve their selectivity based on the dynamic nature investigated with MD simulations (111).

5.2.1 The structural stability of the systems

Among the important parameters used to evaluate the structural changes that occurred during the simulations, are RMSD and RMSF. RMSF was also used to describe relative mobility of specific regions of the systems. Like mentioned in earlier sections, ligand-free systems were constructed in addition to the ligand-bound systems to investigate the influence the respective ligands had on the dynamic profiles of the proteins. Regarding the RMSDs, collectively, the ligand-bound structures (except pimavanserin in 5-HT_{2A} receptor) were less stable compared to the ligand-free systems. The reported RMSD values were in general a bit higher in the ligand-bound systems as well. Further, in the ligand-bound systems, the plots seemed to increase in the beginning before establishing a stable path out the simulation. Oppositely, in the ligand-free systems, the plots seemed more stable in the beginning before slight increasing were observed towards the ends of the simulations.

The overall RMSD values for the ligand-free systems were lower than the ligand-bound, which further renders them more stable, as seen in figure 10 and 11. Based on this, it is reasonable to assume that the presence of ligands in the binding cavities, affect the dynamic and structural behaviours of both the dopamine D_2 and serotonin 5-HT_{2A} receptors. This is most likely a result of interactions that were formed between the drugs and the binding site

residues within the receptors. It was expected that the biggest changes would be seen in the partial agonist and especially agonist plots, simply because drugs with these intrinsic activities are expected to have a significant influence on their target. Pimavanserin and risperidone are both antagonists on their respective receptors and their plots seem more stable, ergo they seem to affect their targets less. However, it is important to elucidate the fact that the G-protein was coupled to the receptors in the bromocriptine and aripiprazole systems, but not in the pimavanserin and risperidone systems. It is very possible that the G-protein also had an influence on the overall plots and RMSD values.

When it comes to the RMSF plots for all of the systems, they were in good agreement with what is already known about secondary structures. The highest peaks and biggest fluctuations were observed in the loop regions and particularly the amino and carboxyl terminuses as these are studied to be the most flexible and variable segments (57, 72). Regions with less peaks and low RMSF values corresponded to the transmembrane helices where the amino acids are stabilized by the secondary structure, similarly to what was discovered by Salmas et al 2016 (16). The regions representing the beta strands were also relatively low compared to the loop regions and in this case, beta strands were only observed in the systems containing the G-protein. Loops are generally more exposed to the surface compared to other secondary structures which are hidden in cores and more conserved. Thus, loop are usually more susceptible to changes, often have lower sequence conservation and can adopt many different structural forms (56).

Both the RMSD and RMSF plots for aripiprazole revealed higher flexibility compared to the other plots correspondingly to the findings in Salmas et al (16). In the same article they suggested that the reason for this was the extended structure of the drug and hydrogen bonds that were forming and breaking between some of the TMs. However, this was not investigated further in the present study.

5.2.2 Protein-ligand interactions

The interactions of bromocriptine, aripiprazole, risperidone and pimavanserin were investigated based on the results from the MD simulations. What was seen in all systems, was the ability to make a salt bridge interaction between protonated nitrogen in the drugs and conserved Asp(3.32) in the dopamine D_2 and serotonin 5-HT_{2A} receptor. From earlier, it is known that particularly this interaction is a part of the aminergic receptors pharmacophore and crucial for receptor binding (16, 44, 47, 59, 80, 112, 113). The other interactions that seemed to be necessary for receptor binding included both polar and non-polar interactions such as hydrogen bonds, hydrophobic interactions ($\pi - \pi$ stacking, vdW and cation- π interactions) and water bridges. This was described in detail in earlier sections. A comparison of bromocriptine, aripiprazole and risperidone in the dopamine D_2 receptor revealed that bromocriptine established a stable hydrogen bond to Ser197(5.46), $\pi - \pi$ stacking and water bridge interactions to His393(6.55) that were not found in the partial agonist nor antagonist system. The hydrogen bond established between bromocriptine and Ser197(5.46) has been reported to be necessary for receptor activation (64, 67, 113) and was observed in both of the simulations that were run with bromocriptine in the present study.

Interestingly, in the aripiprazole-D_2 receptor complex, two stable hydrogen bonds were observed with Cys182 (in ECL2) that were not observed in any of the other systems. These hydrogen bonds were present throughout the simulation which most likely means they have a significant importance in the effect of aripiprazole on the dopamine D_2 receptor. Activation of the dopamine D_2 receptor, includes interactions with serines in TM5 (Ser5.42 or Ser5.43 or Ser5.46) and these were lacking in the aripiprazole- D_2 receptor complex. Thus, this is likely to result in reduced receptor activation which can contribute to the reason why aripiprazole is classified as a partial agonist.

Moving further, it was observed a hydrogen bond with Ser193(5.42) in the risperidone- D_2 receptor complex that did not seem to be crucial due to the fraction of approximately 20%. Compared to bromocriptine and aripiprazole, risperidone did not establish any hydrogen bonds of significant importance and earlier publications (16, 44, 59), have not either mentioned hydrogen bonds as important for risperidone binding to an inactive state conformation of the D_2 receptor. Other interactions however, such as hydrophobic interactions (vdW and $\pi - \pi$ stacking interactions) with the hydrophobic aromatic network in

the D_2 receptor, have been mentioned and is in good agreement with the findings of the present study. In contrast to the active structure of the dopamine D_2 receptor, the inactive structure seems to be more compact which also allows for the «ionic lock» to constrict the receptor. Similarly to what was reported by Salmas et al in 2015 (59), the more spread-out active structure on the other hand, reveals an outward movement of TM5 and TM6 which creates a suitable site for the binding of a G-protein at the bottom of these helices as seen in figure 23.

Regarding pimavanserin, its binding profile to the serotonin 5-HT_{2A} receptor in the present study included hydrogen bond and salt bridge to Asp155(3.32), hydrophobic interactions to Trp336(6.48), Phe339(6.51), Leu229(ECL2) among others. Water bridges were created to especially Leu229(ECL2) and Asn343(6.55). Kimura et al (44) reported similar findings in 2019.

5.2.3 Binding modes of the antipsychotic drugs

When it comes to the binding poses, the different antipsychotic drugs seem to bind and occupy different regions which probably has something to say for their binding affinities and intrinsic activities. Firstly, it is relevant to mention that multiple previous publications have categorized the drugs into different groups mainly based on their structures. The structures of the antipsychotic drugs are shown in figure 8. Class I drugs, such as clozapine, olanzapine share bulky structures while class II drugs like aripiprazole and risperidone have a more extended chemical structure (59, 67). In this case, only based on structure, pimavanserin is more similar to class II drugs. Class II drugs, risperidone in particular, extends into a deep binding pocket in the dopamine D_2 receptor, which is situated below the actual orthosteric site according to Wang et al 2018 (79) and also confirmed in the present study. The predicted binding site of antagonists such as risperidone in the dopamine D_2 receptor, includes the extended deep pocket and is found to consist of TM2, TM3, TM4, TM6 and TM7 with minimal interactions to residues in TM5 like described earlier (64). Further, Kimura et al 2019 (44) pointed out that pimavanserin due to its structure, occupied a side extended cavity which they suggested contributed to the high selectivity for the 5-HT_{2A} receptor. This is because the side extended cavity of other serotonergic receptors most likely are too shallow to

accommodate pimavanserin. However, due to short time, this was not investigated thoroughly in the present study.

Bromocriptine and aripiprazole did not extend into a deeper binding pocket, but they occupied the same regions in the orthosteric binding pocket, interacting with TM3-TM6. These TMs are described to make up the actual orthosteric binding pocket (67). Further, a part of the structure of aripiprazole seems to additionally occupy an extended binding pocket located closer to the extracellular surface in a similar manner to risperidone. This binding pocket is different from the binding pocket observed below the orthosteric binding pocket. A figure displaying the comparison of the discussed ligands is provided in earlier sections, figure 25. Kling et al (114) described similar findings in 2014.

A quite interesting feature that was observed in all frames for all the drugs from the conformational transition analysis (figures 2-5 supplementary material), was the movement of water molecules throughout the MD simulations. Some of the hydrogen bonds that were established in the present study were mediated through water molecules as seen in figures 15-23. Other water molecules interacted with each other in addition to residues in the binding pocket correspondingly to what was explained by Venkatakrishnan et al in 2013 (115). Because water molecules were present in the binding site of all of the systems, it can be assumed that they play an important role in the binding of drugs to their target receptor. According to Zuk et al (116) activation of G-protein-coupled receptors correlates with the formation of continuous internal water pathways. In 2019, Venkatakrishnan et al published their results where they concluded that the water molecules observed in the crystal structures of GPCRs are not equal. While some of these molecules are stable, most are mobile. They further suggested that a network of hydrogen bonds was formed by stable water molecules located near the G-protein binding site, which seemed to be conserved in class A GPCRs. However, the water molecules in the ligand binding pocket varied among the class (117).

In contrast to previous articles that investigated the effect of water molecules in whole systems (i.e., the whole proteins including both orthosteric and G-protein binding site), here, only water molecules that were present in the ligand binding sites were studied. The binding sites of the dopamine D_2 and serotonin 5-HT_{2A} receptors in the current study, were set to include residues and waters within 5 angstroms from the ligand. For example, in the bromocriptine system, 24 water molecules were observed in frame 1 while 26, 43, 31 and 34 water molecules were observed in frames 1001, 2001, 3001 and 4001 respectively. None of

the water molecules remained at the same position throughout the whole simulation in any of the systems MD was run on. This can confirm the theory about water molecules located in the ligand binding sites being highly mobile (117). In frame 1 in the bromocriptine – D_2 complex, water molecule SPC15 made direct interactions to a carboxylate group in bromocriptine. Both SPC19410 and SPC21489 interacted with Ile184 (ECL2) which then established a hydrogen bond to bromocriptine as seen in supplementary figure 6. Many of the water molecules in the binding sites of both the D_2 and 5-HT_{2A} receptors additionally interacted with each other as expected (115).

Finally, all of the ligands were accommodated in the orthosteric binding sites of their respective targets and like discussed, some of the ligands occupied additional spaces in the receptors. Unfortunately, in this thesis, the role of ECL2 was not taken into consideration but it is believed to have an important functional role in deciding how the ligands bind to their target receptors. ECL2 is known to play an important role in ligand recognition, selectivity and activation (57, 118). In the dopamine D_2 receptor, residues in ECL2 such as Ile183(ECL2), Ile184(ECL2) and Cys182(ECL2), as well as Leu229(ECL2) in the serotonin 5-HT_{2A} receptor, were involved in stable interactions with bromocriptine, aripiprazole and pimavanserin. This further shows the importance of ECL2 in receptor activation. This equated to the observations made by Kling et al in 2014 (114).

During activation of the G-protein-coupled receptors, it is believed that the loop adopts different conformations. In the beginning, the loop adopts an open conformation to accommodate the entry of the ligand into the orthosteric site. Following accommodation, the ECL2 then closes over the orthosteric site like a lid and is stabilised by contributing to interactions with the ligand (56, 57). The interactions formed between the drug and ECL2, are important for the specificity aspect as well. Interestingly, the interactions formed between the ECL2 and bromocriptine and aripiprazole were mostly hydrogen bonds. A small fraction of the interactions between bromocriptine and Ile184(ECL2) in the dopamine D_2 receptor were hydrophobic. Furthermore, the tiny fraction of interactions that were seen in the risperidone-D_2 receptor (antagonist) were hydrophobic. In the pimavanserin-5-HT_{2A} receptor complex, the interactions between Leu229(ECL2) and the drug, were both polar and non-polar. According to Wheatly et al (56), Peeters et al (57) and Kling et al (114), some of the differences in the ECL2 in agonists versus antagonist lies in the actual geometry of the loop as this further affects how the drug is accommodated but also what interactions that are able to form.

5.3 Future expectations

Antipsychotics drugs are commonly used across the globe in the treatment of disorders such as psychosis and schizophrenia. Many individuals suffering from these disorders begin treatment with antipsychotics and remain on treatment for long periods of time. In addition to producing effects that alleviate the symptoms, antipsychotics unfortunately produce side effects. Some of them are transient, while other may develop into more adverse reactions that either require medical intervention or discontinuation like it has been discussed in this thesis. For example in treatment – resistant schizophrenia, clozapine is the "gold standard" medication of choice but serious adverse effects like weight gain and agranulocytosis are associated with this drug (32). Therefore, it is of great interest to develop effective drugs that are deficient of such side effects.

Aminergic receptors such as the dopamine D_2, 5-HT_{2A}, 5-HT_{2C} and histamine H_1 receptors, have high structural conservation of the ligand binding sites which creates a challenge in the development of receptor-selective drugs. The binding sites in these receptors greatly overlap and explains why most antipsychotics produce side effects in addition to their ability to cause favourable reactions. The similarities between the aminergic receptors may contribute to reduced receptor selectivity for drugs that bind to multiple receptors, such as atypical antipsychotics. However, there have been discovered a few structural differences between the aminergic receptors that can be used as starting points to develop more selective drugs.

For instance, the 5-HT_{2A} receptor has an extended side cavity between TM4 and TM5 close to the orthosteric site with Gly238(5.42) in the entrance. This position is occupied by Ala(5.42) in dopamine D_2, Ile(5.42) in 5-HT_{2C} and Lys(5.42) in histamine H_1 receptors. Compared to glycine, the side chains of alanine, isoleucine and lysine are larger and block the entrance of the side-extended cavity in a way that drugs cant extends into this side cavity. In a study where the docking poses of pimavanserin were studied (44) it was revealed that the isobutoxybenzyl group of pimavanserin occupied the side cavity. They also did a mutagenesis study where Gly238(5.42) was substituted into a serine which resulted in decreased affinity and activity.

When it comes to the inactive dopamine D_2 receptor structure (in complex with risperidone, figures 19-20) compared to the 5-HT_{2A} receptor (figure 22), it is clear that the involvement of

ECL2 in 5-HT_{2A} receptor for ligand binding is important. In the active dopamine D_2 receptor structure in complex with bromocriptine and aripiprazole, residues Ile184(ECL2) and Cys182(ECL2) in this loop covered the ligand binding site and created stable interactions with the drugs. However, in the inactive structure of the D_2 receptor, the ECL2 is oriented away from the ligand binding site in a way that does not facilitate stable contacts between the drug and the receptor (44). The opposite is observed in the pimavanserin – 5-HT_{2A} receptor complex where interactions with Leu229(ECL2) are amongst the most stable and persistent throughout the MD simulation. Thus, this means that interactions established between the drug and ECL2 in the 5-HT_{2A} receptor, are necessary for drug binding and for the activity whereas it is not as important for the activity of risperidone in the dopamine D_2 receptor. It therefore seems like the conformation that ECL2 can adapt to accommodate both the drug and residues in close vicinity, is specific to different receptors. Taking this difference into consideration during drug design may contribute to increased specificity for one receptor over the other.

Moving further, the histamine H_1 receptor also has some unique features that differentiates it from other aminergic receptors. While ECL2 in the histamine H_1 consists of 22 residues, the ELC2 of D_2, 5-HT_{2A} and 5-HT_{2C} receptors consists of 12, 13 and 14 residues respectively. Due to the length of the ECL2 in the H_1 receptor, the distance between TM4 and TM5 is increased which again creates more space within the ligand binding pocket. Shimamura et al (80) described similar findings and proposed that large and bulky drugs could be well accommodated within this binding pocket since it is more spacious. An anion binding site located at the entrance of the ligand binding site, consisting of a phosphate ion, that is specific to histamine H_1 receptor, has additionally been discovered. It has further been suggested that the phosphate ion may serve as a positive modulator of ligand binding as the affinities for histamine and some H_1-antagonist, increased with the presence of the phosphate. Among some of the residues in the histamine H_1 receptor believed to coordinate the phosphate ion are Lys191(5.39), Tyr413(6.51) and His450(7.35) and the phosphate ion itself is seemingly involved in ionic interactions with drugs (80).

Even though most class A GPCRs share many structural similarities and conserved residues, there are some features that are unique to each of them like what has been discussed. By investigating and performing more structural studies on each of these receptors, more differences may be revealed which further simplifies the distinction of the receptors. In those cases where it is known what interactions between the drug and receptor that increase the

stability and activity of the drug, it would be reasonable to take advantage of that to ensure desired interactions but also avoid them. In the example of antipsychotic drugs where antagonism of the histamine H_1 receptor is associated with certain side effects, it would make sense to try to avoid drug-protein contacts that improve the drugs affinity to the receptor. On the contrary, it is an extremely difficult compromise to establish desirable interactions (to ensure sufficient activity), avoid undesirable interactions as well as establish interactions that are selective enough to avoid deleterious "off-target" interactions with related targets. However, this has successfully been done, resulting in drugs like for instance pimavanserin, the only non-dopaminergic antipsychotic drug (in treatment of Parkinson's disease psychosis).

Understanding of functional selectivity or biased agonism in addition to increased knowledge regarding the signalling pathways of GPCRs, represents promising avenues that in the future will lead to the development of more specific drugs. This way, one can develop compounds that are biased for either G-protein or arrestin signalling and thereby promote the beneficial pathway and subsequently inhibit potential deleterious pathways. Lysergic acid diethylamide (LSD) and β_2-antagonist carvedilol are two examples of compounds that display biased agonism. Carvedilol is a β_2-adrenoreceptor antagonist used in the treatment of heart failure. The antagonist property of the drug inhibits the toxic effects the endogenous ligands (noradrenaline and adrenaline) have on the heart mediated by G-protein, while it also has cardioprotecting properties by stimulating cell survival through the arrestin pathway (119). Similarly, LSD differentially activates both the G-protein and arrestin signalling pathways on the $5\text{-}HT_{2B}$ receptor and is believed to recruit arrestin over the activation of G-proteins resulting in hallucinations and altered thoughts (120). It is now understood that some drugs have the capacity to preferentially activate either G-protein signalling or arrestin-signalling. The next step would be to get a clearer understanding of the molecular basis of the coupling and how the drugs selectively influence different conformations leading to the activation of either pathway.

One way to gain insight into this can be by obtaining protein structures with even higher resolution than current and also protein structures with different ligands in the orthosteric site coupled to diverse binding proteins. Additionally, it would be interesting to obtain protein structures of the GPCRs in different states such as fully -, partially activated and inactivated receptor to understand how different drugs modulate function. Finally, in order to design new drugs based on the properties and 3D structure of different GPCRs like discussed above, a

strategy known as structure-based drug design (SBDD), can be utilized. With this strategy, the features of the target are exploited to design a drug that potentially establishes crucial drug-receptor interactions (121). Ligand-based drug design (LBDD) is another approach in drug design that rather depends on the physiochemical properties of the drug of interest when the structure of the target is not identified.

6 Conclusion

Class A GPCRs are interesting drug targets as ubiquitous neurotransmitters such as dopamine and serotonin bind to them and they are additionally associated with a variety of disorders, including psychosis disorders, schizophrenia and depression. In summary, computational approaches were applied to investigate the binding affinities and interactions between antipsychotic drugs and class A GPCRs dopamine D_2, 5-$HT_{2A,}$ 5-HT_{2c} and histamine H_1 receptors mediating antipsychotic effects as well as important side effects. The docking scores from IFD were viewed in context of the binding affinities (K_i value) of the drugs to the different receptors. The results indicate that there is a context between binding affinity and reported side effects that could be used to understand and distinguish between typical and atypical antipsychotics. Moreover, the development of novel drugs in the treatment of for example schizophrenia is highly needed as many people experience side effects as a result of off-target effects involving 5-HT_{2C}, histamine H_1, α_1 adrenergic and muscarinic receptors.

MD simulations revealed that antipsychotic drugs with different intrinsic activity, bind to the dopamine D_2 receptor in distinct ways, thus ligand-specific conformations were captured. One of the findings showed that an agonist like bromocriptine on the dopamine D_2 receptor, established a stable hydrogen bond to Ser197(5.46) that was not maintained in the partial agonist nor antagonist systems. This in particular is believed to help explain the reduced efficacy observed with aripiprazole. Further risperidone (antagonist on dopamine D_2 receptor) extended into a deep binding pocket in the receptor unlike the agonist and partial agonist aripiprazole, establishing hydrophobic interactions with Trp386(6.48), Phe382(6.44) and Phe389(6.51) among others. Aripiprazole seemed to bind to the dopamine D_2 receptor in ways that resembled the binding modes of both an agonist and antagonist. Ultimately, the concept of functional selectivity or biased agonism which is also the proposed mechanism of action of aripiprazole, takes into account a ligands ability to activate different signalling pathways and has without a doubt, relevance for drug design in the future.

7 Supplementary material

***Table 1**: overview table showing the classification of dopamine receptors with subtypes, functional role, G-protein coupling and agonists/antagonists on the receptors (18).*

Table 39.1 Dopamine receptors

		D_1 type		D_2 type		
	Functional role	*D_1*	*D_5*	*D_2*	*D_3*	*D_4*
Distribution						
Cortex	Arousal, mood	+++	–	++	–	+
Limbic system	Emotion, stereotypic behaviour	+++	+	++	+	+
Striatum	Prolactin secretion	+++	+	++	+	+
Ventral hypothalamus and anterior pituitary	Prolactin secretion	–	–	++	+	–
Agonists						
Dopamine		+ (Low potency)		+ (High potency)		
Apomorphine		PA (Low potency)		+ (High potency)		
Bromocriptine		PA (Low potency)		+ (High potency)		
Quinpirole		Inactive		Active		
Antagonists						
Chlorpromazine		++	++	++	++	++
Haloperidol		++	+	+++	++	+++
Spiperone		++	+	+++	+++	+++
Sulpiride		–	–	++	++	+
Clozapine		+	+	+	+	++
Aripiprazole		–	–	+++ (PA)	–	++
Raclopride		–	-	+++	++	+
Signal transduction		G_s coupled – activates adenylyl cyclase		G_i/G_o coupled – inhibits adenylyl cyclase, activates K^+ channels, inhibits Ca^{2+} channels, may also activate phospholipase C		
Effect		Mainly postsynaptic inhibition		Pre- and postsynaptic inhibition Stimulation/inhibition of hormone release		

PA, partial agonist.

Affinity data based on data contained in the IUPHAR/BPS Guide to Pharmacology database (www.guidetopharmacology.org)

***Table 2**: overview table showing the classification of serotonin receptors with subtypes, functional role, G-protein coupling and agonists/antagonists on the receptors (18).*

Table 15.1 Some significant drugs acting at the main 5-HT receptor subtypes

Receptor	Location	Main function	Signalling system	Significant drugs	
				Agonists	*Antagonists*
5-HT_{1A}	CNS	Neuronal inhibition Behavioural effects: sleep, feeding, thermoregulation, anxiety	G protein (G_i/G_o) ↓ cAMP (may also modulate Ca^{2+} channels)	8-OH-DPAT, triptans, clozapine, buspirone (PA), cabergoline	Methiothepin, yohimbine, ketanserin, pizotifen, spiperone
5-HT_{1B}	CNS, vascular smooth muscle, many other sites	Presynaptic inhibition Behavioural effects Pulmonary vasoconstriction	G protein (G_i/G_o) ↓ cAMP (may also modulate Ca^{2+} channels)	8-OH-DPAT, triptans, clozapine, cabergoline, dihydroergotamine	Methiothepin, yohimbine, ketanserin, spiperone
5-HT_{1D}	CNS, blood vessels	Cerebral vasoconstriction Behavioural effects: locomotion	G protein (G_i/G_o) ↓ cAMP (may also modulate Ca^{2+} channels)	8-OH-DPAT, triptans, clozapine, cabergoline, dihydro-ergotamine/ ergotamine	Methiothepin, yohimbine, ketanserin, methysergide, spiperone
5-HT_{1E}	CNS	–	G protein (G_i/G_o) ↓ cAMP (may also modulate Ca^{2+} channels)	8-OH-DPAT, triptans; clozapine, dihydroergotamine	Methiothepin, yohimbine, methysergide
5-HT_{1F}	CNS, uterus, heart, GI tract	–	G protein (G_i/G_o) ↓ cAMP (may also modulate Ca^{2+} channels)	8-OH-DPAT, triptans; clozapine dihydro-ergotamine/ergotamine, lamistidan	Methiothepin, yohimbine, methysergide
5-HT_{2A}	CNS, PNS, smooth muscle, platelets	Neuronal excitation Behavioural effects Smooth muscle contraction (gut, bronchi, etc.) Platelet aggregation Vasoconstriction/vasodilatation	G protein (G_q/G_{11}) ↑ IP_3, Ca^{2+}	LSD, cabergoline, methysergide (PA), 8-OH-DPAT, ergotamine (PA)	Ketanserin, clozapine, methiothepin, methysergide
5-HT_{2B}	Gastric fundus	Contraction	G protein (G_q/G_{11}) ↑ IP_3, Ca^{2+}	LSD, cabergoline, methysergide (PA), 8-OH-DPAT, ergotamine (PA)	Ketanserin, clozapine, methiothepin, yohimbine
5-HT_{2C}	CNS, lymphocytes	–	G protein (G_q/G_{11}) ↑ IP_3, Ca^{2+}	LSD, cabergoline, methysergide (PA), 8-OH-DPAT, ergotamine (PA)	Ketanserin, clozapine, methiothepin, methysergide
5-HT_3	PNS, CNS	Neuronal excitation (autonomic, nociceptive neurons) Emesis Behavioural effects: anxiety	Ligand-gated cation channel	2-Me-5-HT, chloromethyl biguanide	Dolesatron, granisetron, ondansetron, palonosetron, tropisetron
5-HT_4	PNS (GI tract), CNS	Neuronal excitation GI motility	G protein (G_s) ↑ cAMP	Metoclopramide, tegaserod, cisapride	Tropisteron
5-HT_{5A}	CNS	Modulation of exploratory behaviour (rodents)?	G protein (G_s) ↑ cAMP	Triptans, 8-OH-DPAT	Methiothepin, clozapine, methysergide, yohimbine, ketanserin
5-HT_6	CNS, leukocytes	Learning and memory?	G protein (G_s) ↑ cAMP	LSD, ergotamine	Methiothepin, clozapine, spiperone, methysergide, dihydro-ergotamine
5-HT_7	CNS, GI tract, blood vessels	Thermoregulation? Circadian rhythm?	G protein (G_s) ↑ cAMP	Buspirone, cisapride, 8-OH-DPAT, LSD,	Methiothepin, clozapine, methysergide, buspirone, dihydro-ergotamine, ketanserin, yohimbine

The receptor classification system is based upon the IUPHAR database at www.iuphar-db.org.
Many drugs here are not used clinically; others have been withdrawn (e.g. fenfluramine), or are not currently available in the UK (e.g. dolesatron, tropisetron), but are included as they are often referred to in the literature.
2-Me-5-HT, 2-methyl-5-hydroxytryptamine; 8-OH-DPAT, 8-hydroxy-2-(di-n-propylamino) tetraline; CNS, central nervous system; DAG, diacylglycerol; GI, gastrointestinal; IP_3, inositol trisphosphate; LSD, lysergic acid diethylamide; PA, partial agonist; PNS, peripheral nervous system.
The list of agonists and antagonists is not exhaustive.

```
#  Multiple input structures can be specified by adding additional
#  INPUT_FILE lines or including multiple structures in a single
#  file.
#
#  If beginning with an existing Pose Viewer file, simply specify
#  it as the INPUT_FILE (making sure the name ends in "_pv.mae"
#  or "_pv.maegz") and ensure that the first GLIDE_DOCKING stage
#  is commented out.  The ligand used in producing the Pose Viewer
#  file must also be provided to the second GLIDE_DOCKING stage,
#  using the LIGAND_FILE keyword.

INPUT_FILE      IFD_antipsy_asp155n_rec.mae

# Prime Loop Prediction
#  Perform a loop prediction on the specified loop, including
#  side chains within the given distance.  Only return
#  structures within the specified energy range from the
#  lowest energy prediction, up to the maximum number of
#  conformations given.
#
#  Note: This stage is disabled by default.  Uncomment the
#   lines below and edit the fields appropriately to enable it.
#STAGE PRIME_LOOP
#  START_RESIDUE A:11
#  END_RESIDUE A:16
#  RES_SPHERE 7.5
#  MAX_ENERGY_GAP 30.0
#  MAX_STRUCTURES 5
#  USE_MEMBRANE no

STAGE GLIDE_DOCKING2
  BINDING_SITE residues A:155
  INNERBOX 10.0
  OUTERBOX auto
  LIGAND_FILE  IFD_antipsy_asp155n.maegz
  LIGANDS_TO_DOCK all
  GRIDGEN_RECEP_CCUT  0.25
  GRIDGEN_RECEP_VSCALE 0.50
  GRIDGEN_FORCEFIELD OPLS3e
  DOCKING_PRECISION SP
  DOCKING_LIG_CCUT  0.15
  DOCKING_CV_CUTOFF  100.0
  DOCKING_LIG_VSCALE 0.50
  DOCKING_POSES_PER_LIG 20
  DOCKING_FORCEFIELD OPLS3e
  DOCKING_RINGCONFCUT 2.5
  DOCKING_AMIDE_MODE penal
  DOCKING_[[FEATURE:1]]
    DOCKING_PATTERN1   "[N+][H] 1,2 include"
  DOCKING_[[FEATURE:2]]
    DOCKING_PATTERN1   "[N+][H] 1,2 include"
  GRIDGEN_HBOND_CONSTRAINTS "atom0 1420","atom1 1419"
  DOCKING_[[CONSTRAINT_GROUP:1]]
  DOCKING_USE_CONS atom0:1,atom1:2
  DOCKING_NREQUIRED_CONS 2

STAGE COMPILE_RESIDUE_LIST
  DISTANCE_CUTOFF       5.0

STAGE PRIME_REFINEMENT
  NUMBER_OF_PASSES      1
  USE_MEMBRANE no
  OPLS_VERSION OPLS3e

STAGE SORT_AND_FILTER
  POSE_FILTER   r_psp_Prime_Energy
  POSE_KEEP     30.0

STAGE SORT_AND_FILTER
  POSE_FILTER   r_psp_Prime_Energy
  POSE_KEEP     20#

STAGE GLIDE_DOCKING2
  BINDING_SITE ligand Z:999
  INNERBOX 10.0
  OUTERBOX auto
  LIGAND_FILE  IFD_antipsy_asp155n.maegz
  LIGANDS_TO_DOCK self
  GRIDGEN_RECEP_CCUT  0.25
  GRIDGEN_RECEP_VSCALE 1.00
  GRIDGEN_FORCEFIELD OPLS3e
  DOCKING_PRECISION SP
  DOCKING_LIG_CCUT  0.15
  DOCKING_CV_CUTOFF  0.0
  DOCKING_LIG_VSCALE 0.80
  DOCKING_POSES_PER_LIG 1
  DOCKING_FORCEFIELD OPLS3e
  DOCKING_RINGCONFCUT 2.5
  DOCKING_AMIDE_MODE penal
  DOCKING_[[FEATURE:1]]
    DOCKING_PATTERN1   "[N+][H] 1,2 include"
  DOCKING_[[FEATURE:2]]
    DOCKING_PATTERN1   "[N+][H] 1,2 include"
  GRIDGEN_HBOND_CONSTRAINTS "atom0 1420","atom1 1419"
  DOCKING_[[CONSTRAINT_GROUP:1]]
  DOCKING_USE_CONS atom0:1,atom1:2
  DOCKING_NREQUIRED_CONS 2

STAGE SCORING
  SCORE_NAME  r_psp_IFDScore
  TERM 1.0,r_i_glide_gscore,0
  TERM 0.05,r_psp_Prime_Energy,1
  REPORT_FILE report.csv
```

***Figure 1**: syntax containing the constraints that were used in the IFD. The red boxes display the exact text that was used*

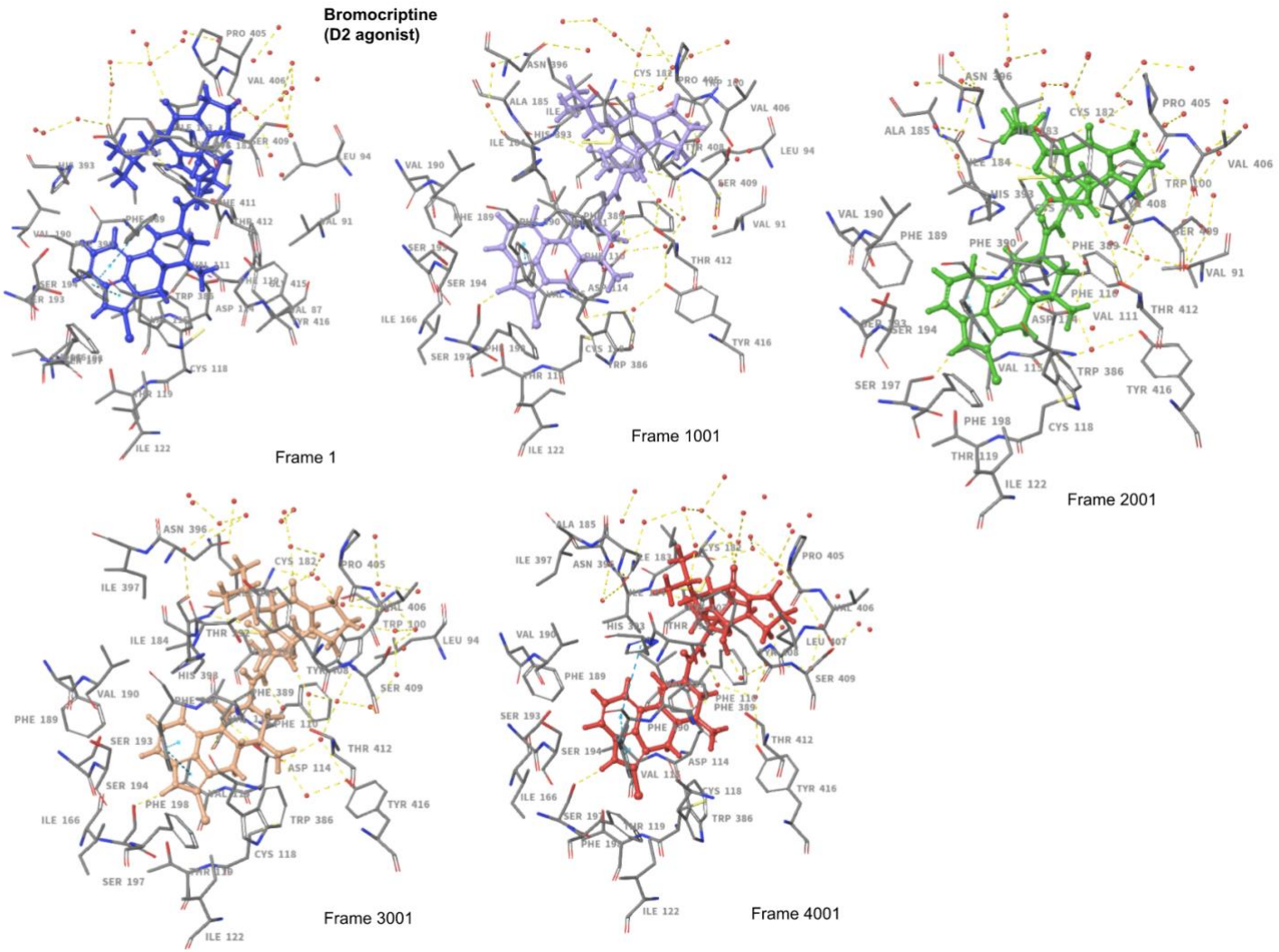

Figure 2*: in dept presentation of the ligand-residue contacts formed in the five frames (1, 1001, 2001, 3001 and 4001) described in the results section for the conformational transition analysis. Bromocriptine is coloured in blue, lilac, green, beige and red for each frame respectively while binding site residues are coloured gray. Yellow dotted lines represent hydrogen bonds, red spheres are water molecules, blue dotted lines are* $\pi - \pi$ *stacking interactions, pink line is ionic interaction.*

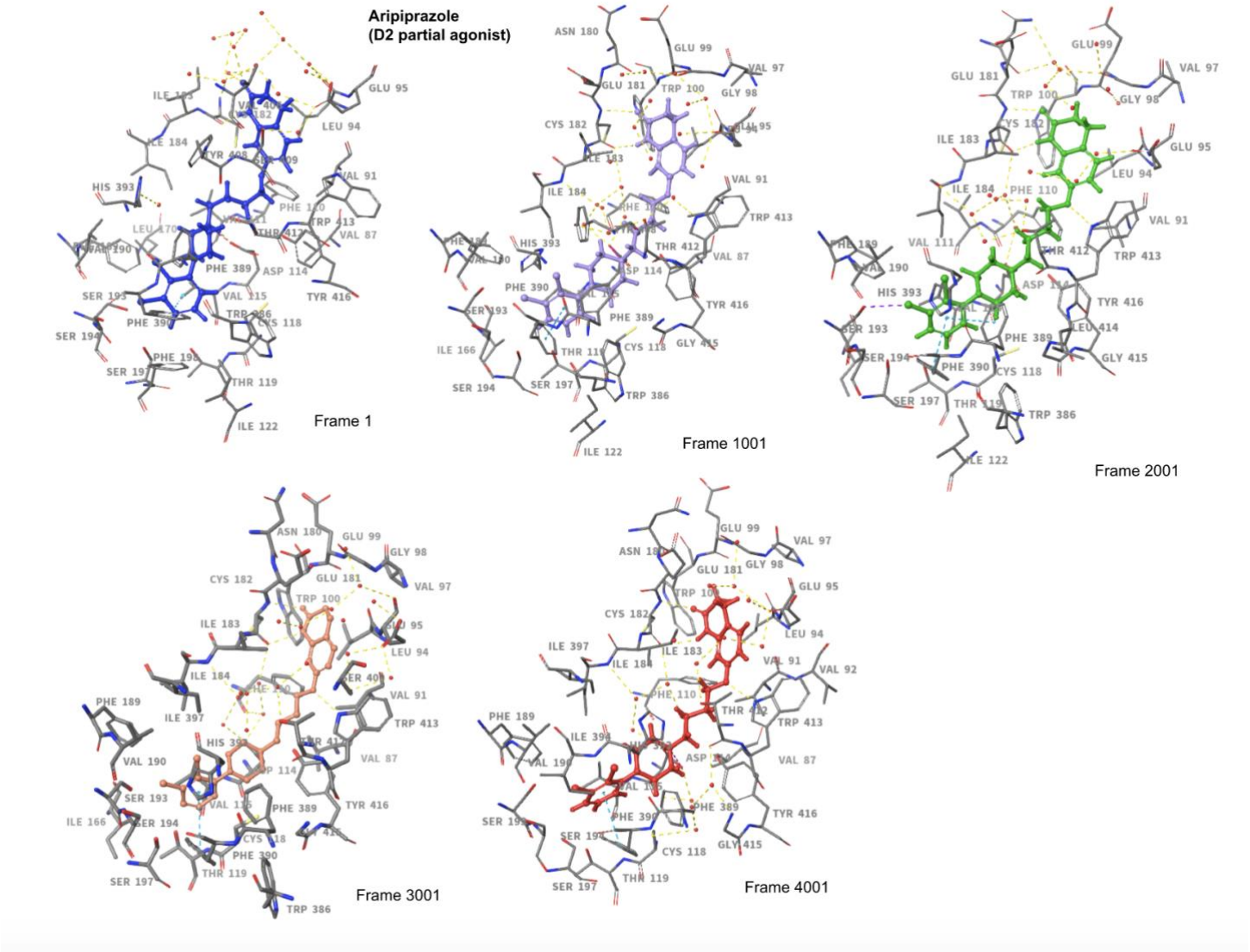

Figure 3*: in dept presentation of the ligand-residue contacts formed in the five frames (1, 1001, 2001, 3001 and 4001) described in the results section for the conformational transition analysis. Aripiprazole is coloured in blue, lilac, green, beige and red for each frame respectively while binding site residues are coloured gray. Yellow dotted lines represent hydrogen bonds, red spheres are water molecules, blue dotted lines are* $\pi - \pi$ *stacking interactions, pink line is ionic interaction while the purple dotted line is a halogen interaction.*

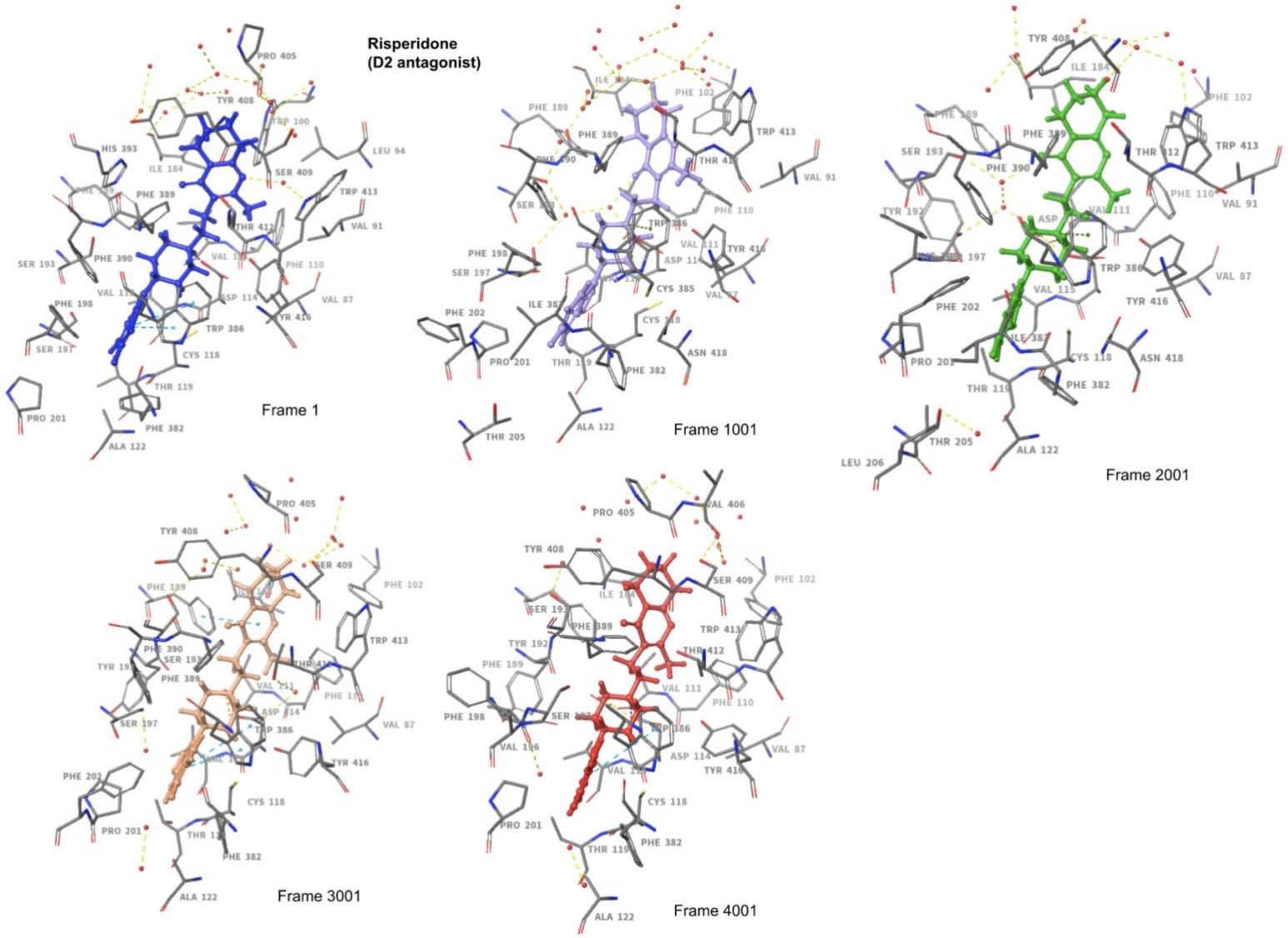

Figure 4*: in dept presentation of the ligand-residue contacts formed in the five frames (1, 1001, 2001, 3001 and 4001) described in the results section for the conformational transition analysis. Risperidone is coloured in blue, lilac, green, beige and red for each frame respectively. Yellow dotted lines represent hydrogen bonds, red spheres are water molecules, blue dotted lines are* $\pi - \pi$ *stacking interactions, pink line is ionic interaction and green represents* $\pi - cation$ *interaction.*

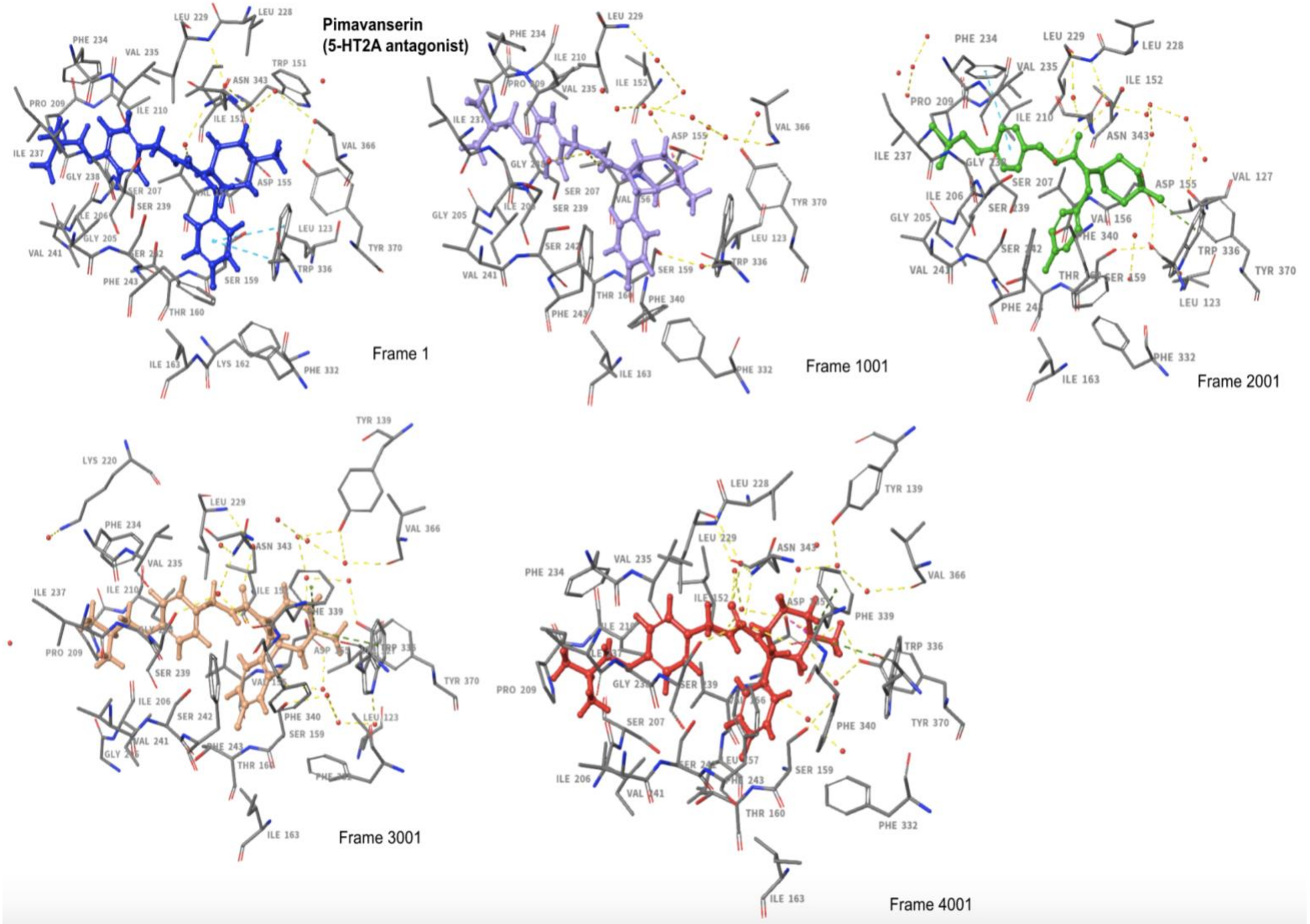

Figure 5*: in dept presentation of the ligand-residue contacts formed in the five frames (1, 1001, 2001, 3001 and 4001) described in the results section. Pimavanserin is coloured in blue, lilac, green, beige and red for each frame respectively while binding site residues are coloured gray. Yellow dotted lines represent hydrogen bonds, red spheres are water molecules, blue dotted lines are* $\pi - \pi$ *stacking interactions, pink line is ionic interaction and green represents* $\pi - cation$ *interaction*

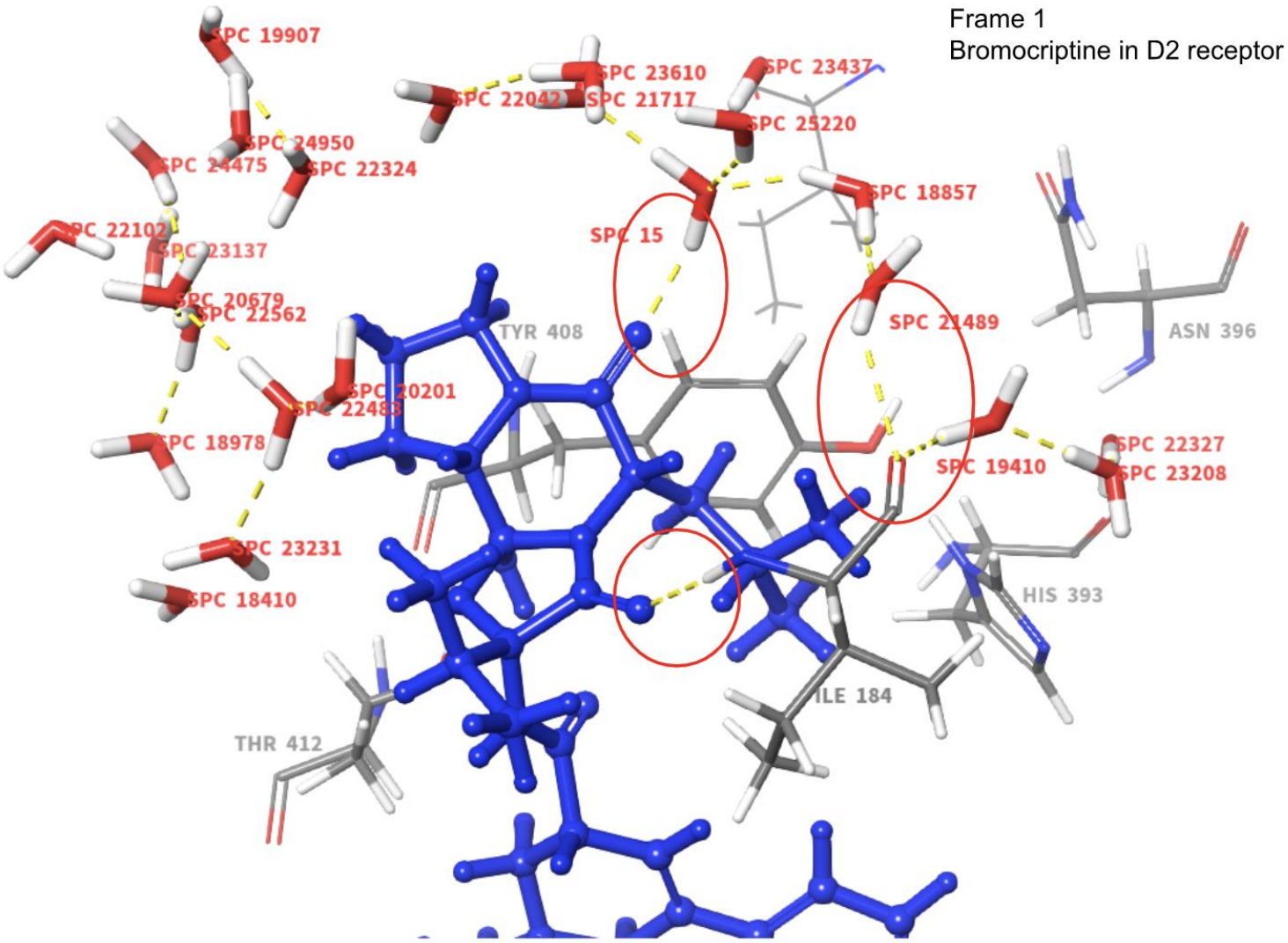

***Figure 6**: water molecules in the orthosteric site in frame 1 of the bromocriptine – D_2 receptor simulation. Bromocriptine is displayed in blue, surrounding binding site residues in gray and water molecules in red. Hydrogen bonds are shown as yellow dotted lines and the rings highlights the interactions established between water molecules, residues and bromocriptine.*

8 Reference list

1. Services USDoHaH. Introduction to the Nervous System: National Cancer Institute; [Available from: https://training.seer.cancer.gov/anatomy/nervous/.
2. J. Gordon Betts KAY, James A. Wise, Eddie Johnson, Brandon Poe, Dean H. Kruse, Oksana Korol, Jody E. Johnson, Mark Womble, Peter DeSaix. Anatomy and Physiology: Basic Structure and Function of the Nervous System: OpenStax; 1999-2021 25.04.2013.
3. George J. Augustine PD, Dona M. Chikaraishi PD, Michael D. Ehlers MD, Ph.D., Gillian Einstein PD, David Fitzpatrick PD, William C. Hall PD, et al. Neuroscience, NEURAL SIGNALING. edition T, editor2004.
4. J.Alexander J. Blood-brain barrier (BBB) and the complement landscape: ScienceDirect; 2018 [Volume 102:[Available from: https://www.sciencedirect.com/science/article/abs/pii/S0161589018304723?via%3Dihub.
5. Cornell B. Blood-Brain Barrier: BioNinja; 2016 [Available from: https://ib.bioninja.com.au/options/option-a-neurobiology-and/a2-the-human-brain/blood-brain-barrier.html.
6. Banks WA. Characteristics of compounds that cross the blood-brain barrier. BMC neurology. 2009;9 Suppl 1(Suppl 1):S3-S.
7. Hook V, Kind T, Podvin S, Palazoglu M, Tran C, Toneff T, et al. Metabolomics Analyses of 14 Classical Neurotransmitters by GC-TOF with LC-MS Illustrates Secretion of 9 Cell-Cell Signaling Molecules from Sympathoadrenal Chromaffin Cells in the Presence of Lithium. ACS Chem Neurosci. 2019;10(3):1369-79.
8. Gemperline E, Chen B, Li L. Challenges and recent advances in mass spectrometric imaging of neurotransmitters. Bioanalysis. 2014;6(4):525-40.
9. Kandimalla R, Reddy PH. Therapeutics of Neurotransmitters in Alzheimer's Disease. J Alzheimers Dis. 2017;57(4):1049-69.
10. ACADEMY K. Neuron action potentials: The creation of a brain signal 2021 [cited 2021 02.01.2021]. Available from: https://www.khanacademy.org/test-prep/mcat/organ-systems/neuron-membrane-potentials/a/neuron-action-potentials-the-creation-of-a-brain-signal.
11. Lemke TL, Williams, David A. . Foye's Principles of Medicinal Chemistry. Seventh, International Edition ed: Lippincott Williams and Wilkins; 2012. 1520 p.
12. Kizirian A. Synaptic Transmission by Somatic Motorneurons 2021 [Available from: https://antranik.org/synaptic-transmission-by-somatic-motorneurons/.
13. Campus LI. Synaptic Dopamine reuptake and degradation. In: degradation SDra, editor. Lundbeck Institute Campus Webpage: Lundbeck Institute Campus; 2016. p. Dopamine is released from the presynaptic terminal, diffuses over the synaptic cleft and activates Dopaminergic receptors (D1-D5 receptors). After release from the nerve terminal, Dopamine is taken up via a presynaptically located Dopamine transporter and degraded by the Mono amine oxidase B (MAO-B).
14. Siafis S, Tzachanis D, Samara M, Papazisis G. Antipsychotic Drugs: From Receptor-binding Profiles to Metabolic Side Effects. Curr Neuropharmacol. 2018;16(8):1210-23.
15. Gittelman JX, Perkel DJ, Portfors CV. Dopamine modulates auditory responses in the inferior colliculus in a heterogeneous manner. J Assoc Res Otolaryngol. 2013;14(5):719-29.
16. Salmas RE, Yurtsever M, Durdagi S. Atomistic molecular dynamics simulations of typical and atypical antipsychotic drugs at the dopamine D2 receptor (D2R) elucidates their inhibition mechanism. Journal of Biomolecular Structure and Dynamics. 2017;35(4):738-54.

17. Pinoli M. The Cross-Talk Between The Dopaminergic System And Innate Immunity: An Evolving Concept: Brain Immune; 2017 [Available from: http://www.brainimmune.com/cross-talk-between-dopaminergic-system-and-innate-immunity/.
18. H. P. Rang JMR, R. J. Flower, and G. Henderson. Rang & Dale's Pharmacology. 8th edition ed: Churchill Livingstone; 2015. 808 p.
19. Eske J. Dopamine and serotonin: Brain chemicals explained: Medical News Today; 2019 [Available from: https://www.medicalnewstoday.com/articles/326090.
20. Seo D, Patrick CJ, Kennealy PJ. Role of Serotonin and Dopamine System Interactions in the Neurobiology of Impulsive Aggression and its Comorbidity with other Clinical Disorders. Aggress Violent Behav. 2008;13(5):383-95.
21. Fischer AG, Ullsperger M. An Update on the Role of Serotonin and its Interplay with Dopamine for Reward. Front Hum Neurosci. 2017;11:484-.
22. Daw ND, Kakade S, Dayan P. Opponent interactions between serotonin and dopamine. Neural Netw. 2002;15(4-6):603-16.
23. Kapur S, Remington G. Serotonin-dopamine interaction and its relevance to schizophrenia. Am J Psychiatry. 1996;153(4):466-76.
24. Wong PT, Feng H, Teo WL. Interaction of the dopaminergic and serotonergic systems in the rat striatum: effects of selective antagonists and uptake inhibitors. Neurosci Res. 1995;23(1):115-9.
25. (HQ) WH. What are neurological disorders? : The world Health Organization; 2016 [Available from: https://www.who.int/news-room/q-a-detail/what-are-neurological-disorders.
26. Kiran T Thakur EA, Panteleimon Giannakopoulos, Nathalie Jette, Mattias Linde, Martin J Prince, Timothy J Steiner, and Tarun Dua. Mental, Neurological, and Substance Use Disorders: Disease Control Priorities. Third ed: Washington (DC): The International Bank for Reconstruction and Development; 2016 14.03.2016.
27. Government M. Neurological Disorders: Department of Public Health and Human Services; [Available from: https://dphhs.mt.gov/schoolhealth/chronichealth/neurologicaldisorders.
28. Zis P, Hadjivassiliou M. Treatment of Neurological Manifestations of Gluten Sensitivity and Coeliac Disease. Current Treatment Options in Neurology. 2019;21(3):10.
29. Bhandari S. What can trigger schizophrenia? : WebMD; 2020 [Available from: https://www.webmd.com/schizophrenia/qa/how-do-environmental-factors-cause-schizophrenia.
30. Khanna P, Suo T, Komossa K, Ma H, Rummel-Kluge C, El-Sayeh HG, et al. Aripiprazole versus other atypical antipsychotics for schizophrenia. Cochrane Database Syst Rev. 2014;2014(1):CD006569-CD.
31. Patrick GL. An Introduction to Medicinal Chemistry

: Oxford University Press; 2013. 816 p.
32. Aringhieri S, Carli M, Kolachalam S, Verdesca V, Cini E, Rossi M, et al. Molecular targets of atypical antipsychotics: From mechanism of action to clinical differences. Pharmacology & Therapeutics. 2018;192:20-41.
33. Armstrong JF FE, Harding SD, Pawson AJ, Southan C, Sharman JL, Campo B, Cavanagh DR, Alexander SPH, Davenport AP, Spedding M, Davies. Ligand actions: Guide to PHARMACOLOGY; 2003-2014 [Available from: https://www.guidetopharmacology.org/GRAC/helpPagePopup.jsp#glossary.
34. Yartsev A. Full agonists, partial agonists and inverse agonists

: Deranged Physiology 2015 [updated 01/31/2019. Available from: https://derangedphysiology.com/main/cicm-primary-exam/required-

reading/pharmacodynamics/Chapter%20417/full-agonists-partial-agonists-and-inverse-agonists.
35. Tuplin EW, Holahan MR. Aripiprazole, A Drug that Displays Partial Agonism and Functional Selectivity. Curr Neuropharmacol. 2017;15(8):1192-207.
36. de Bartolomeis A, Tomasetti C, Iasevoli F. Update on the Mechanism of Action of Aripiprazole: Translational Insights into Antipsychotic Strategies Beyond Dopamine Receptor Antagonism. CNS Drugs. 2015;29(9):773-99.
37. Leucht S, Cipriani A, Spineli L, Mavridis D, Örey D, Richter F, et al. Comparative efficacy and tolerability of 15 antipsychotic drugs in schizophrenia: a multiple-treatments meta-analysis. The Lancet. 2013;382(9896):951-62.
38. Leucht S, Corves C, Arbter D, Engel RR, Li C, Davis JM. Second-generation versus first-generation antipsychotic drugs for schizophrenia: a meta-analysis. The Lancet. 2009;373(9657):31-41.
39. Leucht S, Leucht C, Huhn M, Chaimani A, Mavridis D, Helfer B, et al. Sixty Years of Placebo-Controlled Antipsychotic Drug Trials in Acute Schizophrenia: Systematic Review, Bayesian Meta-Analysis, and Meta-Regression of Efficacy Predictors. American Journal of Psychiatry. 2017;174(10):927-42.
40. Negative symptoms: a path analytic approach to a double-blind, placebo- and haloperidol-controlled clinical trial with olanzapine. American Journal of Psychiatry. 1997;154(4):466-74.
41. Wang S, Che T, Levit A, Shoichet BK, Wacker D, Roth BL. Structure of the D2 dopamine receptor bound to the atypical antipsychotic drug risperidone. Nature. 2018;555(7695):269-73.
42. Kirk SL, Glazebrook J, Grayson B, Neill JC, Reynolds GP. Olanzapine-induced weight gain in the rat: role of 5-HT2C and histamine H1 receptors. Psychopharmacology. 2009;207(1):119.
43. Eison AS, Mullins UL. Regulation of central 5-HT2A receptors: a review of in vivo studies. Behav Brain Res. 1996;73(1-2):177-81.
44. Kimura KT, Asada H, Inoue A, Kadji FMN, Im D, Mori C, et al. Structures of the 5-HT2A receptor in complex with the antipsychotics risperidone and zotepine. Nature Structural & Molecular Biology. 2019;26(2):121-8.
45. Amato D, Beasley CL, Hahn MK, Vernon AC. Neuroadaptations to antipsychotic drugs: Insights from pre-clinical and human post-mortem studies. Neuroscience & Biobehavioral Reviews. 2017;76:317-35.
46. Alvir JMJ, Lieberman JA, Safferman AZ, Schwimmer JL, Schaaf JA. Clozapine-Induced Agranulocytosis -- Incidence and Risk Factors in the United States. New England Journal of Medicine. 1993;329(3):162-7.
47. Kondej M, Stępnicki P, Kaczor AA. Multi-Target Approach for Drug Discovery against Schizophrenia. Int J Mol Sci. 2018;19(10):3105.
48. Fredriksson R, Lagerström MC, Lundin L-G, Schiöth HB. The G-Protein-Coupled Receptors in the Human Genome Form Five Main Families. Phylogenetic Analysis, Paralogon Groups, and Fingerprints. Mol Pharmacol. 2003;63(6):1256.
49. Zhou Q, Yang D, Wu M, Guo Y, Guo W, Zhong L, et al. Common activation mechanism of class A GPCRs. Elife. 2019;8:e50279.
50. Bortolato A, Doré AS, Hollenstein K, Tehan BG, Mason JS, Marshall FH. Structure of Class B GPCRs: new horizons for drug discovery. Br J Pharmacol. 2014;171(13):3132-45.
51. Vohra S, Taddese B, Conner AC, Poyner DR, Hay DL, Barwell J, et al. Similarity between class A and class B G-protein-coupled receptors exemplified through calcitonin gene-related peptide receptor modelling and mutagenesis studies. J R Soc Interface. 2012;10(79):20120846-.

52. Zhang D, Zhao Q, Wu B. Structural Studies of G Protein-Coupled Receptors. Mol Cells. 2015;38(10):836-42.
53. Eilers M, Hornak V, Smith SO, Konopka JB. Comparison of class A and D G protein-coupled receptors: common features in structure and activation. Biochemistry. 2005;44(25):8959-75.
54. Kobilka BK. G protein coupled receptor structure and activation. Biochim Biophys Acta. 2007;1768(4):794-807.
55. Woolley MJ, Watkins HA, Taddese B, Karakullukcu ZG, Barwell J, Smith KJ, et al. The role of ECL2 in CGRP receptor activation: a combined modelling and experimental approach. J R Soc Interface. 2013;10(88):20130589-.
56. Wheatley M, Wootten D, Conner MT, Simms J, Kendrick R, Logan RT, et al. Lifting the lid on GPCRs: the role of extracellular loops. Br J Pharmacol. 2012;165(6):1688-703.
57. Peeters MC, van Westen GJP, Li Q, Ijzerman AP. Importance of the extracellular loops in G protein-coupled receptors for ligand recognition and receptor activation. Trends in Pharmacological Sciences. 2011;32(1):35-42.
58. Isberg V, de Graaf C, Bortolato A, Cherezov V, Katritch V, Marshall FH, et al. Generic GPCR residue numbers - aligning topology maps while minding the gaps. Trends in pharmacological sciences. 2015;36(1):22-31.
59. Salmas RE, Yurtsever M, Stein M, Durdagi S. Modeling and protein engineering studies of active and inactive states of human dopamine D2 receptor (D2R) and investigation of drug/receptor interactions. Molecular Diversity. 2015;19(2):321-32.
60. Trzaskowski B, Latek D, Yuan S, Ghoshdastider U, Debinski A, Filipek S. Action of molecular switches in GPCRs--theoretical and experimental studies. Curr Med Chem. 2012;19(8):1090-109.
61. Erlandson SC, McMahon C, Kruse AC. Structural Basis for G Protein–Coupled Receptor Signaling. Annual Review of Biophysics. 2018;47(1):1-18.
62. Han M, Gurevich VV, Vishnivetskiy SA, Sigler PB, Schubert C. Crystal Structure of β-Arrestin at 1.9 Å: Possible Mechanism of Receptor Binding and Membrane Translocation. Structure. 2001;9(9):869-80.
63. Rajagopal S, Rajagopal K, Lefkowitz RJ. Teaching old receptors new tricks: biasing seven-transmembrane receptors. Nat Rev Drug Discov. 2010;9(5):373-86.
64. Yin J, Chen K-YM, Clark MJ, Hijazi M, Kumari P, Bai X-c, et al. Structure of a D2 dopamine receptor–G-protein complex in a lipid membrane. Nature. 2020;584(7819):125-9.
65. Beaulieu J-M, Gainetdinov RR. The Physiology, Signaling, and Pharmacology of Dopamine Receptors. Pharmacological Reviews. 2011;63(1):182.
66. Khan ZU, Mrzljak L, Gutierrez A, de la Calle A, Goldman-Rakic PS. Prominence of the dopamine D2 short isoform in dopaminergic pathways. Proc Natl Acad Sci U S A. 1998;95(13):7731-6.
67. Kalani MYS, Vaidehi N, Hall SE, Trabanino RJ, Freddolino PL, Kalani MA, et al. The predicted 3D structure of the human D2 dopamine receptor and the binding site and binding affinities for agonists and antagonists. Proc Natl Acad Sci U S A. 2004;101(11):3815-20.
68. Simpson MM, Ballesteros JA, Chiappa V, Chen J, Suehiro M, Hartman DS, et al. Dopamine D4/D2 Receptor Selectivity Is Determined by A Divergent Aromatic Microdomain Contained within the Second, Third, and Seventh Membrane-Spanning Segments. Mol Pharmacol. 1999;56(6):1116.
69. Yin J, Chen, K.M., Clark, M.J., Hijazi, M., Kumari, P., Bai, X., Sunahara, R.K., Barth, P., Rosenbaum, D.M. Structure of a D2 dopamine receptor-G-protein complex in a lipid membrane: Protein data bank; 17 June 2020 [Available from: https://www.rcsb.org/structure/6VMS, 10.2210/pdb6vms/pdb

70. Delgado PL. Depression: the case for a monoamine deficiency. J Clin Psychiatry. 2000;61 Suppl 6:7-11.
71. Zhang G, Stackman RW. The role of serotonin 5-HT2A receptors in memory and cognition. Frontiers in Pharmacology. 2015;6(225).
72. Torrens-Fontanals M, Stepniewski TM, Aranda-García D, Morales-Pastor A, Medel-Lacruz B, Selent J. How Do Molecular Dynamics Data Complement Static Structural Data of GPCRs. Int J Mol Sci. 2020;21(16):5933.
73. Gani OABSM. Signposts of Docking and Scoring in Drug Design. Chemical Biology & Drug Design. 2007;70(4):360-5.
74. Śledź P, Caflisch A. Protein structure-based drug design: from docking to molecular dynamics. Current Opinion in Structural Biology. 2018;48:93-102.
75. LLC S. Desmond User Manual. 2015. p. 45-68.
76. Monticelli L, Tieleman DP. Force Fields for Classical Molecular Dynamics. In: Monticelli L, Salonen E, editors. Biomolecular Simulations: Methods and Protocols. Totowa, NJ: Humana Press; 2013. p. 197-213.
77. legemiddelregister Nr. Statistikk fra Reseptregisteret

: Folkehelse Instituttet; 2005 [Available from: http://www.reseptregisteret.no/Prevalens.aspx.
78. H.M. Berman JW, Z. Feng, G. Gilliland, T.N. Bhat, H. Weissig, I.N. Shindyalov, P.E. Bourne. Protein Data Bank: RCSB PDB; 2000 [Available from: rcsb.org
79. Wang S, Che, T., Levit, A., Shoichet, B.K., Wacker, D., Roth, B.L. Structure of the D2 Dopamine Receptor Bound to the Atypical Antipsychotic Drug Risperidone: Protein Data Bank; 2018 [Available from: https://www.rcsb.org/structure/6CM4, http://dx.doi.org/10.1038/nature25758.
80. Shimamura T, Han, G.W., Shiroishi, M., Weyand, S., Tsujimoto, H., Winter, G., Katritch, V., Abagyan, R., Cherezov, V., Liu, W., Kobayashi, T., Stevens, R., Iwata, S., GPCR Network (GPCR). Structure of the human histamine H1 receptor in complex with doxepin: Protein Data Bank; 2011 [Available from: https://www.rcsb.org/structure/3RZE, http://doi.org/10.2210/pdb3RZE/pdb.
81. Kimura TK, Asada, H., Inoue, A., Kadji, F.M.N., Im, D., Mori, C., Arakawa, T., Hirata, K., Nomura, Y., Nomura, N., Aoki, J., Iwata, S., Shimamura, T. Crystal structure of 5-HT2AR in complex with risperidone

: Protein Data Bank; 2019 [Available from: https://www.rcsb.org/structure/6A93, http://doi.org/10.2210/pdb6A93/pdb.
82. Peng Y, McCorvy, J.D., Harpsoe, K., Lansu, K., Yuan, S., Popov, P., Qu, L., Pu, M., Che, T., Nikolajse, L.F., Huang, X.P., Wu, Y., Shen, L., Bjorn-Yoshimoto, W.E., Ding, K., Wacker, D., Han, G.W., Cheng, J., Katritch, V., Jensen, A.A., Hanson, M.A., Zhao, S., Gloriam, D.E., Roth, B.L., Stevens, R.C., Liu, Z. Crystal structure of 5-HT2C in complex with ritanserin

: Protein Data Bank; 2018 [Available from: https://www.rcsb.org/structure/6BQH, http://doi.org/10.2210/pdb6BQH/pdb.
83. Dr. Henry I. Mosberg DAM, Kim Henrick, Drs. Eugene Krissinel, Gabor Tusnady, Drs. Simon Hubbard, Vladimir Maiorov, Simon Sherman. 6vms » D2 dopamine receptor, with Gi protein: Orientations of Proteins in Membranes (OPM) database; 2005-2019 [Available from: 2020https://opm.phar.umich.edu/proteins/5168.
84. The Multiplicity of Serotonin Receptors: Uselessly diverse molecules or an embarrasment of riches?

BL Roth, WK Kroeze, S Patel and E Lopez: The Neuroscientist, 6:252-262, 2000 [Internet]. The Neuroscientist. 2000 [cited 11.02.2021]. Available from: https://pdsp.unc.edu/databases/kidb.php.
85. Scrödinger. FORCE FIELDS: Scrödinger Inc; [Available from: https://www.schrodinger.com/science-articles/force-field.
86. Sherman WD, T.; Jacobson, M. P.; Friesner, R. A.; Farid, R.,Beard, H. Induced Fit Docking protocol 2015-2. New York, NY, 2015.: Schrödinger, LLC, 2015.; 2015. p. 12-55.
87. Sastry GMA, M.; Day, T.; Annabhimoju, R.; Sherman, W. Protein Preparation Wizard New York, LLC, 2020: Epik, Schrödinger; 2020 [Schrödinger Release 2020-4:[Available from: https://www.schrodinger.com/products/protein-preparation-wizard.
88. CROSSLINKER PANEL: I have a crystal structure with missing loops. I would like to build the loops from a known sequence of residues. What are my options? : KNOWLEDGE BASE, Schrödinger Inc; 2018 [updated 28.01.2018. Available from: https://www.schrodinger.com/kb/1835.
89. Skyner RE, McDonagh JL, Groom CR, van Mourik T, Mitchell JBO. A review of methods for the calculation of solution free energies and the modelling of systems in solution. Physical Chemistry Chemical Physics. 2015;17(9):6174-91.
90. Alex Bateman ABaCW, supported by key staff,. P14416 (DRD2_HUMAN). 01.01.1990 ed: European Bioinformatics Institute (EMBL-EBI), the SIB Swiss Institute of Bioinformatics and the Protein Information Resource (PIR). 2002-2021.
91. SAPHRIS (asenapine) sublingual tablets. Schering Corporation 2009.
92. Nuplazid prescribing information. Acadia Pharmaceuticals Inc.; 2016.
93. Kimie Yonemura KM, Yukiteru Machiyama. PROFILES OF THE AFFINITY OF ANTIPSYCHOTIC DRUGS FOR NEUROTRANSMITTER RECEPTORS AND THEIR CLINICAL IMPLICATION. The Kitakanto Medical Journal. 1998;48(2):87-102.
94. Corena-McLeod M. Comparative Pharmacology of Risperidone and Paliperidone. Drugs R D. 2015;15(2):163-74.
95. Anthony Busti M, PharmD The Inhibitory Constant (Ki) and its Use in Understanding Drug Interactions: EBM Consult, LLC; [Available from: https://www.ebmconsult.com/articles/inhibitory-constant-ki-drug-interactions.
96. What is considered a good GlideScore? : Schrödinger, Inc; 2021 [updated 04.12.2010. Available from: https://www.schrodinger.com/kb/639.
97. What are the advantages and disadvantages of Glide regular docking and induced fit docking? : Schrödinger, Inc; 2011 [updated 16.05.2011. Available from: https://www.schrodinger.com/kb/739.
98. Education Y. 2021. [cited 2021]. Available from: http://www.csb.yale.edu/userguides/datamanip/autodock/html/Using_AutoDock_305.9.html.
99. Appl H, Holzammer T, Dove S, Haen E, Straßer A, Seifert R. Interactions of recombinant human histamine H1, H2, H3, and H4 receptors with 34 antidepressants and antipsychotics. Naunyn-Schmiedeberg's Archives of Pharmacology. 2012;385(2):145-70.
100. Divac N, Prostran M, Jakovcevski I, Cerovac N. Second-generation antipsychotics and extrapyramidal adverse effects. Biomed Res Int. 2014;2014:656370-.
101. Shahi MK, Kar SK, Singh A. Asymmetric, Tender Gynecomastia Induced by Olanzapine in a Young Male. Indian J Psychol Med. 2017;39(2):215-6.
102. Bhattacharjee J, El‐Sayeh HG. Aripiprazole versus typical antipsychotic drugs for schizophrenia. Cochrane Database of Systematic Reviews. 2008(3).
103. Kroeze WK, Hufeisen SJ, Popadak BA, Renock SM, Steinberg S, Ernsberger P, et al. H1-Histamine Receptor Affinity Predicts Short-Term Weight Gain for Typical and Atypical Antipsychotic Drugs. Neuropsychopharmacology. 2003;28(3):519-26.

104. Booth RG, Fang L, Huang Y, Wilczynski A, Sivendran S. (1R, 3S)-(-)-trans-PAT: a novel full-efficacy serotonin 5-HT2C receptor agonist with 5-HT2A and 5-HT2B receptor inverse agonist/antagonist activity. Eur J Pharmacol. 2009;615(1-3):1-9.
105. Reynolds GP, Kirk SL. Metabolic side effects of antipsychotic drug treatment – pharmacological mechanisms. Pharmacology & Therapeutics. 2010;125(1):169-79.
106. Nasrallah HA. Atypical antipsychotic-induced metabolic side effects: insights from receptor-binding profiles. Molecular Psychiatry. 2008;13(1):27-35.
107. Bitter I, Dossenbach MRK, Brook S, Feldman PD, Metcalfe S, Gagiano CA, et al. Olanzapine versus clozapine in treatment-resistant or treatment-intolerant schizophrenia. Progress in Neuro-Psychopharmacology and Biological Psychiatry. 2004;28(1):173-80.
108. Crossley NA, Constante M, McGuire P, Power P. Efficacy of atypical v. typical antipsychotics in the treatment of early psychosis: meta-analysis. Br J Psychiatry. 2010;196(6):434-9.
109. Moore DC. Drug-Induced Neutropenia: A Focus on Rituximab-Induced Late-Onset Neutropenia. P T. 2016;41(12):765-8.
110. Roos K, Wu C, Damm W, Reboul M, Stevenson JM, Lu C, et al. OPLS3e: Extending Force Field Coverage for Drug-Like Small Molecules. Journal of Chemical Theory and Computation. 2019;15(3):1863-74.
111. Chan HCS, Wang J, Palczewski K, Filipek S, Vogel H, Liu Z-J, et al. Exploring a new ligand binding site of G protein-coupled receptors. Chemical Science. 2018;9(31):6480-9.
112. Peng Y, McCorvy JD, Harpsøe K, Lansu K, Yuan S, Popov P, et al. 5-HT(2C) Receptor Structures Reveal the Structural Basis of GPCR Polypharmacology. Cell. 2018;172(4):719-30.e14.
113. Sukalovic V, Soskic V, Sencanski M, Andric D, Kostic-Rajacic S. Determination of key receptor–ligand interactions of dopaminergic arylpiperazines and the dopamine D2 receptor homology model. Journal of Molecular Modeling. 2013;19(4):1751-62.
114. Kling RC, Tschammer N, Lanig H, Clark T, Gmeiner P. Active-state model of a dopamine D2 receptor-Gαi complex stabilized by aripiprazole-type partial agonists. PLoS One. 2014;9(6):e100069-e.
115. Venkatakrishnan AJ, Deupi X, Lebon G, Tate CG, Schertler GF, Babu MM. Molecular signatures of G-protein-coupled receptors. Nature. 2013;494(7436):185-94.
116. Żuk J, Bartuzi D, Matosiuk D, Kaczor AA. Preferential Coupling of Dopamine D(2S) and D(2L) Receptor Isoforms with G(i1) and G(i2) Proteins-In Silico Study. Int J Mol Sci. 2020;21(2):436.
117. Venkatakrishnan AJ, Ma AK, Fonseca R, Latorraca NR, Kelly B, Betz RM, et al. Diverse GPCRs exhibit conserved water networks for stabilization and activation. Proceedings of the National Academy of Sciences. 2019;116(8):3288.
118. Basith S, Cui M, Macalino SJY, Park J, Clavio NAB, Kang S, et al. Exploring G Protein-Coupled Receptors (GPCRs) Ligand Space via Cheminformatics Approaches: Impact on Rational Drug Design. Frontiers in Pharmacology. 2018;9(128).
119. Andresen BT. A pharmacological primer of biased agonism. Endocr Metab Immune Disord Drug Targets. 2011;11(2):92-8.
120. Wacker D, Wang S, McCorvy JD, Betz RM, Venkatakrishnan AJ, Levit A, et al. Crystal Structure of an LSD-Bound Human Serotonin Receptor. Cell. 2017;168(3):377-89.e12.
121. Batool M, Ahmad B, Choi S. A Structure-Based Drug Discovery Paradigm. Int J Mol Sci. 2019;20(11):2783.